

K.P. DATEMA

VIRUS-MEMBRANE INTERACTIONS
spectroscopic studies

PROEFSCHRIFT

ter verkrijging van de graad van
doctor in de landbouwwetenschappen,
op gezag van de rector magnificus,
dr. C.C. Oosterlee,
in het openbaar te verdedigen
op dinsdag 8 september 1987
des namiddags te vier uur in de aula
van de Landbouwuniversiteit te Wageningen.

RECEIVED

15N 423020

VIRUS-MEMBRANE INTERACTIONS

spectroscopic studies

CENTRALE LANDBOUWCATALOGUS



0000 0234 3719

Promotor: dr. T.J. Schaafsma, hoogleraar in de moleculaire fysica
Co-promotor: dr. M.A. Hemminga, universitair hoofddocent

STELLINGEN

- 1 Het staat niet vast dat tijdens plantevirusinfectie de mantel-eiwitten worden geïncorporeerd in het plasmamembraan van de plant.

Dit proefschrift, Hoofdstuk 2.

- 2 De doving van de tryptofaanfluorescentie van het M13-mantel-eiwit in dimyristoylphosphatidylcholine vesikels door stralingsloze energieoverdracht naar parinaarzuur in de bilaag, sluit niet uit dat het M13-mantel-eiwit in geaggregeerde vorm voorkomt.

Kimelman, D., Tecoma, E.S., Wolber, P.K., Hudson, B.S., Wickner, W. & Simoni, R.D. (1979), Biochemistry 18, 5874-5880.

- 3 De transmembraanconformatie van fd-mantel-eiwit in modelmembranen, zoals Valentine et al. zich die voorstellen, wordt onvoldoende ondersteund door hun experimentele resultaten.

Valentine, K.G., Schneider, D.M., Leo, G.C., Colnago, L.A. & Opella, S.J. (1986), Biophys. J. 49, 36-38.

- 4 Leo et al. hebben aangetoond, dat fd-mantel-eiwit in bilagen in de gel-fase niet beweeglijk is op de microseconde-tijdschaal. Zij hebben echter niet onderzocht of dit ook in de vloeibaar-kristallijne fase het geval is, waardoor de relevantie van hun onderzoek aanzienlijk beperkt wordt.

Leo, B.C., Colnago, L.A., Valentine, K.G. & Opella, S.J. (1987), Biochemistry 26, 854-861.

- 5 De waarneming van Oldfield et al., dat de ordening van de vet-zuurstaarten van de lipiden in aanwezigheid van fi-mantel-eiwit verlaagd is, verliest aan betekenis omdat niet is nagegaan of de lipiden georganiseerd waren in een bilaagstructuur.

Oldfield, E., Gilmore, R., Glaser, M., Gutowski, H.S., Hshung, J.C., Kang, S.Y., King, T.E., Meadows, M. & Rice, D. (1978), Proc. Natl. Acad. Sci. U.S.A. 75, 4657-4660.

- 6 De resultaten, die met spin-label-ESR verkregen worden over lipide-eiwit-interacties in membranen, verdienen meer aandacht dan de verfijning van de theorie, die ten grondslag ligt aan de techniek.
- 7 Volgens de morfo-fonologische regels, die gelden voor het Romeinse gedeelte van het Nederlandse vocabularium, moet het woord soniceren uitgesproken worden als [so:niserə] en niet als [so:nikerə].
- 8 Het anoniem blijven van de beoordelaars van wetenschappelijke manuscripten beoogt een ongehinderde selectie van kwalitatief hoogstaand werk. Het staat echter niet vast, dat deze anonimiteit de kwaliteit van de beoordeling verhoogt.
- 9 De minister bekostigt via de Nederlandse Organisatie voor Zuiver Wetenschappelijk Onderzoek (ZWO) beurzen om pas gepromoveerden voor het universitaire onderzoek te behouden. Voor pas gepromoveerden verliest deze optie veel aan betekenis, omdat te verwachten valt dat onvoldoende vaste universitaire posities vacant zullen komen.
- 10 Het gebruik van personal computers vormt een goede stimulans voor optimale benutting en kennisname van de vele toepassingsmogelijkheden.
- 11 In vergelijking met reeds gepromoveerden betalen de promovendi nieuwe stijl (AIO's) een hoge prijs voor een doctoraat met nog onbekende maatschappelijke waarde.

Stellingen behorende bij het proefschrift

"Virus-Membrane Interactions. Spectroscopic Studies"

Klaas Pieter Datema, 8 september 1987.

aan Irena
en mijn ouders

VOORWOORD

In dit proefschrift wordt verslag gedaan van een onderzoek, dat is uitgevoerd van 1983 tot 1987 bij de vakgroep moleculaire fysica. Vele leden van de vakgroep waren hierbij betrokken, waarvan ik met name de volgende personen wil noemen: Prof. Dr. T.J. Schaafsma was mijn promotor. Het onderzoek is uitgevoerd binnen de "virusgroep", waarvan mijn co-promotor, Marcus Hemminga, werkgroep leider is. Ruud Spruijt en Cor Wolfs zijn nauw betrokken geweest bij dit onderzoek als biochemisch analisten.

Tijdens dit onderzoek heeft onze werkgroep nauw samengewerkt met andere laboratoria, zowel binnen als buiten Wageningen. In Wageningen zijn experimenten gedaan in samenwerking met Dick Verduin (Virologie) en Ton Visser (Biochemie), buiten Wageningen in samenwerking met Derek Marsh (M. Planck Institut für Biophysikalische Chemie, Göttingen), Anthony Watts (University of Oxford) en Myer Bloom (University of British Columbia, Vancouver).

Ik bedank allen hartelijk voor hun bijdrage.

Klaas Pieter Datema
juni 1987

CONTENTS

1	GENERAL INTRODUCTION	1
1.1	Plant viruses	5
1.2	Bacteriophage M13	9
1.3	Optical spectroscopy	15
1.4	Magnetic resonance	22
1.5	Outline of this thesis	29
2	EFFECT OF PLANT VIRUSES ON MEMBRANES	37
2.1	Interaction of Plant Viruses and Viral Coat Proteins with Mixed Model Membranes (Biochemistry, in press)	39
3	EFFECT OF THE MEMBRANE ON BACTERIOPHAGE M13 COAT PROTEIN	59
3.1	Time-Resolved Tryptophan Anisotropy Investigation of Bacteriophage M13 Coat Protein in Micelles and Mixed Bilayers (Biochemistry, in press)	61
3.2	Dynamic Properties of M13 Coat Protein in Mixed Bilayers. A Deuterium NMR Study of the Exchangeable Proton Sites	85
4	EFFECT OF BACTERIOPHAGE M13 COAT PROTEIN ON THE MEMBRANE	93
4.1	Spin Label ESR of Bacteriophage M13 Coat Protein Incorpo- ration into Mixed Lipid Bilayers (Biochemistry, in press)	95
4.2	Deuterium NMR Investigation of Bacteriophage M13 Coat Protein in DMPC Liposomes Using Palmitic Acid as a Probe	109
5	SUMMARIZING DISCUSSION	135
	SAMENVATTING	141
	ABBREVIATIONS	147
	CURRICULUM VITAE	149

CHAPTER 1

GENERAL INTRODUCTION

1 GENERAL INTRODUCTION

For an animal, a plant or bacterium, a cell constitutes the fundamental unit of structure and function. For a virus, a cell provides the machinery to make the components for the assembly of new viruses.

The genetic information, specific for a particular virus, is present in the nucleotide sequence of the nucleic acid. In spite of this, a virus can not reproduce itself independently; it must penetrate a host cell and use its metabolic systems. After penetration, the host cell produces the necessary viral components, encoded by the viral nucleic acid. The new virus particles are assembled and leave the host to repeat the reproductive cycle in another host cell.

Most bacterial and plant viruses are non-enveloped viruses, which consist of single- or double-stranded ribonucleic (RNA) or desoxyribonucleic acid (DNA), mainly encapsidated by several identical protein molecules. Many animal viruses are more complicated; the nucleoprotein particle is surrounded by a lipid bilayer, forming membrane-enveloped viruses. A variety of virus particles is shown in Fig.1.

With respect to the early events in infection, enveloped viruses are distinctly different from non-enveloped viruses due to the presence of the surrounding membrane. The virus membrane or envelope, has three functions: it protects the nucleoprotein during the extracellular stage of the reproductive cycle, it is responsible for penetration of the nucleoprotein into the host and it is involved in the assembly of new virus particles in the infected cell.

The general features of the infection mechanism of some enveloped viruses are known (Helenius et al., 1980; White et al., 1983; Crowell & Lonberg-Holm, 1986). These viruses enter the host after attachment of its membrane spike glycoproteins to the cell membrane. Penetration of the nucleoprotein particle occurs either after endocytosis of the virus or directly by passage through the plasma membrane (Fig.2). In

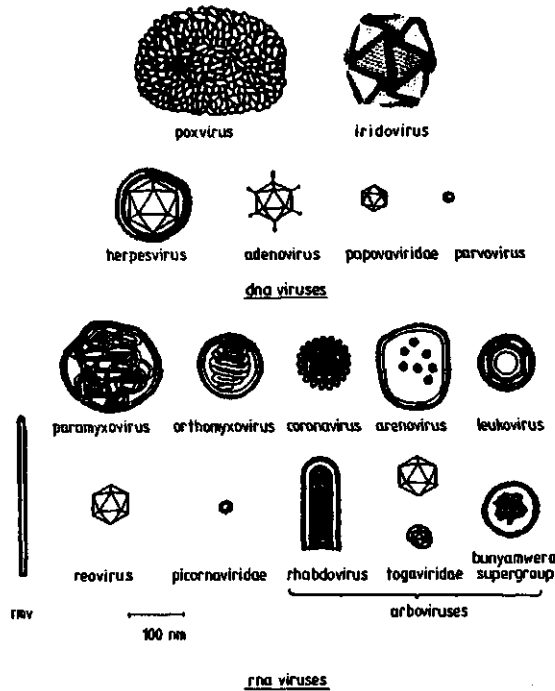


Figure 1. Schematic structure of various viruses.

case of adsorptive endocytosis the endosome is formed by invagination of the cell membrane, surrounding the attached virus.

Non-enveloped viruses may follow a similar endocytotic pathway, but eventually the virus particles have to pass the membrane. These latter processes are poorly understood for both animal and plant viruses. Even for the well-characterized bacterial virus M13 the molecular details of the infection mechanism, have not been completely elucidated.

1.1 PLANT VIRUSES

Structure of plant viruses. The majority of the plant viruses con-

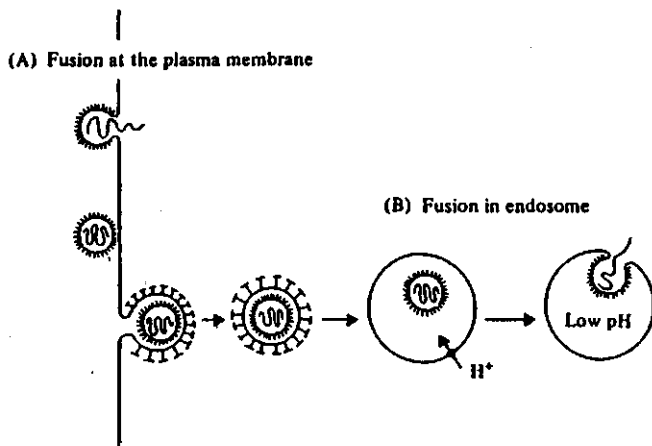


Figure 2. Pathways for entry of enveloped viruses. In pathway A the viral membrane fuses with the plasma membrane and releases the nucleoprotein in the cytoplasm. In pathway B the entire virus particle enters by endocytosis through coated pits into acidic endosomes, where fusion occurs between the viral and the host membrane. (From White et al., 1983).

sist of single-stranded RNA of positive sense, surrounded by a protein coat (Kaper, 1975; Francki, 1985). The protein coat may be rod-shaped, e.g. tobacco mosaic virus (TMV) or spherical, e.g. cowpea chlorotic mottle virus (CCMV), brome mosaic virus (BMV) and southern bean mosaic virus (SBMV). The protein coat of CCMV, BMV and SBMV is a T=3 icosahedron that consists of 180 coat protein molecules with $M=19,400$, $20,300$ and $28,218$, respectively. The rod-shaped protein coat of TMV consists of numerous copies of identical coat protein molecules with $M=17,400$. The detailed molecular structure of TMV (Bloomer et al., 1978; De Wit, 1978) and a number of spherical plant viruses, like CCMV (Verduin, 1978; Vriend, 1983) and SBMV (Harrison et al., 1978; 1980; Abad-Zapatero et al., 1980; Rossmann, 1984), has been investigated. In

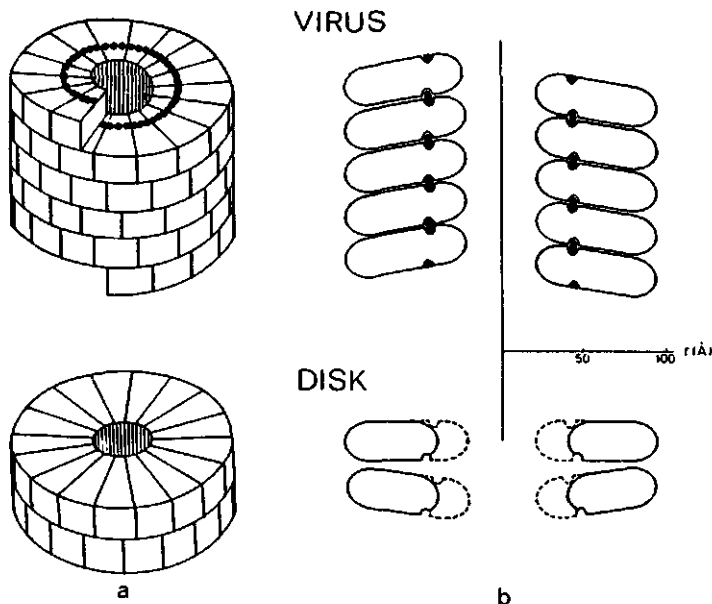


Figure 3. (a) Coat protein packing in the TMV protein disk (below) and in the virus (above). Schematic diagrams of the two-layer (34 coat protein) disk and part of the virus helix.(b) Side views of sections through the central axis of the disk and the virus to show the RNA location in the virus and the diameter of the aggregates (From Lomonosoff & Wilson, 1985).

the virus particle protein-RNA and protein-protein interactions occur. In TMV, besides the electrostatic interaction of the RNA with helical parts of the coat protein molecules, the strong hydrophobic protein-protein interactions dictate the particle structure (Fig.3, Lauffer, 1975; Bloomer et al., 1978; Lomonosoff & Wilson, 1985). In spherical viruses, like CCMV, similar hydrophobic intersubunit bonds stabilize the particle. The positively charged N-termini of the coat protein are important because of electrostatic interaction with the negatively charged RNA, that occurs during the assembly of the virus particle. Recently, a model for CCMV assembly has been proposed (Vriend et al., 1986).

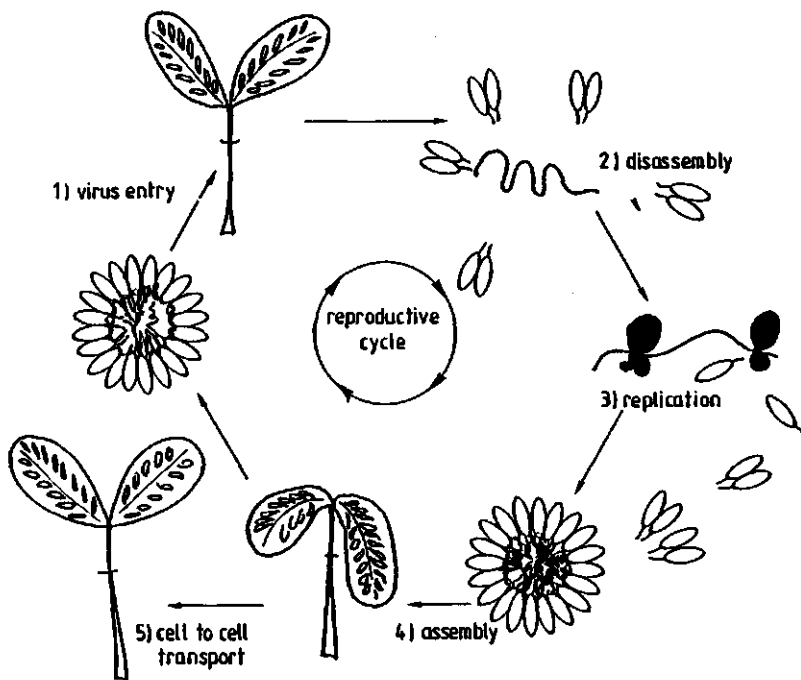


Figure 4. General features of the reproductive cycle of plant viruses. Several stages are indicated: virus entry (1) dissociation or uncoating (2) replication and translation (3) assembly of new virus particles (4) and transport from cell to cell (5).

Plant virus infection. In the reproductive cycle of a plant virus several steps can be distinguished: initial interactions (binding and penetration), disassembly or uncoating, replication and translation, assembly of virus particles and transport from cell to cell (Fig.4). In contrast to their structure, little is known about the early events in plant virus infection (Wilson, 1985). Possible initial interactions are attachment of the virus to the host cell, similar to the attachment of bacteriophage M13 to Escherichia coli, or direct penetration via local, transient wounding of the plasma membrane (Burgess et al.,

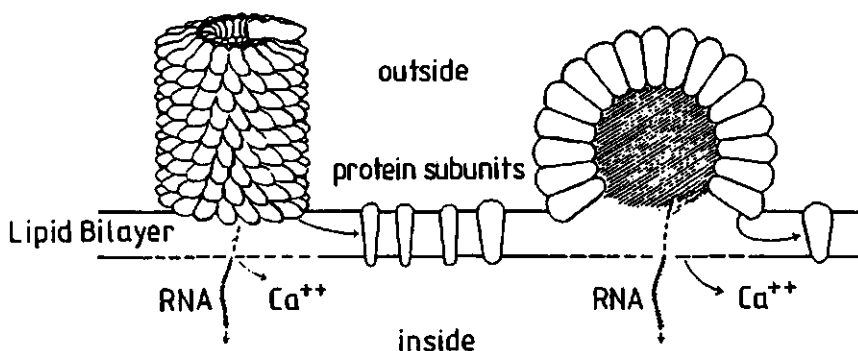


Figure 5. Hypothetical model for plant virus disassembly and membrane passage. The nucleic acid is released in the cytoplasm, while the coat proteins are incorporated in the plasma membrane. Co-transport of ions, like Ca^{2+} , can provide the free energy to drive penetration and disassembly (From Durham, 1978).

1973a,b; Kassanis et al., 1977).

Also, about the mechanism of plant virus dissociation in vivo little is known. Various host cell components may be involved. Components, that were reported to affect plant virus dissociation are: the cell wall (Gaard & De Zoeten, 1979; De Zoeten, 1981), the plasma membrane (Kiho & Shimomura, 1976; Kiho et al., 1979a,b; Watts et al., 1981; Watts & King, 1984; Hull & Maule, 1985), lipids (Kiho & Abe, 1980; Banerjee et al., 1981a,b; Abdel-Salam et al. 1982) and ribosomes (Wilson, 1984).

Models for plant virus infection. Several models describing the initial plant virus-cell interaction have been proposed.

Already in 1963 Caspar speculated about the role of the hydrophobic portion of the host membranes in uncoating of viral RNA (Caspar, 1963). The observation that divalent cations are important factors in plant virus assembly (Durham et al., 1977) and evidence that coat protein of the bacterial virus M13 spans the cytoplasmic bilayer of E.

coli during infection (Marvin & Wachtel, 1975), led Durham to propose a model for plant virus infection (Fig.5). In this model the coat protein subunits become integral membrane proteins of the plasma membrane, stabilized by hydrophobic lipid-protein interactions (Durham, (1978).

Recently, Wilson proposed that destabilized TMV and SBMV nucleocapsids disassemble as a consequence of translation of the viral RNA by the ribosomes of the host cell, i.e. a co-translational disassembly (Wilson, 1985). Evidence that this mechanism of uncoating of viral nucleic acid occurs in vivo has been presented recently (Shaw et al., 1986). The model does not discriminate between membrane passage, in which (the lipids of) the host membranes take part, or penetration of the cell through membrane lesions.

1.2 BACTERIOPHAGE M13

Structure of M13. The filamentous bacteriophage M13 consists of a circular, single stranded DNA molecule of 6407 nucleotides (Van Wezenbeek et al., 1980), protected by a tubular protein coat of approximately 2700 subunits of coat protein molecules (Marvin & Hohn, 1969; Kaper, 1975; Denhardt, 1975; Ray, 1977; Rasched & Oberer, 1986). The virus contains 12% DNA and 88% coat protein by weight. M13 has a diameter of 6 nm and a length of about 870 nm.

98% of the protein coat is formed by the so-called B-protein (the bulk or major coat protein), M=5,240, that is encoded by gene 8 (Marvin & Hohn, 1969; Van Wezenbeek et al., 1980). Spectroscopic studies have shown that the secondary structure of the B-protein in M13 particles is entirely α -helix (Van Asbeck et al., 1969; Day, 1966; 1969). The N-terminal end is located at the outside of the particle and the C-terminal end at the inside, interacting with DNA (Marvin & Wachtel, 1975).

⁺ H ₃ N-Ala-Glu-Gly-Asp-Asp-Pro-Ala-Lys-Ala-Ala	acidic
-Phe-Asn-Ser-Leu-Gln-Ala-Ser-Ala-Thr-Glu	domain
-Tyr-Ile-Gly-Tyr-Ala-TRP-Ala-Met-Val-Val	hydrophobic
-Val-Ile-Val-Gly-Ala-Thr-Ile-Gly-Ile-Lys	domain
-Leu-Phe-Lys-Lys-Phe-Thr-Ser-Lys-Ala-Ser-COO ⁻	basic domain

Figure 6. The amino acid sequence of the major (gene-8 product) M13 coat protein. Three domains are indicated: an acidic N-terminus of 20 residues, a hydrophobic domain of 20 residues and a basic C-terminus of 10 residues. The single tryptophan, used for fluorescence anisotropy decay measurements is at position 26 (After Beck et al., 1978; Van Wezenbeek et al., 1980).

The amino acid sequence of the major coat protein has been established (Nakashima & Koningsberg, 1974; Beck et al., 1978; Van Wezenbeek et al., 1980). It has 50 amino acid residues (Fig.6): an acidic domain of 20 residues at the N-terminus, a hydrophobic, central domain of 20 residues and a basic domain of 10 residues at the C-terminus. In the major coat protein of the related bacteriophages fd and f1 the asparagine residue at position 12 is substituted by an aspartic acid residue (Beck et al., 1978; Van Wezenbeek et al., 1980). Furthermore, the protein coat contains four or five molecules of A-protein (the adsorption or assembly protein), M=42,600, which are located at one end of the filamentous virus particle (Fig.7, Marco, 1975; Goldsmith & Konigsberg, 1977; Woolford et al., 1977) and two additional minor capsid protein molecules, designated C- and D-protein, M=3,500 and M=11,500, respectively (Simons et al., 1979).

Reproductive cycle of M13. The rate of adsorption of M13 to the target *E. coli* cell is limited solely by diffusion and requires no activation energy (Tzagoloff & Pratt, 1964). For the initial interac-

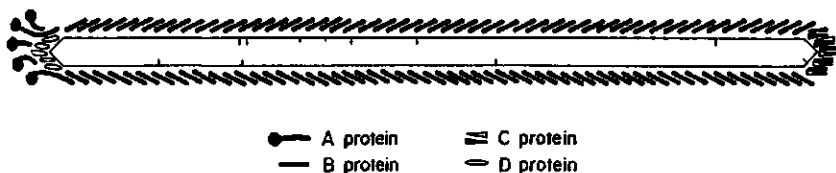


Figure 7. Schematic representation of the positions of structural proteins in bacteriophage M13 (From Webster et al., 1981).

tion with the F-pilus of the host cell the A-protein, located at one tip of the M13 particle, is required (Pratt et al., 1969; Henry & Pratt, 1969). The mechanism of penetration is such, that both DNA and protein of the virus enter the cell (Trenkner et al., 1967). In fact, the major coat protein migrates into the plasma membrane and becomes an integral membrane protein (Smilowitz, 1974; Wickner, 1975; 1976; Chang et al., 1979), while DNA replication takes place in the cytoplasm of the host cell (Fig.8). The newly synthesized, circular DNA is associated with gene-5 protein, forming a linear complex (Pratt et al., 1974).

At the same time new coat protein is synthesized in the cytoplasm as a water soluble precursor of the major coat protein or procoat. The procoat has an extra 23 amino acid (leader) sequence at the N-terminus (Konings et al., 1975; Sugimoto et al., 1977; Model et al., 1979). It is proposed that the procoat is also inserted into the plasma membrane as a double, U-shaped transmembrane protein as a result of the electric membrane potential (Fig.9, Smilowitz et al., 1972; Pratt et al., 1974; Wickner et al., 1978; Date et al., 1980). A leader peptidase outside the cytoplasmic membrane cleaves the double transmembrane procoat to mature, single transmembrane coat protein (Chang et al., 1978a; Kuhn et al., 1986).

During the membrane-associated assembly of new virions gene-5 pro-

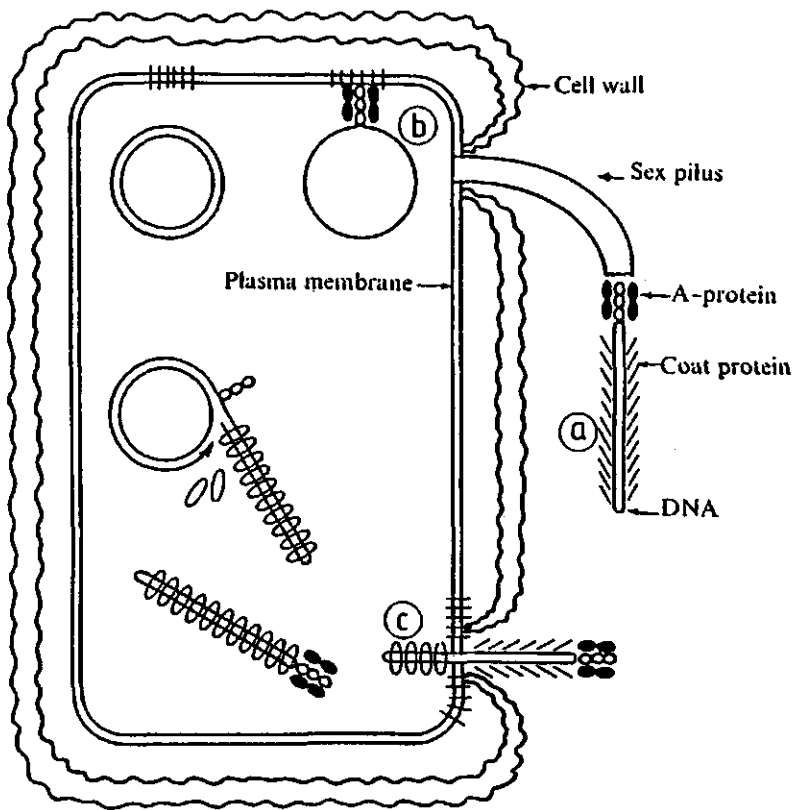


Figure 8. Schematic illustration of some features of the reproductive cycle of bacteriophage M13. (a) Virus attachment by means of a minor coat protein, the A-protein, (b) DNA entry in the cytoplasm, while the major (gene-8 product) coat protein, the B-protein, is incorporated in the cytoplasmic membrane and (c) membrane-bound assembly of new virus particles, without lysis of the host cell (From Marvin & Wachtel, 1975).

tein is removed from the DNA and replaced by the major (gene-8) coat protein. Concomittantly, the nucleoprotein particle is extruding from the plasma membrane into the exterior of the bacterium. Both newly synthesized coat protein, and parental coat protein are used for the

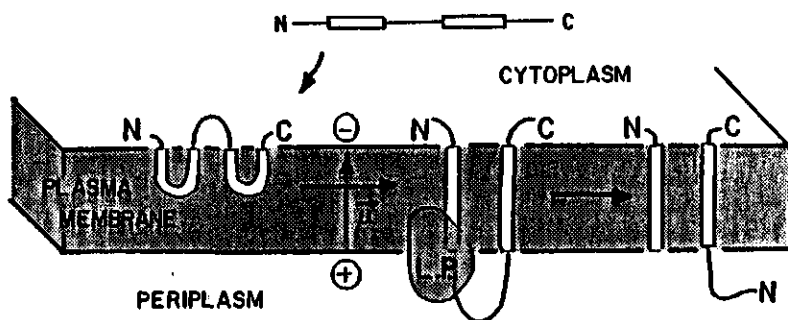


Figure 9. Insertion of the M13 procoat, which has an additional 23 amino acid (leader) sequence into the plasma membrane. After insertion in a U-shape the procoat is cleaved to mature coat protein by a leader peptidase (From Kuhn et al., 1986).

assembly. The virus is released without lysis, i.e. killing of the *E. coli* cell (Hoffmann-Berling & Maze, 1964).

Structure and dynamics of the coat protein in the virus and membrane modelling systems. The structure and dynamics of coat protein of M13 and the related fd in the virus particle, micelles and vesicles have been subject of a number of biophysical investigations, to be reviewed below.

In the virus particle the coat protein secondary structure was determined to be entirely α -helix (Van Asbeck, 1969; Day, 1969) with the helical axis approximately parallel to the filament axis, while the DNA backbone is completely disordered (Cross & Opella, 1981; Cross et al., 1983). Refinement of its structure and position by one and two dimensional NMR indicates that the amino acid residues 40-45 are in a somewhat distorted α -helix, (Cross & Opella, 1985), that the helical axis of residues 28-32 is tilted away with respect to the filament axis by 20° , the axis of residue 33 to 39 by 7° and the axis of residue 40-48 by 14° (Valentine et al., 1985), in agreement with the

slightly slewed helix found from diffraction studies (Marvin et al., 1974; Banner et al., 1981). The coat protein exhibits rapid reorientation on the 10^{-4} s timescale only at the terminal residues at the N-terminus, while the C-terminus is immobile on the timescale 10^{-6} s at the inside of the assembled virus particles (Valentine et al., 1985; Colnago et al., 1987, cf. Fig.7). The motions of the aromatic residue Trp-26 are slow on the 10^{-3} s timescale, but the Phe-11, Phe-42, Phe-45 and Tyr-21, Tyr-24 undergo 180° flips about the $C_\beta-C_\gamma$ bond axis at a rate higher than 10^6 s $^{-1}$, as determined from 2H , ^{13}C and ^{15}N NMR (Gall et al., 1982; Opella et al., 1987).

In SDS micelles the coat protein is dimeric (Makino et al., 1975). The protein secondary structure is 50% α -helix (25 residues) and 30% β -structure (15 residues) as determined from CD (Nozaki et al., 1976; 1978), while laser Raman yields slightly more α -helix and less β -structure (Williams et al., 1984). The hydrophobic core (20 residues) is predominantly β -structure (Chamberlain et al., 1978). The termini are α -helix in micelles (Nozaki et al., 1976; 1978). The backbone of the hydrophobic core, which is buried within the micelle, and part of the hydrophilic domains are rigid in SDS and DCC micelles, i.e. their rotational-correlation time equals that of the micelle as observed by ^{13}C NMR. In contrast, at the extreme ends Ala-1 and Ala-49 are moving more rapidly (Cross & Opella, 1980; Henry et al., 1986a). Hydrogen-exchange rates of the protein in SDS micelles indicate that the N-terminal region up to Asp-12 is well exposed to proton-exchange, as well as Ala-49 at the C-terminus, while the residues 41-46 are much less accessible, possibly due to some hydrogen-bonded structure (Henry et al., 1986b).

In model membranes the coat protein has partly α -helix and β -structure or almost entirely β -structure, depending on the lipid composition of the membrane, the L/P ratio and the preparation method (Nozaki et al., 1976; 1978; Williams & Dunker, 1977; Chamberlain et al., 1978). Also α -helix structure has been suggested (Valentine et

al., 1985), although this paper presents no direct experimental evidence for such a structure. The membrane-bound form of the protein has four mobile sites at the N-terminus while the protein backbone is immobile and does not undergo rapid rotation within the bilayer (Leo et al., 1987; Bogusky et al., 1987). M13 coat protein (L/P = 30) has been found to increase the acyl chain order parameter significantly, while having only a small effect on the rate of acyl chain rotation on the nanosecond timescale, as seen by fluorescence anisotropy measurements of parinaric acid (Wolber & Hudson, 1982). Quenching of the single Trp-26 of the coat protein by parinaric acid in the bilayer has been found to be very efficient, demonstrating the absence of extensive protein aggregation (Kimelman et al., 1979).

In such artificially formed phospholipid vesicles it has been shown that the coat protein spans the membrane, but it is still possible that it has a U-shape in such an orientation and that both the N- and the C-terminus are located at the same side of the membrane (Wickner, 1976; Chamberlain et al., 1978; Bayer & Feigenson, 1985). In the cytoplasmic membrane of *E. coli* antibody- (Wickner, 1975) and tritium-labeling (Ohkawa & Webster, 1981) experiments have shown that the N-terminus is exposed at the outside, while the C-terminus is exposed at the cytoplasmic side. The asymmetric orientation of the coat protein in vivo is also indicated by oriented incorporation in inverted vesicles after synthesis of the coat protein in an in vitro system (Chang et al., 1979).

1.3 OPTICAL SPECTROSCOPY

Optical spectroscopy offers an excellent means to investigate protein structure and dynamics in membrane modelling systems, such as micelles and small unilamellar vesicles (SUVs). Systems containing large structures are much less suitable due to light scattering. The

techniques to be considered here are circular dichroism and time-resolved fluorescence spectroscopy.

Circular dichroism (CD). CD spectroscopy in the far UV can be used to determine the secondary structure of the polypeptide chain. For this purpose the CD spectrum of the protein is compared to a set of reference spectra, derived from proteins containing known amounts of α -helix, β -structure and other structure. Several basis sets of reference spectra exist (Greenfield & Fasman, 1969; Saxena & Wetlaufer, 1971; Chen et al., 1974; Chang et al., 1978b; Hennessey & Johnson, 1981). One example is given in Fig.10 (Greenfield & Fasman, 1969).

The CD spectrum of a protein at any wavelength between 190 and 250 nm can be expressed in terms of a basis set as

$$\theta_{\text{tot}}(\lambda) = f_{\alpha}\theta_{\alpha}(\lambda) + f_{\beta}\theta_{\beta}(\lambda) + f_{\text{rc}}\theta_{\text{rc}}(\lambda) \quad (1)$$

in which $\theta_{\text{tot}}(\lambda)$, $\theta_{\alpha}(\lambda)$, $\theta_{\beta}(\lambda)$ and $\theta_{\text{rc}}(\lambda)$ are the mean residue ellipticities, θ , at wavelength λ of the protein of which the structure is to be analyzed, the reference α -helix, β -structure and other structure with fractions f_{α} , f_{β} and f_{rc} , respectively. Each f has a value between 0 and 1, and the sum of the fractions is 1.

The method of secondary structure determination from CD has been tested for several proteins of which the three dimensional structure has been determined by X-ray diffraction. The accuracy of the determination depends on the amount of secondary structure, such that more accurate results are obtained for proteins with a high degree of α - or β -structure (Greenfield & Fasman, 1969).

It is possible to improve the accuracy of the determination of the secondary structure analysis for large proteins, using a variety of methods (Chen et al., 1974; Hennessey & Johnson, 1981; Mao et al., 1982; Mao & Wallace, 1984; Wallace & Mao, 1984; Wallace & Teeters,

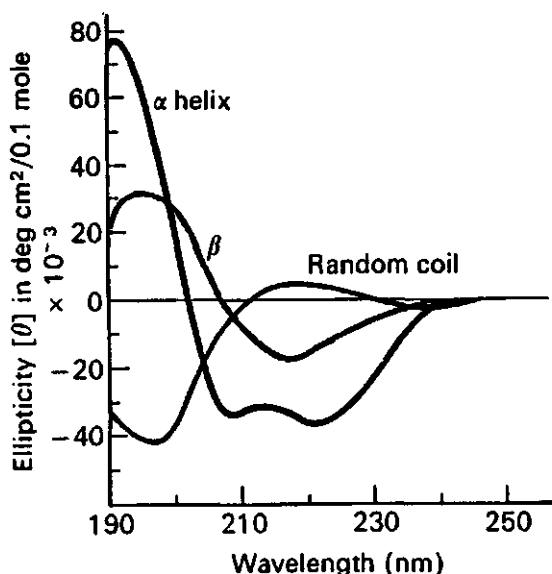


Figure 10. Circular Dichroism (CD) spectra of a polypeptide, poly-L-lysine in various conformations (From Greenfield & Fasman, 1969).

1987). For the relatively small M13 coat protein, studied in this thesis, these methods are not relevant.

CD and absorption spectra of membrane proteins can be distorted by optical artifacts, like light scattering due to the size of the vesicle and hypochromism due to protein aggregation, as is the case in virus particles (Mao & Wallace, 1984, Wallace & Mao, 1984; Wallace & Teeters, 1987). Hypochromism is minimized if the protein is incorporated at high lipid to protein ratio in SUVs, making correction of the spectra unnecessary (Mao & Wallace, 1984).

Time-resolved fluorescence spectroscopy. Time-resolved fluorescence anisotropy measurements can provide detailed information about the

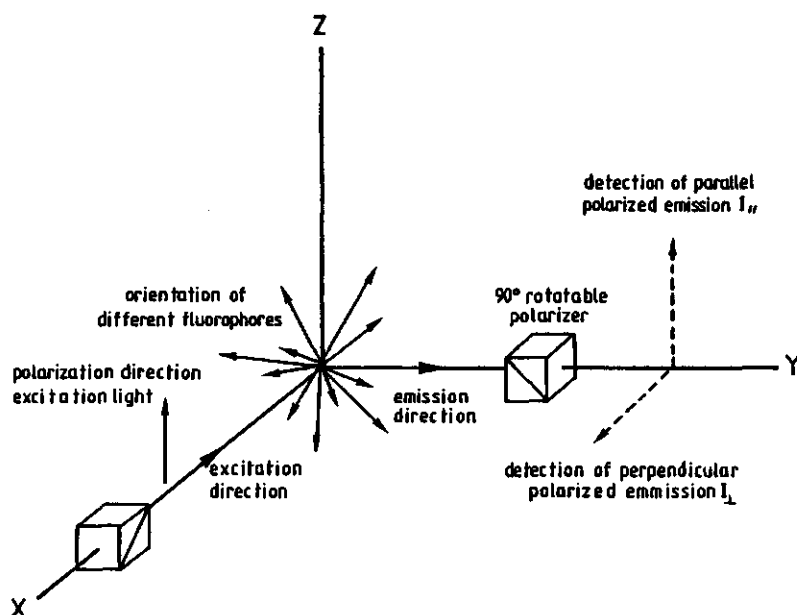


Figure 11. Experimental set-up for a time-resolved anisotropy measurement. The polarization of the excitation pulse is indicated, as well as the parallel, $I_{||}$, and perpendicular, I_{\perp} , detection directions.

dynamical properties of the fluorescent probe and its environment during the lifetime of the excited singlet state. Lifetimes of fluorescent probes range from picoseconds to hundreds of nanoseconds (Zannoni et al., 1983), which makes the technique suitable for a real-time investigation of the dynamics of proteins in solution (whole protein rotation, segmental protein mobility, amino acid side chain motion), of lipids in membranes (restricted acyl chain rotation) and of integral membrane proteins in micelles or membranes (protein backbone mobility, side chain motion).

In a time-resolved fluorescence anisotropy measurement (Fig.11) a short (several picoseconds), monochromatic and polarized laser pulse excites the probe molecules to a higher energy level. Next, the

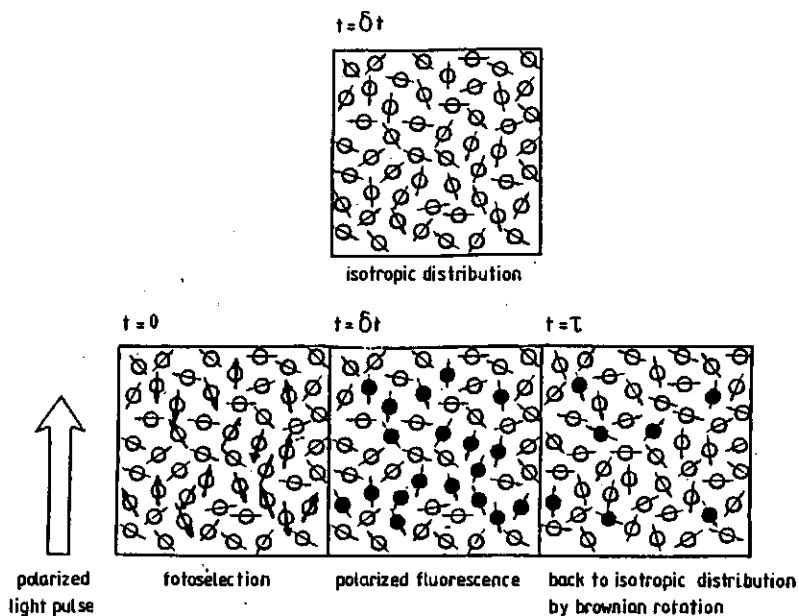


Figure 12. Principle of fluorescence anisotropy decay measurements of isotropically tumbling probe molecules (fluorophores). At $t=0$ a polarized light pulse excites the probe molecules, that have their excitation dipole moments parallel to the pulse. In the following time interval the fluorescence anisotropy decays to the equilibrium value by rotation of the probes. The anisotropy reaches zero, when the distribution of the probe molecules has become isotropic again.

emission from the fluorophore is measured at a higher wavelength as a function of time. The intensity components parallel and perpendicular to the polarization of the excitation pulse are measured by time-correlated single photon counting (for experimental description, see: O'Connor & Phillips, 1984). From the two decays, $I_{\parallel}(t)$ and $I_{\perp}(t)$ (Fig.11), the total fluorescence is obtained by

$$S(t) = I_{\parallel}(t) + 2I_{\perp}(t) \quad (2)$$

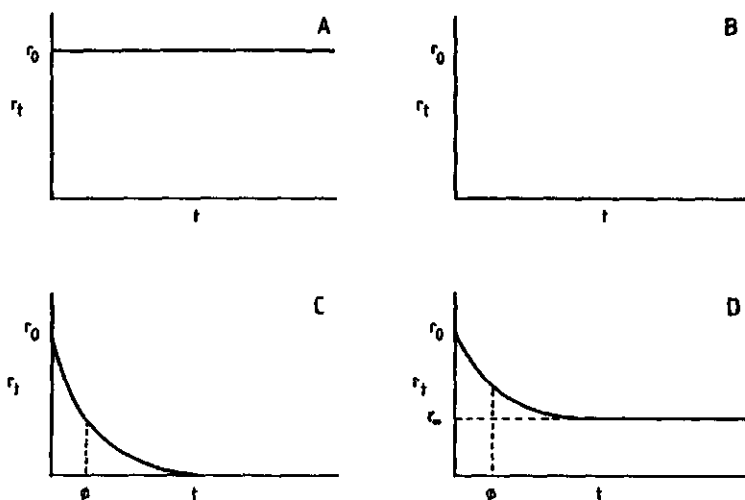


Figure 13. Illustration of the anisotropy decay, $r(t)$, in some specific cases: isotropically tumbling probe molecules with (a) $\tau_F \ll \phi$, resulting in $r(t) = \text{constant} \neq 0$, with (b) $\tau_F \gg \phi$, resulting in $r(t) = 0$ at all times, with (c) $\tau_F \approx \phi$, resulting in a time-dependent anisotropy, containing information on the molecular motion, ϕ and (d) anisotropically tumbling probe molecules, like probe molecules ordered in one direction in bilayers, with $\tau_F \approx \phi$, resulting in a time-dependent anisotropy, containing information on the molecular motion and $r(\infty) = \text{constant} \neq 0$, containing information on the orientational order.

in which $S(t)$ is the convolution product of the undistorted total fluorescence, $s(t)$, and the pulse response, $P(t)$. The fluorescence lifetime(s), τ_F , characterize(s) the decay of the emitted radiation, $S(t)$ (Zannoni et al., 1983). The anisotropy is defined by

$$r(t) = [i_{\parallel}(t) - i_{\perp}(t)] / [i_{\parallel}(t) + 2i_{\perp}(t)] \quad (3)$$

in which $i_{\parallel}(t)$ and $i_{\perp}(t)$ are the (deconvoluted) parallel and perpendicular polarized components derived from the experimental $I_{\parallel}(t)$ and

$I_1(t)$ components. The fluorescence anisotropy, $r(t)$, contains information on the molecular motion if τ_F is of the same order of magnitude as the molecular motion, characterized by ϕ (Zannoni et al., 1983). This is made clear in Fig.12 and 13.

If $\tau_F \ll \phi$, the non-equilibrium distribution of the fluorophores after the photoselection will be completely preserved during the time interval that fluorescence can be observed (Fig.12 and 13a).

If $\tau_F \gg \phi$, the rapid molecular motion has already reduced the non-equilibrium distribution of the fluorophores to zero before fluorescence can be observed (Fig.12 and 13b).

If, however, $\tau_F \approx \phi$, the fluorescence anisotropy decay is related to the molecular motion(s) of the fluorophore (Fig.12 and 13c). If the condition $\tau_F \approx \phi$ is satisfied, the acquisition of information on the molecular motion from the fluorescence anisotropy decay requires theoretical analysis. The analysis can be on the basis of a particular model of which the choice depends on the system under investigation (Kinosita et al., 1977; 1982; Lipari & Szabo, 1980; 1981; Zannoni et al., 1983; Cundall & Dale, 1983; Dale, 1983; Van der Meer et al., 1984; Beecham & Brand, 1985).

For fluorophores in isotropic liquids, illustrated in Fig.12 and 13c, every orientation is equally probable and the anisotropy will finally decay to zero, $r(\infty) = 0$; the system will reach its equilibrium. Information on the molecular motion is obtained from analysis of the fluorescence anisotropy decay.

In vesicle bilayers that consist of lipid molecules, which are ordered in one direction, but highly disordered in the plane perpendicular to the normal of the bilayer, the molecular distribution of the fluorophore is anisotropic, although the vesicle is isotropic as a whole. The molecular anisotropy remains unaffected since the rotation of small unilamellar vesicles is too slow (Burnell et al., 1980) on the nanosecond timescale of the fluorescence anisotropy experiment. As a consequence, in the long time limit, $t \rightarrow \infty$, $r(t)$ does not decay to

zero, but to a constant value, $r(\infty)$, depending on the orientational order of the fluorophore (Fig.13d). Therefore, apart from information on the molecular motion from the decay, also information on the orientational order is available from $r(\infty)$. The degree of orientational constraint to the fluorescence anisotropy is related to the second rank, orientational order parameter, S , by (Heyn, 1979; Jaehnig, 1979)

$$r(\infty) = r(0) \cdot S^2 \quad (4)$$

1.4 MAGNETIC RESONANCE

In this section an outline of the magnetic resonance techniques, as applied in chapter 2-4, is presented. In particular, attention will be paid to the information which can be obtained from magnetic resonance about virus-membrane interactions.

In large anisotropic structures, such as viruses and membranes, solid state nuclear magnetic resonance (NMR) techniques are most appropriate. High resolution NMR is less suitable, because of the incomplete motional averaging of orientation-dependent tensor interactions, e.g. dipole-dipole, quadrupolar and chemical shift anisotropy interaction. Spin-label ESR suffers from the same complication. The latter technique is only suitable by choosing spin labels with appropriate motional characteristics. The techniques to be considered here are spin-label electron spin resonance (ESR), phosphorus NMR and deuterium NMR.

Spin label ESR. Measurements of nitroxide spin labelled phospholipid molecules in membranes are sensitive to molecular motion at the timescale determined by the ^{14}N hyperfine splitting anisotropy of the nitroxide free radical group, $\tau_c = h/(A_{zz} - A_{xx}) \approx 3 \cdot 10^{-8}$ s.

Spin label ESR studies of model membranes containing protein were first performed in 1973 by Jost et al.. After incorporation of cytochrome C oxidase they observed a second component, apart from the sharp three line spectrum, typical for bilayers in the fluid phase (Jost et al., 1973).

Other integral membrane proteins reconstituted in liquid-crystalline phase bilayers, exhibit a similar second component, arising from motionally-restricted lipid molecules (Marsh, 1981; Marsh & Watts, 1982; Griffith et al., 1982; Devaux, 1983; Devaux & Seigneuret, 1985). In addition, the preferences of several phospholipids, differing only in the headgroup, have been summarized for these proteins (Marsh, 1985). Whether a well-resolved second component is observed depends primarily on the $2A_{\max}$ value of the spin label, but also on the rate of exchange between the bulk and motionally-restricted sites. A two-site exchange model is commonly used for the interpretation (Brotherus et al., 1981; Marsh, 1985).

The inherent high sensitivity of ESR as compared to NMR makes spin label ESR particularly well suitable in case of small sample quantities. In comparison, deuterium NMR requires up to a 1,000 times more material than spin label ESR.

Phosphorus NMR. The phosphorus (^{31}P) nucleus in the phosphate of the headgroup of the phospholipid molecule provides an excellent intrinsic membrane probe in the study of virus membrane interactions. ^{31}P ($I=\frac{1}{2}$) has a natural abundance of 100%, so that isotope labelling is not required for ^{31}P NMR spectroscopy.

The ^{31}P NMR spectrum, in our case recorded at 121.48 MHz in a magnetic field of 7.05 T, is determined by the chemical shift anisotropy (CSA) and the phosphorus-proton (^{31}P - ^1H) dipolar interactions,

$$H_{\text{TOT}} = H_Z + H_{\text{CSA}} + H_{\text{DIP}} \quad (5)$$

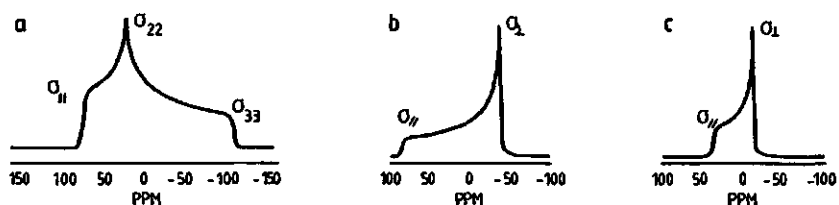


Figure 14. Theoretical ^{31}P NMR spectra of a phospholipid molecule in a membrane: (a) static, (b) rapid, axial rotation around an axis at one fixed angle (c) or within a cone. (After Smith, 1984).

in which H_Z , H_{CSA} and H_{DIP} are the contributions of the Zeeman interaction, the chemical shift anisotropy interaction and the ^{31}P - ^1H dipole-dipole interaction to the spin Hamiltonian, H_{TOT} , respectively. The chemical shift anisotropy Hamiltonian of ^{31}P in phospholipids is described by a tensor interaction (Seelig, 1978), caused by reduction of the local magnetic field through shielding of electrons surrounding the ^{31}P nucleus. This interaction depends on the magnetic field strength. The dipolar Hamiltonian, on the other hand, is independent of the external magnetic field and results in a spectral broadening of 1-5 kHz, depending on the motional freedom of the phosphate group and the distance to the nearest methylene groups (Seelig, 1978). The various phospholipids in a solid are very similar with respect to their principal axis CSA tensor values, σ_{11} , σ_{22} and σ_{33} . The values of a static phosphodiester are typically $\sigma_{11} = -80$ ppm, $\sigma_{22} = -20$ ppm and $\sigma_{33} = 110$ ppm (Seelig, 1978). Therefore, at 7.05 T, the edges of a typical powder pattern are separated by $190 \times 121.48 = 23$ kHz (Fig.14a).

^{31}P NMR spectra of multilamellar or large unilamellar vesicles ($r > 1,000$ nm), however, are axially symmetric (Burnell et al., 1980) with a typical width of 50 ppm, corresponding to 6 kHz at 7.05 T (Fig.14c). The axial symmetry is caused by partial motional averaging, that is

limited by the amplitude of the angular excursion during the averaging and the angle between the axis of rotation and one of the principal components of the CSA tensor (Seelig, 1978; Seelig & Seelig, 1980; Smith, 1984). Therefore, at 7.05 T powder pattern ^{31}P NMR spectra are dominated by a residual CSA interaction, which is broadened by dipolar interactions, which are partly reduced as well. The residual CSA, $\Delta\sigma = \sigma_{\parallel} - \sigma_{\perp}$, can be determined from the edges of the spectrum (Seelig, 1978), but this will involve some error, that depends on the magnitude of the (homogeneous) line broadening of the line width of the individual components in the powder pattern (Seelig, 1978; Rance & Byrd, 1983; Smith, 1984; Dietrich & Trahms, 1987). The ^{31}P - ^1H line broadening can be removed by proton decoupling (Gally et al., 1975; Cullis et al., 1976; Niederberger & Seelig, 1976; Kohler & Klein, 1976; Griffin, 1976) to minimize this type of error in the determination of $\Delta\sigma$. The experimental aspects of solid state ^{31}P NMR, as required for membranes, have been described (Rance & Byrd, 1983; Ellena et al., 1986).

For small unilamellar vesicles ($r < 100$ nm) of bilayers in the liquid-crystalline phase, rapid vesicle tumbling and lateral diffusion of the lipid molecules within the plane of the bilayer average out the ^{31}P CSA and the ^{31}P - ^1H dipolar interactions (Seelig, 1978; Hemminga & Cullis, 1982). Under these conditions the ^{31}P NMR spectrum consists of an isotropic peak of only a few Hz width (Burnell et al., 1980).

For lipids in a hexagonal phase, the lineshape of the spectrum is reversed and its width reduced by a factor of 2 in comparison with a bilayer spectrum, due to an additional averaging mode in the hexagonal cylinders (see, e.g.: Cullis & De Kruijff, 1976; 1979).

In a biological membrane, the lipids are predominantly organized in a bilayer. Therefore, membrane proteins have generally been incorporated in model membranes of phospholipid bilayer systems. However, the lipid structure can be influenced by the presence of membrane proteins and possible roles of lipid polymorphism in biological membranes have been

suggested (De Kruijff et al., 1985). ^{31}P NMR is quite suitable to investigate the polymorphic phase behaviour of lipids in the presence of proteins.

Deuterium NMR. Presently, synthesis of phospholipids, that are selectively deuterated at the headgroup positions (Gally et al., 1981; Seelig & Borle, 1983; Tamm & Seelig, 1983; Sixl & Watts, 1982; 1983; 1985; Sixl et al., 1984) or at acyl chain positions (Jacobs & Oldfield, 1981; Davis, 1983; Smith & Oldfield, 1984; Bloom & Smith, 1985), and production of membrane proteins, that contain specifically deuterated amino acid residues (Keniry et al., 1986; Opella et al., 1987), is routinely performed. Using selectively deuterated lipid and protein probes, lipid-protein interactions have been studied and the specific location of the interaction at the headgroup for several extrinsic proteins (Seelig & Seelig, 1980; Gally et al., 1981; Seelig & Borle, 1983; Tamm & Seelig, 1983; Sixl & Watts, 1982; 1983; 1985; Sixl et al., 1984) and at the acyl chain for several intrinsic proteins (Smith, 1985) has been determined.

The deuterium (^2H) nucleus is a spin $I=1$ particle and has a non-zero electric quadrupole moment, eQ . The spin Hamiltonian of a ^2H nucleus in a high magnetic field is described by

$$H_{\text{TOT}} = H_Z + H_Q + H_{\text{CSA}} + H_{\text{DIP}} \quad (6)$$

in which H_Z , H_Q , H_{CSA} and H_{DIP} are the contribution of the Zeeman interaction, the quadrupolar interaction, the chemical shift anisotropy interaction and the dipole-dipole interaction, respectively.

The quadrupolar interaction of maximally 250 kHz for ^2H in a C- ^2H bond (Davis, 1983) is much smaller than the Zeeman interaction in a magnetic field of 7.05 T. On the other hand, the quadrupolar interaction is much larger than the dipolar and chemical shift anisotropy interactions. Therefore, the quadrupolar interaction can be treated as

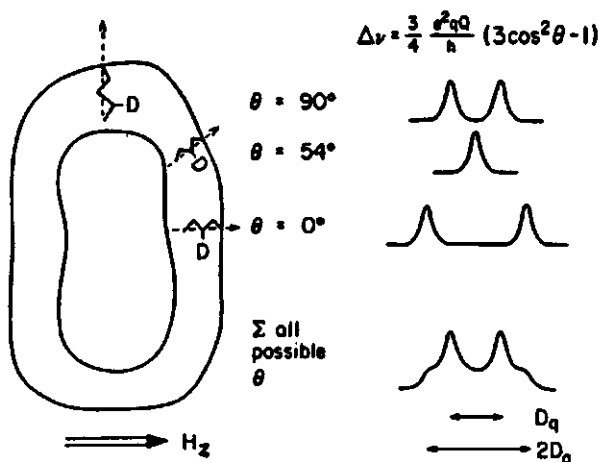


Figure 15. Origin of the deuterium NMR powder spectrum of membranes. θ is the angle between the applied magnetic field, H_z , and the axis of motional averaging (dashed). The parameter D_q describes the splitting in the powder pattern, which corresponds to the $\Delta\nu_q$ for $\theta = 90^\circ$ (From Smith, 1985).

a first order perturbation on the Zeeman interaction,

$$H_{TOT} = H_Z + H_Q, \quad H_Z \gg H_Q \quad (7)$$

The electric quadrupolar Hamiltonian is described by a interaction tensor, described by two unique parameters:

$$\eta = (V_{xx} - V_{yy})/V_{zz} \quad (8)$$

$$V_{zz} = eq \quad (9)$$

where $|V_{yy}| \leq |V_{xx}| \leq |V_{zz}|$ and $0 \leq \eta \leq 1$, and V_{xx} , V_{yy} and V_{zz} are the quadrupolar interaction components, and η the asymmetry parameter.

In practice a 2H NMR spectrum arises from randomly oriented samples, so that a powder pattern lineshape is obtained. A charac-

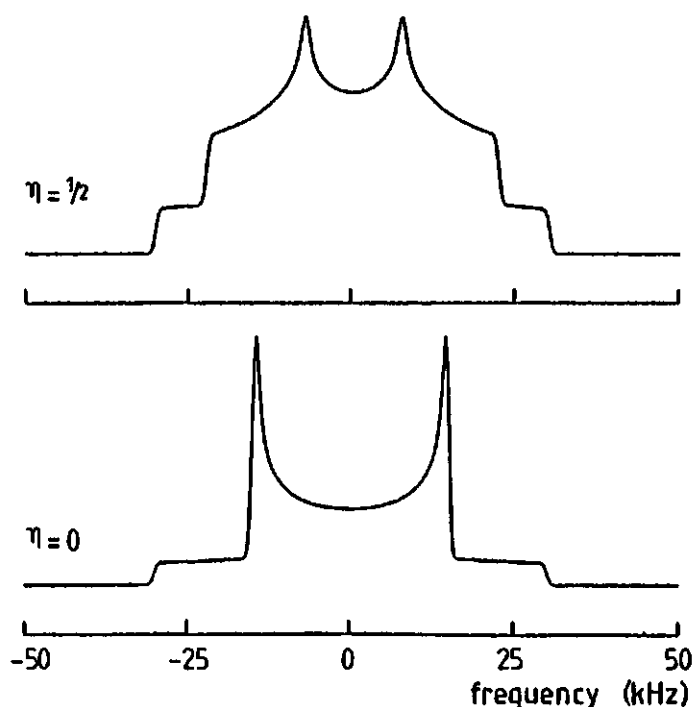


Figure 16. Simulated deuterium NMR spectra with an asymmetry parameter, $\eta = 0.5$ and 0 (From Davis, 1983).

teristic spectrum is shown in Fig.15.

For rapid axial motion ($\tau_c < 10^{-5}$ s) of the probe molecule, the ^2H NMR spectrum is averaged to an axial symmetric powder pattern lineshape in which $\eta=0$ with a quadrupolar splitting, defined as the separation of the singularities at the 90° orientation. This can be expressed in terms of the orientational order parameter for the C- ^2H bond,

$$\Delta\nu_q = (3/4) \cdot (e^2qQ/h) \cdot S_{\text{C-}^2\text{H}} \quad (10)$$

in which $S_{C-2H} = \langle \frac{1}{2}(3\cos^2\theta - 1) \rangle$.

The line shape of the 2H NMR spectrum of a lipid probe is extremely sensitive to the phase transition of the membrane, because of the dramatic changes in molecular order and motion. The spectral parameters (Fig.16, $\Delta\nu_Q$, η) can therefore be used to study the effects of temperature and incorporation of protein molecules in membranes.

1.5 OUTLINE OF THIS THESIS

As a first step towards the elucidation of the molecular mechanisms of non-enveloped virus infection, the interaction between viruses and viral coat proteins and model membranes has been investigated in this thesis. In addition to several plant viruses, a bacterial virus M13 has been chosen for comparison. A number of advanced spectroscopic methods have been chosen to determine the origin of the interactions.

Chapter 2 deals with the effect of plant viruses on membranes. The nature of interaction (hydrophobic or electrostatic) between model membranes and several plant viruses and their coat proteins has been investigated to mimic uncoating and determine the role of the lipid component of the host plasma membrane in the early events of plant virus infection.

TMV, CCMV, BMV and SBMV and their coat proteins have been employed in combination with negatively charged, neutral and positively charged small unilamellar vesicles (SUVs). Various electrostatic and hydrophobic interactions were observed. The experiments showed that plant virus coat protein never incorporates in membranes as integral membrane protein. In addition it was found that the exposed hydrophobic protein domains are able to destabilize membranes and induce membrane fusion.

Chapter 3 deals with the effect of the lipids in the membrane on bacteriophage M13 coat protein.

Time-resolved fluorescence and anisotropy measurements (section 3.1) of the single tryptophan in the coat protein have been carried out at various temperatures and L/P ratios in membranes of mixed lipids, giving information on the order and dynamics of the protein tryptophan and its environment. The results show a constant order over the whole temperature range studied, indicating protein-protein aggregation.

The ^2H NMR measurements (section 3.2) of the exchangeable sites on M13 coat protein in membranes of similar mixed bilayers indicate that the backbone of the coat protein is highly ordered and that the backbone order is unaffected by the rapid lipid motions in liquid-crystalline membranes, in agreement with the protein-protein aggregation concluded from the time-resolved fluorescence anisotropy measurements.

Chapter 4 deals with the effect of bacteriophage M13 coat protein on the lipids of the membrane in which it is incorporated.

From spin label ESR results (section 4.1), obtained with a variety of different spin-labelled phospholipids in M13 coat protein-containing membranes, it is concluded that the presence of the coat protein introduces a second, motionally-restricted component. The two-component spectra have been used to investigate the preference of the different spin-labelled phospholipids for the coat protein. A high preference is found for cardiolipin, a negatively-charged lipid in the target E. coli membrane.

From ^2H NMR measurements (section 4.2) of selectively ^2H labelled palmitic acid in DMPC membranes with various incorporation levels of M13 coat protein the order and dynamics along the acyl chains in the membranes have been studied. No second component is seen in the ^2H NMR spectra in presence of coat protein. The results of both techniques agree with a two site exchange for the fatty acid molecules (at a rate of 10^7 Hz) between the sites in the bulk of the membrane and the motionally-restricted sites.

The concluding chapter 5 discusses and summarizes the observed interactions between the viruses, their coat proteins and the model membranes. Also the possible biological relevance of the observed interactions is indicated.

REFERENCES

- Abad-Zapatero, C., Abdel-Meguid, S.S., Johnson, J.E., Leslie, A.G.W., Rayment, I., Rossmann, M.G., Suck, D., & Tsukihara, T. (1980) Nature **286**, 33-39.
- Abdel-Salam, A., White, J.A., & Sehgal, O.P. (1982) Phytopath. Z. **105**, 334-336.
- Banerjee, S., Vandenbranden, M., & Ruyschaert, J.M. (1981a) Biochim. Biophys. Acta **646**, 360-364.
- Banerjee, S., Vandenbranden, M., & Ruyschaert, J.M. (1981b) FEBS Lett. **133**, 221-224.
- Banner, D.W., Nave, C., & Marvin, D.A. (1981) Nature **289**, 814-816.
- Bayer, R., & Feigenson, G.W. (1985) Biochim. Biophys. Acta **815**, 369-379.
- Beck, E., Sommer, R., Auerswald, E.A., Kurz, Ch., Zink, B., Osterburg, G., Schaller, H., Sugimoto, K., Sugisaki, H., Okamoto, T., & Takanami, M. (1978) Nucl. Acids Res. **5**, 4495-4503.
- Beechem, J.M., & Brand, L. (1985) Ann. Rev. Biochem. **54**, 43-71.
- Bloom, M., & Smith, I.C.P. (1985) in Progress in Protein-Lipid Interactions (Watts, A., & Depont, J.J.H.M., Eds.), Chapt. 2, pp.61-88, Elsevier Science Publishers, New York, NY.
- Bloomer, A.C., Champness, J.N., Bricogne, G., Staden, R., & Klug, A. (1978) Nature **276**, 362-368.
- Bogusky, M.J., Schiksnis, R.A., Leo, G.C., & Opella, S.J. (1987) J. Magn. Reson. **72**, 186-190.
- Brotherus, J.R., Griffith, O.H., Brotherus, M.O., Jost, P.C., Silvius, J.R., & Hokin, L.E. (1981) Biochemistry **20**, 5261-5267.
- Burgess, J., Motoyoshi, F., & Fleming, E.N. (1973a) Planta **111**, 199-208.
- Burgess, J., Motoyoshi, F., & Fleming, E.N. (1973b) Planta **112**, 323-332.
- Burnell, E.E., Cullis, P.R., & De Kruijff, B. (1980) Biochim. Biophys. Acta **603**, 63-69.
- Caspar, D.L.D. (1963) Adv. Protein Chem. **18**, 87-121.
- Chamberlain, B.K., Nozaki, Y., Tanford, C. & Webster, R.E. (1978) Biochim. Biophys. Acta **510**, 18-37.

- Chang, C.T., Wu, C.-S.C., & Yang, J.T. (1978a) Anal. Biochem. **91**, 13-31.
- Chang, C., Blobel, G., & Model, P. (1978b) Proc. Natl. Acad. Sci. USA **75**, 361-365.
- Chang, C., Model, P., & Blobel, G. (1979) Proc. Natl. Acad. Sci. USA **76**, 1251-1255.
- Chen, Y.-H., Yang, J.T., & Chan, K.H. (1974) Biochemistry **13**, 3350-3359.
- Colnago, L.A., Valentine, K.G., & Opella, S.J. (1987) Biochemistry **26**, 847-854.
- Cross, T.A., & Opella, S.J. (1980) Biochem. Biophys. Res. Comm. **92**, 478-484.
- Cross, T.A., & Opella, S.J. (1981) Biochemistry **20**, 290-297.
- Cross, T.A., Tsang, P., & Opella, S.J. (1983) Biochemistry **22**, 721-726.
- Cross, T.A., & Opella, S.J. (1985) J. Mol. Biol. **182**, 367-381.
- Crowell, R.L., & Lonberg-Holm, K. (1986) Virus Attachment and Entry into Cells, Am. Soc. Microbiol., Washington, D.C.
- Cullis, P.R., & De Kruijff, B. (1976) Biochim. Biophys. Acta **436**, 523-540.
- Cullis, P.R., De Kruijff, B., & Richards, R.E. (1976) Biochim. Biophys. Acta **426**, 433-446.
- Cullis, P.R., & De Kruijff, B. (1979) Biochim. Biophys. Acta **559**, 399-420.
- Cundall, R.B., & Dale, R.E. (1983) Time-Resolved Fluorescence Spectroscopy in Biochemistry and Biology, Plenum Press, New York, NY.
- Dale, R.E. (1983) in Time-Resolved Fluorescence Spectroscopy in Biochemistry and Biology, Plenum Press, New York, NY (Cundall, R.B., and Dale, R.E., Eds.) pp. 555-604.
- Date, T., Goodman, J.M., & Wickner, W.T. (1980) Proc. Natl. Acad. Sci. USA **77**, 4669-4673 (1980).
- Davis, J.H. (1983) Biochim. Biophys. Acta **737**, 177.
- Day, L.A. (1966) J. Mol. Biol. **15**, 395-398; (1969) **39**, 265-297.
- De Kruijff, B., Cullis, P.R., Verkleij, A.J., Hope, M.J., Van Echteld, C.J.A., Taraschi, T.F., Van Hoogevest, P., Killian, J.A., Rietveld, A., & Van der Steen, A.T.M. (1985) in Progress in Lipid-Protein Interactions (Watts, A. & De Pont, J.J.H.H.M., Eds.) pp.89-142, Elsevier, NY.
- Denhardt, D.T. (1975) CRC Crit. Rev. Microbiol. **4**, 161-223.
- Devaux, P.F. (1983) in Biological Magnetic Resonance (Berliner, L.J., & Reuben, J., Eds.), vol. 5, pp.183-299, Plenum Press, NY.
- Devaux, P.F., & Seigneuret, M. (1985) Biochim. Biophys. Acta **822**, 63-125.
- De Wit, J.L. (1978) Thesis Wageningen Agricultural University.
- De Zoeten, G.A. (1981) in Plant Diseases and Vectors (Maramorosch, K., & Harris, K.F., Eds.) pp. 221-239, Academic Press, NY.
- Dietrich, R. & Trahms, L. (1987) J. Magn. Reson. **71**, 337-341.
- Durham, A.C.H., Hendry, D.A., & Von Wechmar, M.B. (1977) Virology **77**, 524-533.

- Durham, A.C.H. (1978) Biomedicine 28, 307-314.
- Ellena, J.F., Pates, R.D., & Brown, M.F. (1986) Biochemistry 25, 3742-3748.
- Francki, R.I.B. (1985) The Viruses, Plenum Press, NY.
- Gaard, G., & De Zoeten, G.A. (1979) Virology 96, 21-31.
- Gall, C.M., Cross, T.A., DiVerdi, J.A., & Opella, S.J. (1982) Proc. Natl. Acad. Sci. USA 79, 101-105.
- Gally, H.U., Niederberger, W., & Seelig, J. (1975) Biochemistry 14, 3647-3652.
- Gally, H.U., Pluschke, G., Overath, P., & Seelig, J. (1981) Biochemistry 20, 1826-1831.
- Goldsmith, M., & Konigsberg, W.H. (1977) Biochemistry 16, 2686-2693.
- Greenfield, N., & Fasman, G.D. (1969) Biochemistry 8, 4108-4116.
- Griffin, R.G. (1976) J. Am. Chem. Soc. 98, 851-853.
- Griffith, O.H., Brothier, J., & Jost, P.C. (1982) in Lipid-Protein Interactions (Jost, P.C., & Griffith, O.H., Eds.), vol. 2, Chapt. 6, pp225-237, Wiley-Interscience, NY.
- Harrison, S.L., Olson, A.J., Schut, L.E., Winkler, K.K., & Bricogne, G. (1978) Nature 276, 368-373.
- Harrison, S.L. (1980) Biophys. J. 10, 139-154.
- Heyn, M.P. (1979) FEBS Lett. 108, 359-364.
- Helenius, A., Mellman, I., Wall, D., & Hubbard, A. (1980) Trends Biochem. Sci. 8, 245-250.
- Hemminga, M.A., & Cullis, P.R. (1982) J. Magn. Reson. 47, 307-323.
- Hennessey, J.P., & Johnson, W.C. (1981) Biochemistry 20, 1085-1094.
- Henry, T.J., & Pratt, D. (1969) Proc. Natl. Acad. Sci. USA 62, 800-807 (1969).
- Henry, G.D., Weiner, J.H., & B.D. Sykes (1986a) Biochemistry 25, 590-598.
- Henry, G.D., O'Neil, J.D., Weiner, J.H., & B.D. Sykes (1986b) Biophys. J. 49, 329-331.
- Hoffmann-Berling, H., & Maze, R. (1964) Virology 22, 305-313.
- Hull, R., & Maule, A.J. (1985) in The Viruses (Francki, R.I.B., Ed.) pp.83-115, Plenum Press, NY.
- Jacobs, R.E., & Oldfield, E. (1981) Prog. Nucl. Magn. Reson. Spectrosc. 14, 113-136.
- Jaehnic, F. (1979) Proc. Natl. Acad. Sci. USA 76, 6361-6365.
- Jost, P.C., Griffith, O.H., Capaldi R.A., & Vanderkooi, G.A. (1973) Proc. Natl. Acad. Sci. USA 70, 4756-4763.
- Kaper, J.M. (1975) The Chemical Basis of Virus Structure, Dissociation and Reassembly, vol. 39 (Neuberger, A., & Tatum, E.L., Eds.) Elsevier Publ. Co.
- Kassanis, B., White, R.F., Turner, R.H., & Woods, R.D. (1977) Phytopath. Z. 88, 215-228.
- Keniry, M.A., Gutowski, H.S., & Oldfield, E. (1986) Nature 307, 383-386.
- Kiho, Y., & Shimomura, T. (1976) Japan. J. Microbiol. 20, 537-541.
- Kiho, Y., Shimomura, T., Abe, T., & Nozu, Y. (1979a) Microbiol. Immunol. 23, 735-748.

- Kiho, Y., Abe, T., & Ohashi, T. (1979b) Microbiol. Immunol. **23**, 1067-1076.
- Kiho, Y., & Abe, T. (1980) Microbiol. Immunol. **24**, 617-628.
- Kimelman, D., Tecoma, E.S., Wolber, P.K., Hudson, B.S. Wickner, W.T., & Simoni, R.D. (1979) Biochemistry **18**, 5874-5880.
- Kinosita, K.Jr., Kawato, S., & Ikegami, A. (1977) Biophys. J. **20**, 289-305.
- Kinosita, K.Jr., Ikegami, A., & Kawato, S. (1982) Biophys. J. **37**, 461-464.
- Kohler, S.J., & Klein, M.P. (1976) Biochemistry **15**, 967-973.
- Konings, R.N.H., Hulsebos, T., & Van den Hondel, C.A. (1975) J. Virol. **15**, 570-584.
- Kuhn, A., Wickner, W., & Kreil, G. (1986) Nature **322**, 335-339.
- Lauffer, M.A. (1975) Entropy-Driven Processes in Biology. Polymerization of TMV Protein and Similar Reactions Springer-Verlag, Berlin.
- Leo, G.C., Colnago, L.A., Valentine, K.G., & Opella, S.J. (1987) Biochemistry **26**, 854-862.
- Lomonossoff, G.P., & Wilson, T.M.A. (1985) in Molecular Plant Virology (Davies, J.W., Ed.), Vol I, pp.43-83, CRC Press, Boca Raton, Fl.
- Lipari, G., & Szabo, A.G. (1980) Biophys. J. **30**, 489-506.
- Lipari, G., & Szabo, A.G. (1981) J. Chem. Phys. **75**, 2970-2978.
- Makino, S., Woolford, J.L.Jr., Tanford, C., & Webster, R.E. (1975) J. Biol. Chem. **250**, 4327-4332.
- Mao, D., Wachter, E., & Wallace, B.A. (1982) Biochemistry **21**, 4960-4968.
- Mao, D., & Wallace, B.A. (1984) Biochemistry **23**, 2667-2673.
- Marco, R. (1975) Virology **68**, 280-282.
- Marsh, D. (1981) in Membrane Spectroscopy (Grell, E., Ed.) pp 51-142, Springer-Verlag, Berlin.
- Marsh, D. (1985) in Progress in Protein-Lipid Interactions (Watts, A., & De Pont, J.J.H.M., Eds.), Chapt. 4, pp. 143-172, Elsevier Science Publications, NY.
- Marsh, D., & Watts, A. (1982) in Lipid-Protein Interactions (Jost, P.C., & Griffith, O.H., Eds.), vol. 2, pp53-126, Wiley-Interscience, NY.
- Marvin, D.A., & Hohn, B. (1969) Bact. Revs. **33**, 172-209.
- Marvin, D.A., Wiseman, R.L., & Wachtel, E.J. (1974) J. Mol. Biol. **88**, 581-600.
- Marvin, D.A., & Wachtel, E.J. (1975) Nature **253**, 19-23.
- Model, P., McGill, R., & Kindt, T.J. (1979) cited in Chang et al. (1979)
- Nakashima, Y., & Konigsberg, W. (1974) J. Mol. Biol. **88**, 598-600.
- Niederberger, W., & Seelig, J. (1976) J. Am. Chem. Soc. **98**, 3704-3706.
- Nozaki, Y., Chamberlain, B.K., Webster, R.E., & Tanford, C. (1976) Nature **259**, 335-337.
- Nozaki, Y., Reynolds, J.A., & Tanford, C. (1978) Biochemistry **17**, 1239-1246.
- O'Connor, D.V., & Phillips, D. (1984) Time-Related Single Photon Counting, Acad. Press, London.

- Ohkawa, I., & Webster, R.E. (1981) J. Biol. Chem. **256**, 9951-9958.
- Opella, S.J., Stewart, P.L., & Valentine, K.G. (1987) Quart. Rev. Biophys. in press.
- Pratt, D., Tzagoloff, H., & Beaudoir, J. (1969) Virology **39**, 42-53.
- Pratt, D., Laws, P., & Griffith, J. (1974) J. Mol. Biol. **82**, 425-439.
- Rance, M., & Byrd, A. (1983) J. Magn. Reson. **52**, 221-240.
- Rasched, I., & Oberer, E. (1986) Microbiol. Rev. **50**, 401-427.
- Ray, D.S. (1977) in Comprehensive Virology (Fraeckel-Conrad, H., & Wagner, R.R, Eds.) vol. 7, pp.105-178, Plenum Press, NY.
- Rossmann, M.G. (1984) in Biological Macromolecules and Assemblies (Jurnak, F.A., & McPherson, A., Eds.) vol. 1, pp. 45-96, Wiley & Sons, NY.
- Saxena, V.P., & Wetlaufer, G.D. (1971) Proc. Natl. Acad. Sci. USA **68**, 969-972.
- Seelig, J. (1978) Biochim. Biophys. Acta **515**, 105-140.
- Seelig, J., & Seelig, A. (1980) Quart. Rev. Biophys. **13**, 19-65.
- Seelig, J., & Borle, F. (1983) Bull. Magn. Reson. **5**, 150-151.
- Shaw, J.G., Plaskitt, K.A., & Wilson, T.M.A. (1986) Virology **148**, 328-336.
- Simons, G.F.M., Konings, R.N.H., & Schoenmakers, J.G.G. (1979) FEBS lett. **106**, 8-12.
- Sixl, F., & Watts, A. (1982) Biochemistry **21**, 6446-6452.
- Sixl, F., & Watts, A. (1983) Proc. Natl. Acad. Sci. USA **80**, 1613-1615.
- Sixl, F., Brophy, P.J., & Watts, A. (1984) Biochemistry **23**, 2032-2039.
- Sixl, F., & Watts, A. (1985) Biochemistry **24**, 7906-7910.
- Smailowitz, H., Carson, J., & Robbins, P.W. (1972) J. Supramol. Struct. **1**, 8-18.
- Smailowitz, H. (1974) J. Virol. **13**, 94-99.
- Smith, I.C.P. (1984) in NATO ASI ser. A, vol. 76, no. biomembranes, pp.81-110.
- Smith, I.C.P. (1985) in Nuclear Magnetic Resonance of Liquid Crystals (Emsley, J.W., Ed.) pp 533-566.
- Smith, R.L., & Oldfield, E. (1984) Science **225**, 280-288.
- Sugimoto, K., Sugisaki, K., & Takanami, M. (1977) J. Mol. Biol. **110**, 487-507.
- Tamm, L., & Seelig, J. (1983) Biochemistry **22**, 1474-1483.
- Trenkner, E., Bonhoeffer, F., & Gierer, A. (1967) Biochem. Biophys. Res. Comm. **28**, 932-939.
- Tzagoloff, H., & Pratt, D. (1964) Virology **24**, 373-380.
- Valentine, K.G., Schneider, D.M., Leo, G.C., Colnago, L.A., & Opella, S.J. (1985) Biophys. J. **49**, 36-38.
- Van Asbeck, F., Beyreuther, K., Koehler, H., Von Wettstein, G., & Braunitzer, G. (1969) Hoppe-Seyler's Z. Physiol. Chem. **350**, 1047-1066.
- Van der Meer, W., Pottel, H., Herreman, W., Ameloot, M., Hendrickx, H., & Schroeder, H. (1984) Biophys. J. **46**, 515-523.
- Van Wezenbeek, P.M.G.F., Hulsebos, T.J.M., & Schoenmakers, J.G.G.

- (1980) Gene 11, 129-148.
- Verduin, B.J.M. (1978) Thesis Wageningen Agricultural University.
- Vriend, G. (1983) Thesis Wageningen Agricultural University.
- Vriend, G., Verduin, B.J.H., & Hemminga, M.A. (1986) J. Mol. Biol. 191, 453-460.
- Wallace, B.A., & Mao, D. (1984) Anal. Biochem. 142, 317-328.
- Wallace, B.A., & Teeters, C.L. (1987) Biochemistry 26, 65-70.
- Watts, W.J., Dawson, J.R.O., & King, J.M. (1981) CIBA Foundation Symposium 80, pp. 56-71.
- Watts, W.J., & King, J.M. (1984) J. gen. Virol. 65, 1709-1712.
- Webster, R.E. Grant, R.A., & Hamilton, L.A.W. (1981). J. Mol. Biol. 152, 357-374.
- White, J., Klelian, M., & Helenius, A. (1983) Q. Rev. Biophys. 16, 151-195.
- Wickner, W. (1975) Proc. Natl. Acad. Sci. USA 72, 4749-4753.
- Wickner, W. (1976) Proc. Natl. Acad. Sci. USA 73, 1159-1163.
- Wickner, W., Mandel, G., Zwizinsky, C., Bates, M., & Killick, T. (1978) Proc. Natl. Acad. Sci. USA 75, 1754-1758.
- Williams, R.W., & Dunker, A.K. (1977) J. Biol. Chem. 252, 6253-6255.
- Williams, R.W., Dunker, A.K., & Peticolas, W.L. (1984) Biochim. Biophys. Acta 791, 131-144.
- Wilson, T.M.A. (1984) Virology 137, 255-265.
- Wilson, T.M.A. (1985) J. gen. Virol. 66, 1201-1207.
- Wolber, P.K., & Hudson, B.S. (1982) Biophys. J. 37, 253-262.
- Woolford, J.L., Steinman, H.M., & Webster, R.E. (1977) Biochemistry 16, 2694-2700.
- Zannoni, C., Arcioni, A., & Cavatorta, P. (1983) Chem. Phys. Lipids 32, 179-250.

CHAPTER 2

EFFECT OF PLANT VIRUSES ON MEMBRANES

2.1 INTERACTION OF PLANT VIRUSES AND VIRAL COAT PROTEINS WITH MIXED MODEL MEMBRANES

Klaas P. Datema, Ruud B. Spruijt, Benedictus J.M. Verduin and
Marcus A. Hemminga

ABSTRACT: The interaction between model membranes and viruses, empty capsids and coat protein dimers has been investigated. Spherical plant viruses (CCMV, BMV and SBMV), a rod-shaped plant virus (TMV) and well-defined aggregation states of their proteins have been used. Turbidity measurements at 550 nm of neutral, positively and negatively charged small unilamellar vesicles interacting with viral material indicated electrostatic and indirect hydrophobic interactions. Electrostatic interaction resulted in lipid-protein complexes, which precipitate. Indirect hydrophobic interaction produced precipitates which contained lipid but no protein. Virus particles and empty capsids of the spherical viruses reacted with charged vesicles through electrostatic interaction. Coat protein dimers of all plant viruses induced vesicle fusion by interaction of the exposed hydrophobic protein domains with neutral vesicles. Further characterization of the precipitates by ^{31}P NMR and electron microscopy indicated that both interactions resulted in formation of multilayer structures. Protein assays after incubation at various salt concentrations showed that protein was never incorporated into the bilayer to form a stable complex held together by direct hydrophobic lipid-protein interactions. From the results it is concluded that such hydrophobic lipid-coat protein interactions do not occur, although exposed hydrophobic protein domains are able to destabilize membranes and induce fusion.

The initial stages of non-enveloped plant virus infection involve penetration of the virus into the cell and subsequent dissociation of the nucleoprotein particle. Conclusions about the site and mechanism of penetration are still controversial. Various components of the cell are reported to affect the dissociation of plant virus particles: the cell wall (Gaard & De Zoeten, 1979; De Zoeten, 1981), the plasma membrane (Kiho et al., 1976; 1979a,b), lipids (Kiho et al., 1980;

Banerjee et al., 1981a,b; Abdel-Salam et al., 1982), protoplast membranes (Watts et al., 1981; Watts & King, 1984; Hull & Maule, 1985) and ribosomes (Wilson, 1984).

At present, several models for initial interactions between virus and cell exist. By analogy with the observation that hydrophobic inter-subunit bonds play a role in TMV nucleocapsid assembly, it was proposed that a hydrophobic environment is involved in the uncoating of the viral RNA in vivo (Caspar, 1963). Also divalent cations have been suggested to regulate assembly and disassembly (Durham et al., 1977). Using this observation, a model including both virus penetration and uncoating was postulated, in which the coat protein subunits become integral membrane proteins stabilized by hydrophobic lipid-protein interactions (Durham, 1978). This model is proven for the filamentous bacteriophage M13, in which the coat protein is assumed to span the cytoplasmic bilayer of Escherichia coli during a particular stage of infection (Marvin & Wachtel, 1975). Recently, Wilson (1985) suggested a cotranslational disassembly of destabilized TMV and SBMV as a mechanism for uncoating of viral nucleic acid and evidence was presented that TMV particles disassemble cotranslationally in vivo (Shaw et al., 1986).

We investigated the nature of the interaction (hydrophobic or electrostatic) between artificial membranes and several plant viruses and their coat proteins to mimic and determine the role of the lipid component of the host plasma membrane in initial interactions. Spherical plant viruses (CCMV, and BMV and SBMV), a rod-shaped plant virus (TMV) and several well-characterized aggregation states of their proteins were used. Binding to negatively charged, neutral and positively charged small unilamellar vesicles (SUVs) was studied. This binding was measured by the change in turbidity at 550 nm caused by aggregation, fusion and transformation to multilayer vesicles. Protein content determinations, ³¹P NMR and electron microscopy were used for characterization of the aggregation products. The results are

discussed with respect to previously proposed models of initial interactions.

MATERIALS AND METHODS

Chemicals. 1,2-didodecanoyl-sn-glycero-3-phosphocholine (dilauroyl phosphatidylcholine, DLPC, 99% purity), 1,2-didodecanoyl-sn-glycero-3-phosphatidic acid, (dilauroyl phosphatidic acid, DLPA, 98% purity), 1,2-ditetradecanoyl-sn-glycero-3-phosphoglycerol (dimyristoyl phosphatidylglycerol, DMPG, 99% purity) and palmitoyl choline iodide ($C_{16}H_{33}OC_2H_4N^+(CH_3)_3I^-$, PALCHOL) were obtained from Sigma Chemical Co., St. Louis. Cetyl trimethyl ammonium bromide ($C_{19}H_{42}N^+Br^-$, CTAB, 99% purity) was obtained from Serva Feinbiochemica GMBH & Co., Heidelberg. Lipids and fatty acids were used without further purification.

Sample Preparation. (a) Vesicle stock suspensions. Vesicle stock suspensions of 5.33 mg/ml DLPC (neutral vesicles), 80/20 w/w mixtures of DLPC/DLPA, DLPC/DMPG (negatively charged vesicles) and of DLPC/PALCHOL, DLPC/CTAB (positively charged vesicles) were prepared in the various buffers also used for solutions of virions and coat protein. DLPC was chosen as bulk lipid since pure DLPC vesicles have the gel to liquid-crystalline phase transition at 0°C. A clear suspension of SUVs was obtained by sonication under N_2 on ice for 5 min with a Branson cell disruptor B30 (duty cycle: 90%, power setting 4 (max 350 W at setting 10)). This resulted in vesicle solutions with $A_{550nm} < 0.1$. After sonication the pH of the vesicle solution was checked and no changes were found.

(b) Virus and coat protein stock solutions. Viruses were purified as described for TMV (Leberman, 1966), CCMV and BMV (Verduin, 1978) and SBMV (Van Lent & Verduin, 1985). Coat protein was prepared as reported for TMV (De Wit et al., 1978), CCMV and BMV (Verduin, 1974). For the preparation of SBMV protein the virus was first swollen in 10

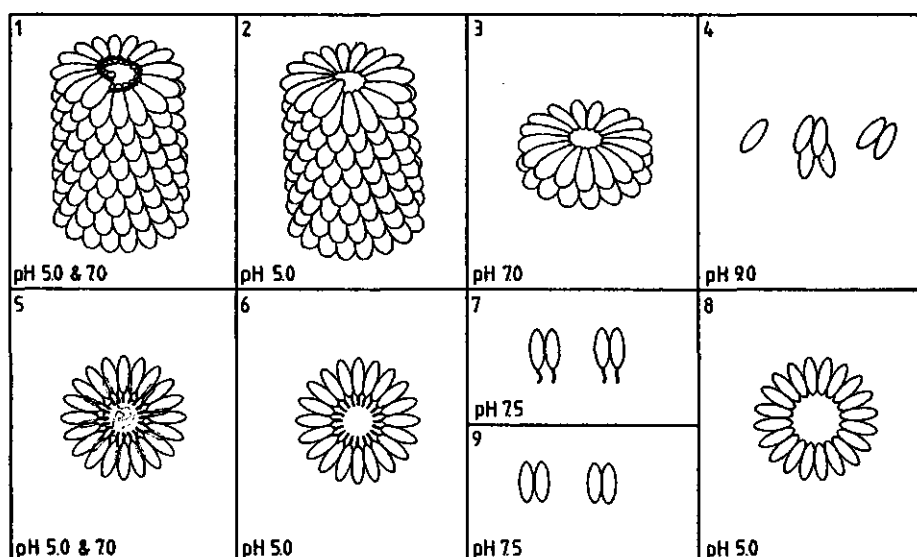


Figure 1. Schematic representation of the plant viruses and various aggregation states of their coat proteins. Rod-shaped TMV virions (1), TMV protein in helix-form (2), in disk-form (3) and as oligomers (4). Spherical CCMV, SBMV or BMV virions (5), empty capsids of CCMV, SBMV or BMV protein (6), dimers of CCMV, SBMV or BMV protein (7), empty capsids of CCMV, SBMV or BMV protein lacking the N-terminal arm (8) and dimers of CCMV, SBMV or BMV protein lacking the N-terminal arm (9). Numbers correspond to the numbering used for stock solutions of virus and coat proteins. (See MATERIALS & METHODS).

mM EDTA, pH 8.0 and then treated like CCMV and BMV. Proteins of CCMV, BMV and SBMV lacking the N-terminal arm, were obtained by trypsin treatment and checked with SDS-PAGE as reported earlier (Vriend et al., 1981). A schematic representation of the plant viruses and the various aggregation states of their proteins is shown in Figure 1. The numbers in this figure correspond to the following 4 mg/ml stock solutions:

- 1) TMV virions in 50 mM sodium acetate/150 mM NaCl, pH 5.0 and in 50 mM potassium phosphate/150 mM NaCl, pH 7.0,
- 2) TMV protein in 50 mM sodium acetate/150 mM NaCl, pH 5.0, mainly

helix-form (De Wit et al., 1978; 1979),

3) TMV protein in 50 mM potassium phosphate/150 mM NaCl, pH 7.0, mainly disk-form (De Wit et al., 1978; 1979),

4) TMV protein in 50 mM Tris-HCl/150 mM NaCl, pH 9.0, mainly oligomers (De Wit et al., 1978; 1979),

5) CCMV, SBMV or BMV virions in 50 mM sodium acetate/150 mM NaCl, pH 5.0 and in 50 mM potassium phosphate/150 mM NaCl, pH 7.0,

6) empty capsids of CCMV, SBMV or BMV protein in 50 mM sodium acetate/200 mM NaCl, pH 5.0,

7) dimers of CCMV, SBMV or BMV protein in 50 mM Tris-HCl/200 mM NaCl, pH 7.5,

8) empty capsids of CCMV, SBMV or BMV protein lacking the N-terminal arm in 50 mM sodium acetate/200 mM NaCl, pH 5.0,

9) dimers of CCMV, SBMV, or BMV protein lacking the N-terminal arm in 50 mM Tris-HCl/200 mM NaCl, pH 7.5.

Coat protein stock solutions were kept at 4°C and used within 7 days after preparation.

(c) Samples for turbidity measurements at 550 nm and electron microscopy. The samples for turbidity measurements at 550 nm were prepared by adding 250 μ l virus or protein stock solution to 750 μ l vesicle stock suspension in the same buffer. The final concentration of lipid was 4 mg/ml buffer and of the virus or coat protein 1 mg/ml buffer. During a 24 h period the 1-ml samples were incubated at 18°C. The samples were measured at one-hour intervals. For each turbidity measurement the samples were transferred to a quartz cuvet. After incubation for turbidity measurements at 550 nm aliquots of the mixed samples were taken for electron microscopy.

(d) Samples for ^{31}P NMR. A unilamellar DLPC vesicle solution (5.33 mg lipid/ml) was prepared in 10 mM Tris-HCl/150 mM NaCl/1 mM EDTA, pH 9.0 by sonication in two 15-ml portions as described in section (a). Titanium particles of the sonicator and residual multilamellar vesicles were removed by centrifugation. (10,000g, 15 min). The

supernatants were mixed resulting in a single homogeneous clear unimellar DLPC vesicle suspension of 30 ml. One 15-ml fraction was incubated with 5 ml TMV protein stock solution number 4 for 24 h at 18°C and the other 15-ml fraction was incubated with 5 ml of identical buffer as reference. Before measurement samples were concentrated by ultracentrifugation (250,000g, 1 h), and resuspended in 10 % (v/v) $^2\text{H}_2\text{O}$ containing 10 mM Tris-HCl/150 mM NaCl/1mM EDTA buffer, pH 9.0 (final volume 2 ml) and treated as indicated in Figure 5.

Absorption measurements. The turbidity of the samples was measured in a Kontron Uvikon 810 spectrophotometer at 550 nm to avoid contributions of absorption of viral material or lipids. Turbidities at 550 nm of identical control vesicle suspensions not exposed to viral material (in all cases less than 0.10) and of viral material were subtracted if necessary.

Determination of the amount of protein associated with membranes after incubation. After the 24-h period of incubation of the vesicle suspensions with protein, the aggregated, fused and multilamellar bilayers together with associated protein were pelleted by centrifugation (8,800g, 10 min). The fraction of residual, unassociated protein in the supernatant was calculated from the protein contribution at 280 nm in the UV spectrum using an extinction coefficient at 280 nm = $1.27 \text{ ml.mg}^{-1}.\text{cm}^{-1}$ for TMV, CCMV and BMV protein and $1.30 \text{ ml.mg}^{-1}.\text{cm}^{-1}$ for SBMV protein. This fraction was subtracted from the 1 mg protein initially added to obtain the complementary fraction of membrane associated protein presented in Table I.

Electron microscopy. Electron micrographs were taken with a Zeiss EM 109 electron microscope equipped with a trans fibre photography camera. The samples were negatively stained with a 2 % solution of uranyl acetate in double-distilled water.

Phosphorus magnetic resonance spectroscopy. The ^{31}P NMR spectra of the DLPC vesicle suspension after 24 h incubation with TMV protein were obtained with a Bruker CXP 300 Fourier Transform spectrometer

operating at a frequency of 121.48 MHz. The spectra were taken in the presence of broadband proton decoupling (20W/12dB) using a sweepwidth of 25,000 Hz and a 16 μ s 45° pulse with a repetition rate of 1 s.

RESULTS

Turbidity measurements and determination of protein associated with membranes. The effect of addition of plant viruses and their coat proteins to neutral and charged SUVs under various conditions was monitored by turbidity measurements at 550 nm. In addition the percentage of protein present in the pellet was determined after centrifugation of the samples.

(a) Effect of intact virions. Addition of TMV or CCMV to positively charged SUVs at pH 5 and 7 increased the turbidity, but not in the case of neutral or negatively charged SUVs (Figure 2A,B,E,F). The turbidity increase for CCMV-lipid mixtures was stronger at pH 7 than at 5. In all cases addition of BMV or SBMV had only a small effect on the turbidity (Figure 2C,D,G,H). Pellets of positively charged SUVs obtained after incubation with TMV at pH 5 and 7 contained all the protein initially added. Pellets of positively charged SUVs obtained after incubation with SBMV at pH 7 and with CCMV at pH 5 and 7 contained approximately 20, 20 and 60 % of the protein, respectively. In all other pellets no protein was detected within experimental error (Table I).

(b) Effect of the proteins. Addition of TMV protein at pH 5, 7 (Figure 2I,M) and 9 (data not shown) to positively charged SUVs increased the turbidity rapidly. No increase of turbidity was found with negatively charged SUVs. Neutral SUVs caused a much slower increase of the turbidity as compared to the positively charged SUVs. The turbidity 24 h after incubation increased as a function of pH from

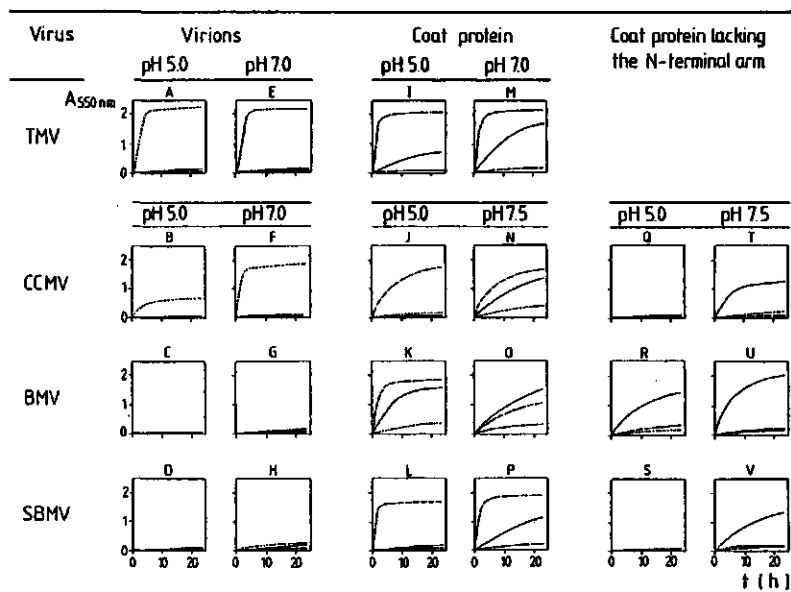


Figure 2. Turbidity of suspensions (final lipid concentration 4 mg/ml) of neutral vesicles (100% DLPC: solid line), positively charged vesicles (80/20 w/w DLPC/CTAB or DLPC/ PALCHOL: dotted line) and negatively charged vesicles (80/20 w/w DLPC/DLPA or DLPC/DMPG: dashed line) after addition of virions (A-H), protein (I-P) and protein lacking the N-terminal arm (Q-V) of TMV (first row: A,E,I,M), CCMV (second row: B,F,J,N,Q,T), BMV (third row: C,G,K,O,R,U) and SBMV (fourth row: D,H,L,P,S,V) as illustrated in Figure 1. All experiments were carried out at 18°C and the same buffer as for vesicle stock suspensions was used for viral particle or protein stock solutions. A,I) pH 5.0 in 50 mM sodium acetate/150 mM NaCl buffer, B,C,D,J, K,L,Q,R,S) pH 5.0 in 50 mM sodium acetate/200 mM NaCl buffer E,F,G,H,M) pH 7.0 in 50 mM potassium phosphate/150 mM NaCl buffer, N,O,P,T,U,V) pH 7.5 in 50 mM Tris-HCl/200 mM NaCl buffer.

5 to 9. Only in pellets of positively charged SUVs obtained after incubation with TMV protein, all the initially added coat protein was found (Table I).

Addition of CCMV, BMV and SBMV protein at pH 5 and 7.5 to positively charged SUVs had no significant effect on the turbidity

Table I. Percentage of Coat Protein Associated with Membranes^a.

Virus	Membrane Charge	Virions		Coat Protein	
		pH 5	pH 7	pH 5	pH 7
TMV	Positive	****	****	****	****
	Neutral
	Negative

Virus	Membrane Charge	Virions		Coat Protein		Coat Protein Lacking the N-terminal Arm	
		pH 5	pH 7	pH 5	pH 7.5	pH 5	pH 7.5
CCMV	Positive	*	***
	Neutral
	Negative	.	.	***	***	.	.
BMV	Positive
	Neutral
	Negative	.	.	****	*	.	.
SBMV	Positive	.	*
	Neutral
	Negative	.	.	****	***	.	.

^a pellets were obtained by centrifugation (8,800g, 10min) of the samples of Figure 2 after 24 h of incubation: . = 0-12%, * = 12-25%, ** = 25-50%, *** = 50-75% and **** = 75-100%. For CCMV and SBMV coat protein the values of DLPA are presented.

(Figure 2J,K,L,N,O,P). For negatively charged SUVs the addition of these proteins increased the turbidity (Figure 2J,K,L,N,O,P) and also protein was found in the pellets: $55 \pm 10\%$ for CCMV at pH 5.0 and

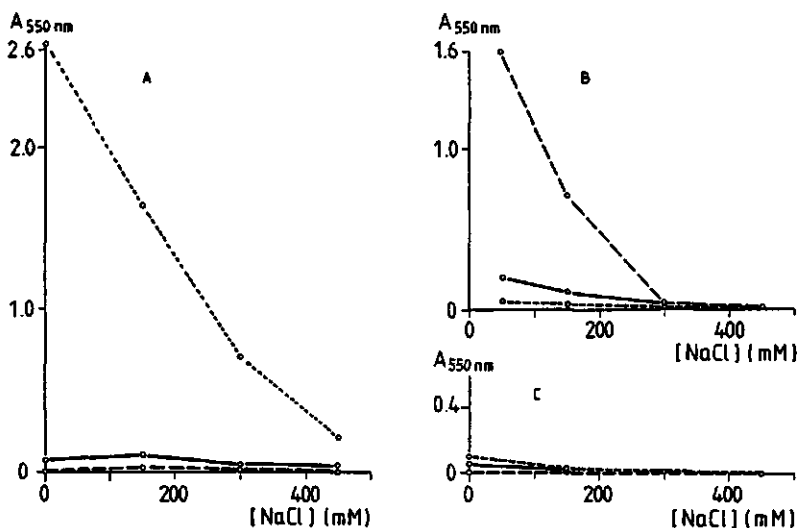


Figure 3. Turbidity of suspensions (final lipid concentration 4 mg/ml) of neutral vesicles (100% DLPC: solid line), positively charged vesicles (80/20 w/w DLPC/PALCHOL: dotted line) and negatively charged vesicles (80/20 w/w DLPC/DLPA: dashed line) 30 min after addition of A) TMV protein in 50 mM potassium phosphate, pH 9.0, B) CCMV protein in 50 mM Tris-HCl, pH 7.5 and C) CCMV protein lacking the N-terminal arm in 50 mM Tris-HCl, pH 7.5 as function of NaCl concentration.

7.5, $85 \pm 10\%$ for BMV and SBMV at pH 5, $20 \pm 10\%$ for BMV at pH 7.5 and $55 \pm 10\%$ for SBMV at pH 7.5 (Table I). The addition of CCMV, BMV and SBMV protein increased the turbidity of neutral SUVs at pH 7.5 (Figure 2N,O,P) and also at pH 5 for BMV protein (Figure 2K). However, no protein was found in pellets of neutral SUVs (Table I).

(c) Effect of proteins lacking the N-terminal arm. After removal of the N-terminal arm of the CCMV, BMV and SBMV protein no significant changes in turbidity were observed with positively and negatively charged SUVs at pH 5 and 7.5 (Figure 2Q-V). The turbidity changes found for neutral SUVs after incubation with intact CCMV, BMV and SBMV protein were preserved with the cleaved proteins. Also cleaved protein



Figure 4. Electron micrographs showing typical shape of unilamellar vesicles after 24 h of incubation of the DLPC/DLPA (80/20 w/w) vesicles (A) and of multilayer structures in pellet after 24 h of incubation of the DLPC/DLPA (80/20 w/w) vesicles with empty capsids of BMV protein in 50 mM sodium acetate/ 200 mM NaCl buffer, pH 5.0 (B).

was not bound (Table I).

Salt concentration dependence of turbidity induced by proteins. The turbidity of the SUV suspensions was measured as a function of NaCl concentration 30 min after addition of TMV protein (Figure 3A), of CCMV protein (Figure 3B) and of CCMV protein lacking the N-terminal arm (Figure 3C). The turbidity reduced with increasing salt concentration. This effect was most clear for positively charged SUVs incubated with TMV protein (Figure 3A) and for negatively charged SUVs incubated with CCMV protein (Figure 3B).

Electron microscopy. After turbidity measurements electron micrographs were taken of the samples. In Figure 4A a typical electron micrograph

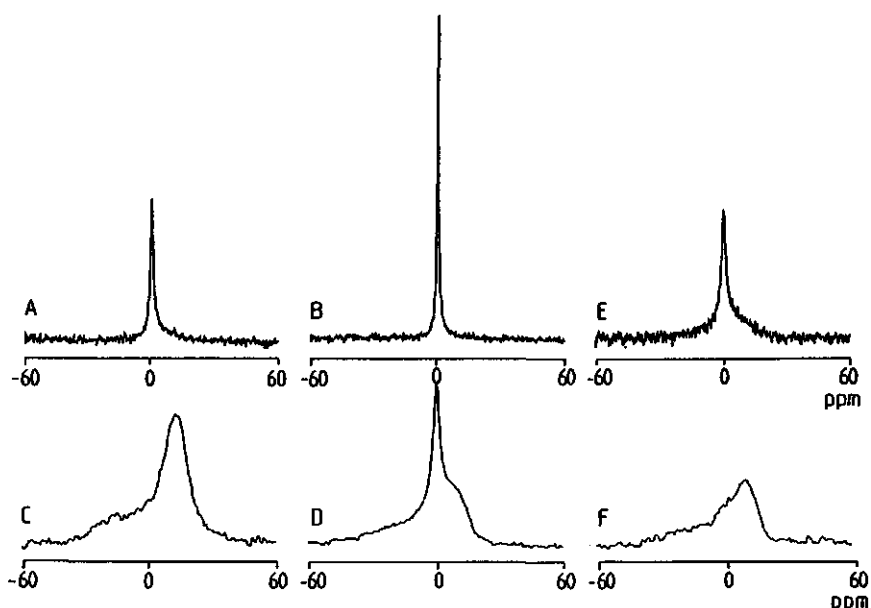


Figure 5. 121.48 MHz ^{31}P NMR spectra of a suspension of DLPC SUVs in 10 mM Tris-HCl/150 mM NaCl/1 mM EDTA buffer, pH 9.0 after 24 h of incubation at 18°C without viral material (A) and (B) sample of (A) after 1 min of sonication; (C) as (A) with TMV protein and (D) sample of (C) after 1 min of sonication; (E) supernatant (8,800g, 10 min) and (F) pellet (8,800g, 10 min) of sample (D). In all cases the number of scans was 1,000 and broadband proton decoupling (20 W/12 dB) was applied. For spectra in (A), (B) and (E) an artificial line broadening of 10 Hz and in (C), (D) and (F) of 100 Hz was used.

of a reference sample of negatively charged SUVs after 24 h of incubation is shown. The diameter of the SUVs ranges from 30 to 100 nm. Identical vesicle sizes were observed for other reference vesicles (data not shown). After 24 h of incubation of negatively charged SUVs with empty capsids of BMV protein at pH 5 (Figure 4B) multilamellar aggregates were formed.

Typical multilayer structures as in Figures 4B were observed in all electron micrographs (data not shown) taken of samples of which the turbidity at 550 nm had increased to values higher than 1 at the end

of the 24 h incubation period after addition of TMV protein or CCMV, BMV or SBMV protein with or without N-terminal arm (Figure 2I-V).

Phosphorus NMR measurements. Figure 5 shows ^{31}P NMR spectra obtained of DLPC SUVs after 24 h of incubation at 18°C with and without TMV protein. The spectrum of the reference SUVs is characterized by one isotropic peak with a linewidth at half height, $\Delta\nu_{1/2}$, of 190 Hz (Figure 5A). After 1 min of sonication $\Delta\nu_{1/2}$ decreased to 70 Hz (Figure 5B). An identical sample incubated for 24 h with TMV coat protein gave a typical powder spectrum characteristic for bilayers with a CSA of ca. 30 ppm (Figure 5C). No peaks were visible that could arise from the presence of rapidly tumbling phospholipid molecules (Burnell et al., 1980) or H_{II} phase lipids (Van Echteld et al., 1982). After 1 min sonication of this sample an isotropic peak with a relative intensity of approximately 20 % was seen (Figure 5D). This peak could be separated from the underlying powder spectrum by centrifugation (8,800g, 10 min). This resulted in an isotropic peak with a $\Delta\nu_{1/2}$ of 370 Hz of the supernatant (Figure 5E) and a powder spectrum of the pellet (Figure 5F) with a CSA of ca. 30 ppm, similar to Figure 5C.

DISCUSSION

The turbidity measurements of neutral and charged SUVs interacting with intact plant viruses or their coat proteins indicated:

(a) Electrostatic interaction. The virus particle or protein contains charged amino acid residues, which interact with oppositely charged membranes. As a consequence, several vesicles are crosslinked. Also charges at the membrane are neutralized, causing aggregation, vesicle fusion and formation of multilayer structures. The precipitated material contains viral coat protein;

(b) Indirect hydrophobic interaction. Dissociated protein causes neu-

tral vesicles to fuse and to form multilayer structures. The precipitated material does not contain protein. As will be discussed later, this effect is caused by exposed hydrophobic protein domains.

For the interactions the following evidence was presented:

1. Rod-shaped TMV. Positively charged vesicles interact with TMV particles at pH 5 and 7 (Figure 2A,E). The same is observed for its coat protein, both in helix and disk conformation (Figure 2I,M) and as oligomers at pH 9 (data not shown). The pellet contains all coat protein (Table I) whereas multilamellar vesicles are formed (Figure 4B). Several arguments suggest that electrostatic forces dominate in the formation of these pellets: (a) The pI of TMV particles is 3.5 (Fraenkel-Conrat & Nariba, 1958). This implies that the virus surface has an overall negative charge at the experimental pH values; (b) Negatively charged SUVs do not interact with TMV and its protein; (c) A reduction of protein-vesicle interaction by high salt concentration is observed by the turbidity measurements at 550 nm as function of salt concentration (Figure 3A).

TMV protein with its hydrophobic areas exposed to the bulk solvent (Bloomer et al., 1978) causes the neutral SUVs to fuse after aggregation (Figure 2I,M). This result agrees with those of Banerjee et al. (1981a,b). In this case no protein is detectable in the pellet. (Table I). This effect parallels the increasing exposure of hydrophobic domains of TMV protein at higher pH values.

An increase in turbidity at 550 nm can only be interpreted as an increase in size of the aggregates. Thus on the basis of turbidity measurements, no discrimination between aggregation, fusion or transformation to multilayer structures can be made. Also, spontaneous aggregation of DLPC SUVs after preparation by sonication was reported (De Kruijff et al., 1976), which was observed as a broadening of the ^{31}P NMR signal. Therefore, ^{31}P NMR spectra were recorded and EM micrographs were taken. After 24 h of incubation of the reference DLPC SUVs the increased linewidth (190 Hz) of the ^{31}P NMR resonance indica-

tes aggregation of the SUVs (Figure 5A,B). The electron micrograph of the reference vesicles after 24 h of incubation shows that no transformation to multilayer structures has occurred (Figure 4A). However, after 24 h of incubation with TMV protein, the ^{31}P NMR spectrum indicates that the majority of the vesicles (minimally ca. 80 %) has become multilamellar (Figure 5F). The rest (maximally ca. 20 %) is aggregated since it appears as a relatively sharp isotropic peak after brief sonication (Figure 5D). These results are in accordance with the multilayer structures observed in electron micrographs of the same samples (data not shown). Formation of multilamellar vesicles implies that fusion of vesicles has taken place.

2. Spherical plant viruses (CCMV, BMV, SBMV). In analogy to TMV, CCMV particles interact with positively charged vesicles (Figure 2B,F), which is explained by the pI value of 3.6 (Bancroft et al., 1971). As a result of the electrostatic interaction the pellets of these samples contain protein at pH 5 (ca. 20 %) and 7 (ca. 60 %, Table I), values at which an increasing number of negatively charged groups per viral particle is present. CCMV protein has an N-terminal arm of twenty-five amino acid residues of which nine residues are basic. This arm, also of coat protein molecules in empty capsids, is known to bind to negatively charged macromolecules in solution (Bancroft, 1971; Vriend et al., 1986). Therefore, binding to negatively charged vesicles is not surprising (Figure 2J,N). Binding is lost after removal of the N-terminal arm by trypsin (Figure 2Q,T).

Dissociated CCMV protein, with and without the N-terminal arm, induces fusion of neutral SUVs and formation of multilayers (Figure 2N,T). This is analogous to the effect of TMV protein on neutral vesicles (Figure 2I,M).

BMV and SBMV have a pI value of 6.8 (Magdolf-Fairchild, 1967) and 6.0 (Rice & Horst, 1972), respectively. These viruses do not interact with SUVs, regardless of their surface charge. SBMV is an exception giving a small electrostatic effect at pH 7, if added to positively

charged SUVs (Figure 2C,D,G,H). This binding, which was also demonstrated by Abdel-Salam et al. (1982) in 0.1 M Tris-HCl, pH 7.5, could be due to the swollen state of SBMV. The near neutral pI values of BMV and SBMV are also reflected in the absence of protein association to positive SUVs (Table I). BMV and SBMV protein, either as capsids or as dimers, interact with negatively charged SUVs (Figure 2K,L,O,P) because of the presence of their basic N-terminal arms. This interaction is lost after removal of the arm (Figure 2R,S,U,V).

Both BMV and SBMV protein dimers induce fusion of neutral SUVs (Figure 2O,P) and this inductive capacity is completely preserved after cleavage of the N-terminal arms (Figure 2U,V). Also BMV empty capsids with and without the N-terminal arm react with neutral SUVs by indirect hydrophobic interaction (Figure 2K,R). This can be attributed to the strong hydrophobic character of BMV protein (Pfeiffer & Hirth, 1974). Again the induction of vesicle fusion increases with increasing hydrophobicity of the protein.

The nature of the interaction between model membranes and several plant viruses and their coat proteins. In the discussion of the results, electrostatic interaction was found to be quite different from induction of vesicle fusion by indirect hydrophobic interaction.

The electrostatic interactions are reduced to zero at high salt concentration (Figure 3). Therefore there is no indication of hydrophobic interaction in the formed complex, i.e. between hydrophobic protein domains and the bilayer interior. Thus the protein is likely to be associated to the headgroups of the bilayers. This process is analogous to that found for aggregation and fusion of negatively charged SUVs by polycations, such as polylysine (Gad et al., 1982; 1985) and polyhistidine (Wang & Huang, 1984; Uster & Deamer, 1985).

Induction of vesicle fusion and formation of multilayers by

indirect hydrophobic interaction is observed only for neutral vesicles. Neutral SUVs aggregate spontaneously (De Kruijff et al., 1976). This is observed in the ^{31}P NMR spectrum (Figure 5A) as a broadening of the isotropic resonance. Brief sonication reverses this aggregation (Figure 5B). Vesicle fusion and further formation of multilamellar structures is inhibited by interfacial water between the apposed bilayer surfaces of two aggregated vesicles (Le Neveu et al., 1976; Papahadjopoulos et al., 1978). A possible mechanism for the indirect hydrophobic interaction is that the hydrophobic sites at the proteins in the solution remove this hydration water, enabling direct molecular contacts of the bilayers and concomittant fusion according to the general theory of vesicle fusion (Wilschut & Hoekstra, 1986). The proposed effect of the protein can be visualized as a pushing out of the interfacial water resulting in a partial dehydration of the bilayer surface. This process is slow, since it requires a collision of the protein with already apposed bilayer surfaces. The protein itself is not inserted in the bilayer, nor does it form a complex with the lipids. Also the protein does not pass through the membrane during the fusion process, since otherwise it would have been locked in the fused vesicles and have appeared in the final multilayer precipitate. The action of the protein may be compared to that of a catalyst in a chemical reaction, enhancing only the rate of fusion between the bilayers.

Since the coat protein is not found associated with the vesicles in the case of hydrophobic interaction (Table I) this implies that the hydrophobic protein domains do not interact directly with the hydrophobic interior of the bilayers.

From these observations it is concluded that, regardless of the type of interaction (hydrophobic, electrostatic), viral coat protein is not incorporated in the bilayer, i.e. by forming a stable complex held together by direct hydrophobic lipid-protein interactions.

Implications of the observed interactions for earlier proposed models of initial interactions between virus and cell. A stable lipid-coat protein complex in which direct hydrophobic forces dominate was not found for any of the viruses and bilayers that were investigated. This strongly disagrees with the model of virus penetration and uncoating proposed by Durham (1978), which we therefore consider incorrect.

Caspar (1963) suggested that the hydrophobic environment of the bilayer interior causes uncoating of TMV RNA in vivo. Although this mechanism of uncoating cannot be excluded rigorously, it is very unlikely on the basis of our results. From Figure 2A-H it is clear that viral particles can interact with the head groups of lipids in the bilayer only by electrostatic interaction, which results in coat protein associated to the outside of the bilayer. In the final complex also no direct hydrophobic forces are involved (Figure 3). Therefore the uncoating process is definitely not initiated and probably also not propagated by hydrophobic lipid-coat protein forces, replacing the hydrophobic intersubunit forces in the virus particle.

Contrary to the suggested uncoating effect of the hydrophobic domain of the bilayer on the virus (Caspar, 1963), for which no information is available from our experiments that focused on the effect of virus-membrane interactions on the membranes, a destabilizing effect of the hydrophobic domains of the viral coat proteins on the membrane has been observed. This suggests that in vivo the virus particle could induce membrane fusion by exposing its hydrophobic protein domains. This could possibly be a mechanism for the virus to enter the cell.

ACKNOWLEDGEMENTS

We thank B. de Kruijff, J.W. Roenhorst, T.J. Schaafsma and J. Wilschut for valuable discussions and critical reading of the

manuscript, C.J.A.M. Wolfs and H.R. Bloksma for help with the preparation of plant virus material and J. Groenewegen for help with electron microscopy.

REFERENCES

- Abdel-Salam, A., White, J.A., & Sehgal, O.P. (1982) Phytopath. Z. **105**, 336-334.
- Bancroft, J.B. (1971) Adv. Virus Res. **16**, 99-134.
- Banerjee, S., Vandenbranden, M., & Ruyschaert, J.M. (1981a) Biochim. Biophys. Acta **646**, 360-364.
- Banerjee, S., Vandenbranden, M., & Ruyschaert, J.M. (1981b) FEBS Lett. **133**, 221-224.
- Bloomer, A.C., Champness, J.N., Bricogne, G., Staden, R., & Klug, A. (1978) Nature (London) **276**, 362-368.
- Burnell, E.E., Cullis, P.R., & De Kruijff, B. (1980) Biochim. Biophys. Acta **603**, 63-69.
- Caspar, D.L.D. (1963) Adv. Protein Chem. **18**, 87-121.
- De Kruijff, B., Cullis, P.R., & Radda, G.K. (1976) Biochim. Biophys. Acta **436**, 729-740.
- De Wit, J.L., Hemminga, M.A., & Schaafsma, T.J. (1978) J. Magn. Res. **31**, 97-107.
- De Wit, J.L., Alma, N.C.M., Hemminga, M.A., & Schaafsma, T.J. (1979) Biochemistry **18**, 3973-3976.
- De Zoeten, G.A. (1981) in Plant Diseases and Vectors (Maramorosch, K. & Harris, K.F., Eds.) pp. 221-239, Academic Press, New York, N.Y.
- Durham, A.C.H., Hendry, D.A., & Von Wechmar, M.B. (1977) Virology **77**, 524-533.
- Durham, A.C.H. (1978) Biomedicine **28**, 307-314.
- Fraenkel-Conrat, H., & Nariba, X. (1958) in Symposium on Protein Structure (Neuberger, A., Ed.) pp. 249, Methuen, London.
- Gaard, G., & De Zoeten, G.A. (1979) Virology **96**, 21-31.
- Gad, A.E., Sliver, B.L., Eytan, G.D. (1982) Biochim. Biophys. Acta **690**, 124-132.
- Gad, A.E., Bental, M., Elyashir, G., & Weinberg, H. (1985) Biochemistry **24**, 6277-6282.
- Hull, R., & Maule, A.J. (1985) in The Viruses (Francki, R.I.B., Ed.) pp. 83-115, Plenum Press, New York, N.Y.
- Kiho, Y., & Shimomura, T. (1976) Japan J. Microbiol. **20**, 537-541.
- Kiho, Y., Shimomura, T., Abe, T., & Nozu, Y. (1979a) Microbiol. Immunol. **23**, 735-748.
- Kiho, Y., Abe, T., & Ohashi, Y. (1979b) Microbiol. Immunol. **23**,

1067-1076.

- Kiho, Y., & Abe, T. (1980) Microbiol. Immunol. 24, 617-628.
- Leberman, R. (1966) Virology 30, 341-347.
- Le Neveu, D.M., Rand, R.P., & Parsegian, V.A. (1976) Nature (London) 259, 601-603.
- Magdolf-Fairchild, B.S. (1967) Virology 31, 142-143.
- Marvin, D.A. & Wachtel, E.J. (1975) Nature (London) 253, 19-23.
- Papahadjopoulos, D., Portis Jr., A., & Pangborn, W. (1978) Ann. N.Y. Acad. Sci 308, 50.
- Pfeiffer, P., & Hirth, L. (1974) Virology 58, 362-368.
- Rice, R.H., & Horst, J. (1972) Virology 49, 602-604.
- Shaw, J.G., Plaskitt, K.A., & Wilson, T.M.A. (1986), Virology 148, 326-336.
- Uster, P.S., & Deamer, D.W. (1985) Biochemistry 24, 1-8.
- Van Echteld, C.J.A., De Kruijff, B., Verkley, A.J., Leunissen-Bijvelt, J., & De Gier, J. (1982) Biochim. Biophys. Acta 692, 126-138.
- Van Lent, J.W.M., & Verduin, B.J.M. (1985) Neth. J. Pl. Path. 91, 205-13.
- Verduin, B.J.M. (1974) FEBS Lett. 45, 50-54.
- Verduin, B.J.M. (1978) J. gen. Virol. 39, 131-147.
- Vriend, G., Hemminga, M.A., Verduin, B.J.M., De Wit, J.L., & Schaafsma, T.J. (1981) FEBS Lett. 134, 167-171.
- Vriend, G., Hemminga, M.A., & Verduin, B.J.M. (1986) J. Mol. Biol. 191, 453-460.
- Watts, W.J., Dawson, J.R.O., & King, J.M. (1981) CIBA Foundation Symposium 80 pp. 56-71.
- Watts, J.W., & King, J.M. (1984) J. gen. Virol. 65, 1709-1712.
- Wang, C.-Y., & Huang, L. (1984) Biochemistry 23, 4409-4416.
- Willschut, J., & Hoekstra, D. (1986) Chem. Phys. Lipids, in press.
- Wilson, T.M.A. (1984) Virology 137, 255-265.
- Wilson, T.M.A. (1985) J. gen. Virol. 66, 1201-1207.

CHAPTER 3

EFFECT OF THE MEMBRANE ON BACTERIO- PHAGE M13 COAT PROTEIN

3.1 TIME-RESOLVED TRYPTOPHAN FLUORESCENCE ANISOTROPY INVESTIGATION OF BACTERIOPHAGE M13 COAT PROTEIN IN MICELLES AND MIXED BILAYERS

Klaas P. Datema, Antonie J.W.G. Visser, Arie van Hoek
Cor J.A.M. Wolfs, Ruud B. Spruijt and Marcus A. Hemminga

ABSTRACT: Coat protein of bacteriophage M13 is examined in micelles and vesicles by time-resolved tryptophan fluorescence and anisotropy decay measurements and circular dichroism experiments. Circular dichroism indicates that the coat protein has α -helix (60%) and β -structure (28%) in 700 mM SDS micelles and predominantly β -structure (94%) in mixed dimyristoyl phosphatidylcholine/dimyristoyl phosphatidic acid (80/20 w/w) small unilamellar vesicles. The fluorescence decay at 344 nm of the single tryptophan in the coat protein after excitation at 295 or 300 nm is a triple exponential. In the micelles the anisotropy decay is a double exponential. A short, temperature independent correlation time of 0.5 ± 0.2 ns reflects a rapid depolarization process within the coat protein. The overall rotation of the coat protein-detergent complex is observed in the decay as a longer correlation time of 9.8 ± 0.5 ns (at 20°C) and has a temperature dependence that satisfies the Stokes-Einstein relation. In vesicles at all lipid to protein molar ratios in the range from 20 to 410 the calculated order parameter is constant with a value of 0.7 ± 0.1 from 10 to 40°C, although the lipids undergo the gel to liquid-crystalline phase transition. The longer correlation time decreases gradually on increasing temperature. This effect probably arises from an increasing segmental mobility within the coat protein. The results are consistent with a model in which the coat protein has a β -structure and the tryptophan indole rings do not experience the motion of the lipids in the bilayer because of protein-protein aggregation.

The interaction of membrane proteins with lipids has received considerable attention in the last decade. The interest in understanding this interaction arises from the notion that lipid composition and dynamics in membranes affect the properties of its proteins. A variety of biophysical techniques has already been applied to membrane proteins

reconstituted in model membranes (for a survey see: Watts & De Pont, 1985). Model membranes can easily be prepared and are free of the complexity of the natural membrane. In particular, time-resolved fluorescence anisotropy measurements (for a review see: Cundall & Dale, 1983; Beechem & Brand, 1985) and nuclear magnetic resonance (NMR) provide complementary information about motion and order of lipids in bilayer systems (for a comparison see: Wolber & Hudson, 1982; Deveaux & Seigneuret, 1985).

The objective of our research is to study the infection mechanism of non-enveloped viruses, like bacteriophage M13 (Hemminga, 1987) and plant viruses (Hemminga et al., 1985), at a molecular level. A suitable system to study the interaction of viral coat proteins with membranes is the M13-Escherichia coli system.

The major (gene-8 product) M13 coat protein is present in the long rodlike virus particle in numerous copies and functions as protection for its single strand DNA. The virus enters E. coli by leaving the coat proteins in the cytoplasmic membrane (Marvin & Wachtel, 1975). After infection and DNA duplication the newly synthesized procoats, a precursor form of the coat protein with a typical bacterial amino terminal leader peptide of 23 residues, also assemble in this membrane. After penetration of the N-terminus of the procoat through the membrane, the procoat is cleaved to mature coat protein by a leader peptidase (Geller & Wickner, 1985). Both progeny as well as parental coat protein are used for the membrane-bound assembly of new M13 particles (Wickner, 1976). The viral DNA is complexed with these coat proteins without lysis of the host cell.

The coat protein consists of 50 amino acid residues (M=5240): a basic C-terminus, a hydrophobic central core of 19 amino acid residues and an acidic N-terminus (Van Asbeck et al., 1969; Nakashima & Konigsberg, 1974). It contains a single tryptophan residue located at the 26th position, i.e. in the hydrophobic region. The tryptophan can be used as an intrinsic fluorescent marker.

Time-resolved fluorescence anisotropy analysis of fluorophores in membranes (for a theoretical description see for example: Kinoshita et al., 1977; 1982; Zannoni et al., 1983; Szabo, 1984; Van der Meer et al., 1984) has several features which make the technique particularly attractive for studying the M13 coat protein in model membranes. First, the time-dependent anisotropy provides a direct, real-time measurement of the reorientational dynamics of the coat protein in the (sub)nanosecond time range. The measurable range is limited by the average fluorescence lifetime characterizing the tryptophan. Second, in time-resolved fluorescence anisotropy analysis motional rates and molecular order manifest themselves separately, which is advantageous for bilayer studies.

We have reconstituted the coat protein of M13 in micelles and mixed SUVs. Time-resolved fluorescence and fluorescence anisotropy measurements of the single tryptophan residue in the coat protein were carried out at various temperatures and protein contents. In addition CD spectra were taken of the coat protein in these micelles and bilayers to determine the secondary structure of the coat protein. Time-resolved fluorescence and fluorescence anisotropies were analysed in terms of multi-exponential functions, giving information about dynamics of the coat protein tryptophan and the structure of its environs in these systems. In SUVs an additional residual anisotropy is present, which is directly related to the order of the coat protein tryptophan. The temperature dependence of the correlation times and of the order of the coat protein in the membrane was determined in the range in which the lipid bilayer undergoes the gel to liquid-crystalline phase transition.

MATERIALS AND METHODS

Materials. DMPC (1,2-dimyristoyl-sn-glycero-3-phosphocholine, 99% pu-

rity) and DMPA (1,2-dimyristoyl-sn-glycero-3-phosphatidic acid, 98% purity) were obtained from Sigma Chemical Co. and used without further purification.

M13 bacteriophage was purified as described by Garssen et al. (1977). The major (gene-8 product) coat protein of M13 was isolated by the method of Knippers and Hoffmann-Berling (1966).

Sample preparation. Micelles were prepared by dissolving coat protein in 0.8, 4, 100 or 700 mM SDS, 10 mM potassium phosphate, pH 5.0. A clear, micellar solution was obtained by vortexing and heating the sample to 55°C. The samples were diluted with the same buffers to $OD_{280nm} = 0.1$.

Vesicles were prepared by cholate dialysis, as described by Hagen et al. (1978) with a few modifications. Stock suspensions of DMPC and DMPA vesicles (both 50 mg/ml) and coat protein (8 mg/ml) in 5.0 mM Tris-HCl buffer, pH 8.0 with 2 w% sodium cholate, 8.0 M urea, 0.1 mM EDTA and 20 mM ammonium sulphate were used. 0.16 ml of DMPC stock suspension, 0.04 ml of DMPA stock suspension and 0.500, 0.250, 0.125, 0.063, 0.031, 0.016 or 0 ml coat protein stock solution were coadded with 0.300, 0.550, 0.675, 0.737, 0.769, 0.784 or 0.800 ml of the same buffer, respectively. Clear and homogeneous suspensions were obtained by vortexing and heating the samples to 55°C. Subsequently, the suspensions were dialysed at 4°C against 4 times 1.5 L of 10 mM Tris-HCl, pH 8.0, 0.2 mM EDTA and 10 v/v% methanol during 48 h with changes at 12, 24 and 36 h. In the last dialysis step no methanol was added to the buffer. This results in opalescent dispersions of unilamellar vesicles. All the samples were sonicated under nitrogen with a Branson cell disruptor B30 (duty cycle: 90%, power setting 4 (max. 350 W at setting 10)) to obtain SUVs. The SUV suspensions were centrifuged (8,800g, 10 min) to precipitate unincorporated, water-insoluble coat protein. At this point, aliquots of the samples were taken to determine the protein and phospholipid concentration (Bartlett, 1959; Peterson, 1977), from which the L/P ratio was calculated. This proce-

dure results in samples of L/P ratios of 20, 30, 70, 140, 210, 410 or ∞ , respectively. The error in these ratios was less than 10%. The samples were homogeneous as tested by sucrose gradient centrifugation. Before measurement the samples were diluted to $OD_{280nm} = 0.1$.

Methods. CD spectra were recorded at room temperature on a Jobin-Yvon Auto-Dichrograph Mark V in the wavelength range 250 - 190 nm. A sample cell of 1-mm path length was used. The spectra are the average of four scans taken from the same sample. To determine the secondary structure the CD spectra were fitted to reference spectra of Greenfield and Fasman (1969) by a least squares fitting procedure using spectral points in the 250 to 190 nm range with 5-nm steps. The basis for this analysis has been described (Cantor & Schimmel, 1980).

The experimental setup for the time-resolved fluorescence measurements has been described previously (Van Hoek et al., 1983; Van Hoek & Visser, 1985; Visser et al., 1985). The excitation wavelengths were 295 and 300 nm. The emission wavelength was selected with an interference filter transmitting at 344 nm with a 10-nm bandpass. Fluorescence was detected by time-correlated single-photon counting (O'Connor & Phillips, 1984).

The total fluorescence decay is determined from the measured polarized fluorescence components parallel, I_{\parallel} , and perpendicular, I_{\perp} , to the electric vector of the excitation as:

$$S(t) = I_{\parallel}(t) + 2I_{\perp}(t) \quad (1)$$

in which $S(t)$ is the convolution product of the (unconvoluted) total fluorescence, $s(t)$, and the excitation pulse response, $P(t)$. The data were analysed as a sum of three exponentials, i.e.

$$s(t) = \sum_{i=1}^3 \alpha_i \exp(-t/\tau_i) \quad (2)$$

in which τ_1 is the fluorescence lifetime with a pre-exponential factor, a_1 , indicating the relative contribution of τ_1 to the initial intensity of the total decay. The experimental data were corrected for background fluorescence measured for identical vesicles without coat protein (in all cases less than 10% of the fluorescence of the sample with coat protein). From these data the lifetimes and relative contributions to the total decay are obtained by a non-linear least squares fitting procedure (Vos et al., 1987).

The fluorescence anisotropy, $r(t)$, is given by:

$$r(t) = [I_{\parallel}(t) - I_{\perp}(t)] / [I_{\parallel}(t) + 2I_{\perp}(t)] \quad (3)$$

in which $I_{\parallel}(t)$ and $I_{\perp}(t)$ are the (deconvoluted) parallel and perpendicular polarized components derived from the experimental $I_{\parallel}(t)$ and $I_{\perp}(t)$ components. $r(t)$ is obtained by fitting the experimental $I_{\parallel}(t)$ and $I_{\perp}(t)$ decays directly to the anisotropy-containing expressions for these two fluorescence components with the use of one set of parameters (Gilbert, 1983; Cross & Fleming, 1984) using Fortran-77 programs (Vos et al., 1987). The model for anisotropy decay analysis consisted of a sum of two exponentials for the coat protein in micelles and of a sum of two exponentials and a constant term for the coat protein in SUVs. In the analysis it is assumed that every lifetime component is coupled to every rotational component (Dale et al., 1977). The quality of the fit is determined by (1) visual inspection, (2) the weighted residuals, (3) the number of zero passages of the auto-correlation function (Ameloot & Hendrickx, 1982), (4) the reduced chi-square value, (5) the Durbin-Watson parameter (O'Connor & Phillips, 1984) and (6) the standard deviations. The standard deviations of the fitted parameters are estimated from the Hessian as described by Bevington (1969), which is one of the output parameters of the Fortran-77 programs.

The orientational order parameter, S , for the coat protein in the

bilayer is calculated from the residual, $r(\infty)$, and the initial, $r(0)$, anisotropies by

$$S = [r(\infty)/r(0)]^{1/2} \quad (4)$$

as given by Heyn (1979) and Jaehnig (1979). For $r(0)$ the average of the series of measurements at each excitation wavelength was used (Table IV).

RESULTS

Circular dichroism. The CD spectrum of M13 coat protein in micelles is shown in Figure 1. Analysis of the spectrum yields 60% α -helix, 28% β -structure and 12% other structure for the coat protein in 700 mM SDS micelles. Below the CMC (which is at 3 mM, Helenius et al., 1979) at 0.8 mM SDS 16 % α -helix, 64% β -structure and 20% other structure was determined (data not shown). The CD spectrum of M13 coat protein in mixed SUVs of DMPC/DMPA (20/80 w/w) at L/P ratio of 25 was best simulated by 2% α -helix, 94% β -structure and 4% other structure (Figure 1). The same CD spectra were observed for the other L/P molar ratios (data not shown).

Time-resolved fluorescence of M13 coat protein in micelles. The total fluorescence decay at 344 nm of M13 coat protein in micelles after excitation at 295 nm was fitted as a triple exponential function (an example of a triple exponential fit, for the decay of M13 coat protein in mixed SUVs, is shown in Figure 4). The lifetimes that characterize the total fluorescence decays of the M13 coat protein-SDS complexes and their relative contributions to the total decay are listed in Table I. In 700 mM SDS the shortest lifetime, τ_1 , and all the amplitudes are independent of temperature. However, τ_2 and τ_3 decrease at increasing temperature (Table I). Below the CMC (3 mM) all

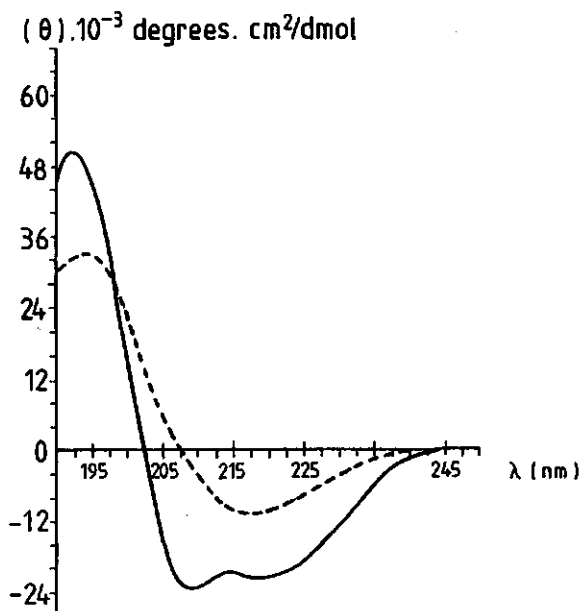


Figure 1. CD spectra of M13 coat protein at 20°C in 700 mM SDS micelles (solid line) and mixed SUVs of DMPC/DMPA (80/20 w/w) at L/P ratio of 25 (dashed line). Mean residue ellipticities are shown.

lifetimes increase, while α_2 , and possibly α_1 , increase at the expense of α_3 .

The fluorescence anisotropy decay was fitted as a double exponential function. In Figure 2 the anisotropy decay at 344 nm of M13 coat protein in 700 mM SDS micelles at 20°C is given. The correlation times and their amplitudes are listed in Table II for various SDS concentrations and temperatures. The short correlation time, ϕ_1 (0.5 ± 0.2 ns), is independent of both the SDS concentration and temperature. The longer correlation time, ϕ_2 , depends on the SDS concentration as well as temperature. The value of ϕ_2 , which is significantly longer below the CMC (3 mM), decreases as a function of temperature (Figure 3). The

Table I. Fluorescence Decay Parameters (344 nm) of the Single Tryptophan of Bacteriophage M13 Coat Protein in SDS Micelles for Excitation at 295 nm ^a.

SDS	T	α_1	τ_1	α_2	τ_2	α_3	τ_3	$\langle\tau\rangle$
		$\pm .05$	$\pm .1$	$\pm .05$	$\pm .1$	$\pm .05$	$\pm .1$	
(mM)	(°C)		(ns)		(ns)		(ns)	(ns)
0.8	20	.30	1.2	.62	3.7	.08	7.5	4.1
4	20	.18	.9	.52	3.1	.30	5.8	4.4
100	20	.23	.3	.30	2.3	.46	5.5	4.7
700	20	.22	.3	.29	2.5	.49	5.7	5.0
700	25	.23	.3	.29	2.5	.47	5.6	4.8
700	30	.27	.3	.28	2.3	.46	5.3	4.6
700	35	.19	.3	.27	2.0	.54	4.9	4.4
700	40	.17	.3	.27	1.8	.56	4.6	4.1

$$^a \langle\tau\rangle = \frac{\sum_{i=1}^3 \alpha_i \tau_i^2}{\sum_{i=1}^3 \alpha_i \tau_i}$$

product, $kT\Phi_2/\eta$, in which η is the viscosity of pure water, is given in Table II and found to be constant within experimental error (10%).

Time-resolved fluorescence of M13 coat protein in vesicles. The lifetimes and their pre-exponential factors in the range of 10 to 40°C are listed in Table III. In Figure 4 the decay after excitation at 295 nm is shown. Similar values as given in Figure 4 were also found for

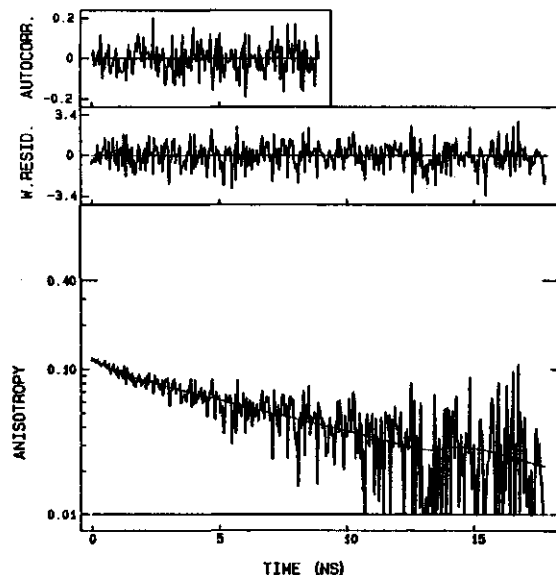


Figure 2. Anisotropy decay at 344 nm of the single tryptophan of bacteriophage M13 coat protein in 700 mM SDS micelles at 20°C after excitation at 295 nm and the best computer fit. The parameters describing the best fit to the experimental decay and the estimated standard deviations are: $\beta_1 = 0.06 \pm 0.014$, $\beta_2 = 0.11 \pm 0.004$; $\phi_1 = 0.50 \pm 0.21$ ns, $\phi_2 = 9.76 \pm 0.51$ ns with the Durbin-Watson parameter = 1.95 and the number of zero passages in the parallel channel = 97 and in the perpendicular channel = 96 (429 channels, 42 ps/channel). The weighted residuals from experimental and fitted curve and the auto-correlation function are given in the top of the figure.

the other L/P ratios from 20 to 410 at 20°C (data not shown).

The fluorescence anisotropy in SUVs was fitted as a double exponential with a constant value ($r(\infty)$). In Figure 5 the anisotropy decays of M13 coat protein in SUVs after excitation at 295 and 300 nm are shown. Table IV summarizes the results at various temperatures. The initial anisotropy, $r(0)$, is 0.16 after 295 nm and 0.23 after 300 nm

Table II. Anisotropy Decay Parameters (344 nm) of the Single Tryptophan of Bacteriophage M13 Coat Protein in SDS Micelles for Excitation at 295 nm ^a.

SDS (mM)	T (°C)	β_1 ±.01	ϕ_1 (ns)	β_2 ±.01	ϕ_2 ±.5 (ns)	r(0) ±.02	V .10 ⁻³ (cm ³)
0.8	20	.06	.5	.09	16.2	.15	
4	20	.07	.5	.10	10.2	.17	24
100	20	.05	.5	.10	9.6	.15	23
700	20	.06	.5	.11	9.8	.17	23
700	25	.06	.5	.11	9.1	.16	25
700	30	.04	.5	.11	7.6	.15	24
700	35	.05	.5	.10	6.9	.15	25
700	40	.05	.5	.09	6.1	.14	24

^a β_1 is the contribution to the initial anisotropy, r(0), of the depolarization mechanism characterized by ϕ_1 ; V, the volume of the protein-micelle complex was calculated with the Stokes-Einstein relation for spherical rotation, $\phi_2 = \eta V/kT$ in which η is the viscosity of water, T the temperature and k the Boltzmann constant.

excitation and in both cases independent of temperature (Table IV). The relative contribution of β_1 to the total anisotropy decay, i.e. $\beta_1/r(0)$, is 19% at 295 nm and 26 % at 300 nm excitation. For other L/P ratios in the range of 20 to 410 at 20°C similar results are found

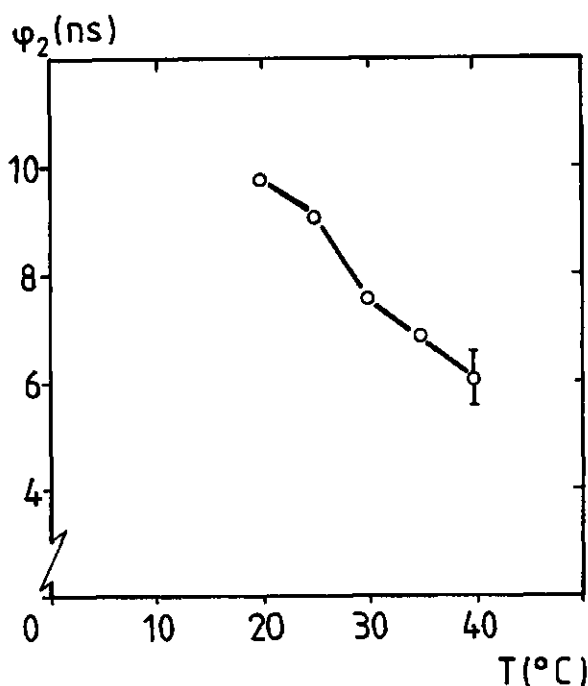


Figure 3. Temperature dependence of the longer correlation time, ϕ_2 , of M13 coat protein in 700 mM SDS obtained from the best computer fits. For experimental details see Table II and the text.

(data not shown). The short correlation time, ϕ_1 , was found to be nearly temperature independent (0.5 ± 0.2 ns). Therefore ϕ_1 was fixed at 0.5 ns in the final computer fitting. The longer correlation time, ϕ_2 , decreases at increasing temperature (Figure 6).

The order parameter, S , calculated from eq. (4), is almost constant (0.7 ± 0.1) at all temperatures at 295 (Figure 6) and 300 nm excitation (Table IV).

DISCUSSION

Table III. Fluorescence Decay Parameters (344 nm) of the Single Tryptophan of Bacteriophage M13 Coat Protein-DMPC/DMPA (80/20 w/w) SUVs at L/P molar ratio 70 ^a.

$\lambda_{exc.}$ (nm)	T (°C)	α_1 $\pm .02$	τ_1 $\pm .1$ (ns)	α_2 $\pm .02$	τ_2 $\pm .1$ (ns)	α_3 $\pm .02$	τ_3 $\pm .1$ (ns)	$\langle \tau \rangle$ (ns)
295	10	.20	.6	.47	2.1	.33	5.7	4.3
	15	.26	.8	.42	2.2	.33	5.5	4.2
	20	.25	.8	.44	2.2	.31	5.5	4.1
	25	.24	.9	.41	2.1	.35	5.1	3.9
	30	.17	.7	.46	1.8	.37	4.8	3.7
	35	.13	.6	.49	1.7	.38	4.7	3.6
	40	.15	.7	.46	1.7	.39	4.5	3.5
300	20	.22	.3	.40	2.2	.38	5.8	4.7
	25	.14	.3	.46	2.2	.40	5.6	4.5
	30	.24	.8	.38	2.3	.38	5.5	4.3
	35	.26	.8	.40	2.4	.34	5.5	4.2
	40	.22	.3	.45	2.0	.33	5.2	4.0

$$^a \langle \tau \rangle = \frac{\sum_{i=1}^3 \alpha_i \tau_i^2}{\sum_{i=1}^3 \alpha_i \tau_i}$$

Micelles

In SDS micelles M13 coat protein forms a dimer (Tanford & Reynolds,

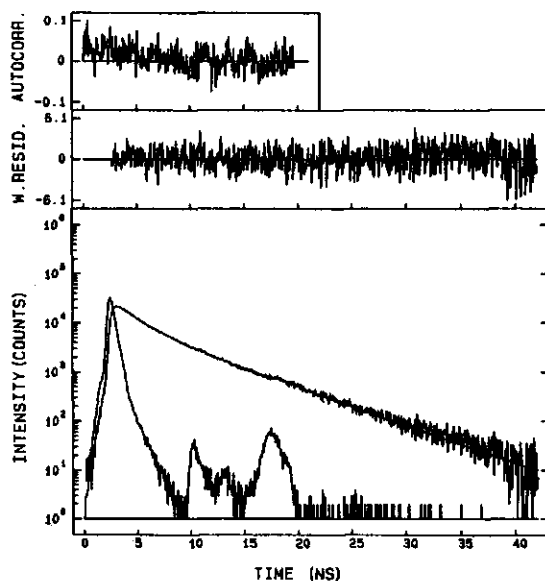


Figure 4. Fluorescence decay at 344 nm of the single tryptophan of bacteriophage M13 coat protein-DMPC/DMPA (80/20 w/w) SUVs of L/P ratio = 70 at 20°C, the best computer fit and the excitation pulse (295 nm). The parameters describing the best fit to the experimental decay and the estimated standard deviations are: $\alpha_1 = 0.25 \pm 0.02$, $\alpha_2 = 0.44 \pm 0.02$, $\alpha_3 = 0.31 \pm 0.01$; $\tau_1 = 0.8 \pm 0.1$ ns, $\tau_2 = 2.2 \pm 0.1$ ns, $\tau_3 = 5.5 \pm 0.1$ ns with the Durbin-Watson parameter = 1.82 and the number of zero passages = 202 (959 channels, 41 ps/channel). The weighted residuals from experimental and fitted curve and the auto-correlation function are given in the top of the figure.

1976). The secondary structure of the coat protein in the SDS micelles is partly α -helix (60%) and partly β -structure (28%, Figure 1). This observation agrees with those previously reported (Nozaki et al., 1976; 1978; Chamberlain et al., 1978). Below the CMC (3 mM) the amount of β -structure increases to 64% at the expense of α -helix (16%). Under the-

Table IV. Anisotropy Decay Parameters (344 nm) of the Single Tryptophan of Bacteriophage M13 Coat Protein-DMPC/DMPA (80/20 w/w) SUVs at L/P molar ratio 70 ^a.

$\lambda_{exc.}$ (nm)	T (°C)	β_1 $\pm .01$	ϕ_1 (ns)	β_2 $\pm .01$	ϕ_2 ± 2 (ns)	$r(\infty)$ $\pm .01$	$r(0)$	S $\pm .09$
295	10	.03	.5	.04	10	.09	.16	0.75
	15	.03	.5	.04	9	.09	.16	0.75
	20	.03	.5	.04	8	.09	.16	0.75
	25	.03	.5	.05	8	.08	.16	0.71
	30	.03	.5	.05	6	.08	.16	0.71
	35	.03	.5	.05	6	.08	.16	0.71
	40	.03	.5	.05	5	.08	.16	0.71
$\langle r(0) \rangle = .16 \pm .005$								
300	20	.06	.5	.07	8	.10	.23	0.66
	25	.06	.5	.09	7	.09	.24	0.60
	30	.06	.5	.08	6	.09	.23	0.63
	35	.06	.5	.08	6	.09	.23	0.63
	40	.06	.5	.07	5	.09	.23	0.64
$\langle r(0) \rangle = .23 \pm .005$								

^a β_1 is the contribution to the initial anisotropy, $r(0)$, of the dipolarization mechanism characterized by ϕ_1 .

se conditions the coat protein is solubilized by SDS molecules. The higher amount of β -structure in the coat protein is probably due to

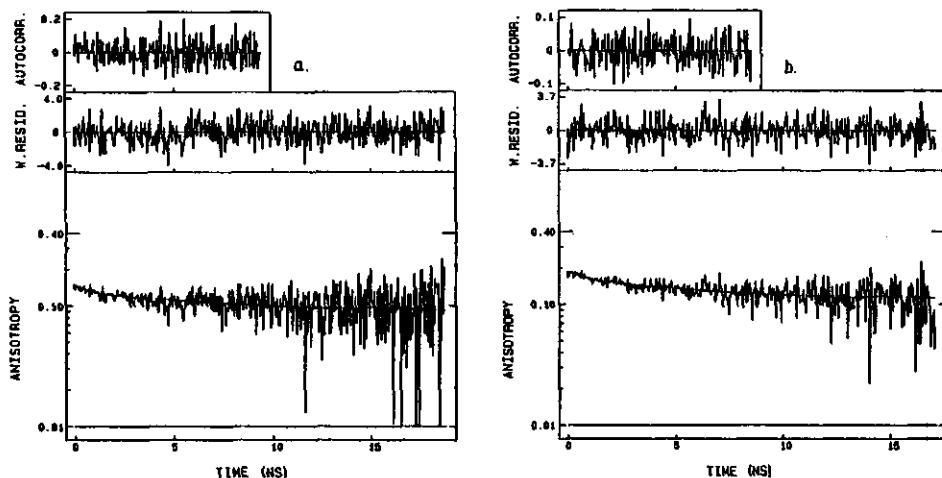


Figure 5. Anisotropy decays at 344 nm of the single tryptophan of bacteriophage M13 coat protein-DMPC/DMPA (80/20 w/w) SUVs of L/P ratio = 70 at 20°C and the best computer fits after excitation at 295 (a) and 300 nm (b). The parameters describing the best fit to the experimental decay and the estimated standard deviations are, for (a): $\beta_1 = 0.03 \pm 0.006$, $\beta_2 = 0.04 \pm 0.006$, $r(\infty) = 0.09 \pm 0.007$; $\phi_1 = 0.5$ ns, $\phi_2 = 8 \pm 2$ ns with the Durbin-Watson parameter = 1.87 and the number of zero passages in the parallel channel = 98 and in the perpendicular channel = 118 (460 channels, 41 ps/channel), for (b): $\beta_1 = 0.06 \pm 0.007$, $\beta_2 = 0.07 \pm 0.010$, $r(\infty) = 0.10 \pm 0.010$; $\phi_1 = 0.5$ ns, $\phi_2 = 8 \pm 2$ ns with the Durbin-Watson parameter = 1.84 and the number of zero passages in the parallel channel = 84 and in the perpendicular channel = 97 (432 channels, 41 ps/channel). Only the initial parts of the anisotropy decays (of totally 1024 channels) are shown. The weighted residuals from the experimental and fitted curves and the auto-correlation functions are given in the top of the figures.

the formation of larger aggregates as seen from the fluorescence anisotropy decay (to be discussed below). These aggregates could be simi-

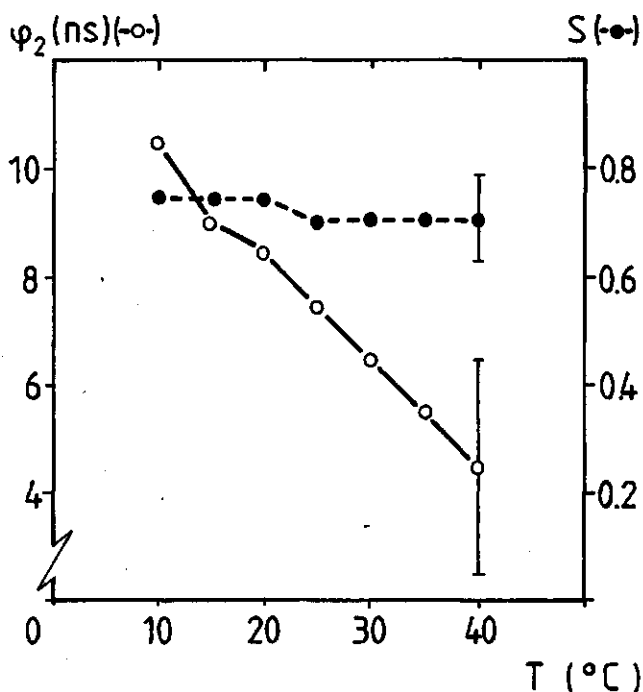


Figure 6. Temperature dependence of the longer correlation time, ϕ_2 (open circles), and order parameter, S (closed circles), of M13 coat protein in mixed SUVs of DMPC/DMPA (80/20 w/w) at L/P ratio of 70. For experimental details see Table IV and the text.

lar to the coat protein polymer observed in vesicles in which also β -structure is dominant (94%), consistent with the work of Nozaki et al. (1978).

For all total fluorescence decays of the tryptophan in M13 coat protein three lifetimes were required to obtain a satisfactory fit according to the criteria listed under Methods. This is in agreement with previously reported multi-exponential decays for other single tryptophan proteins (Grinvald & Steinberg, 1976; Munro et al., 1979). The origin for this lies in the complex photophysics of the tryptophan residue which is partly caused by the presence of different conformers

(Szabo & Rayner, 1980; Chang et al., 1983; Petrich et al., 1983). We suggest that in a similar way in the M13 coat protein different conformers give rise to different lifetimes. These conformers arise from different average orientations of the tryptophan indole ring with respect to the neighbouring amide and carboxyl groups along the backbone of the coat protein.

Below the CMC the fluorescence of the coat protein aggregate, solubilized by detergent molecules, is also triply exponential, but the lifetimes are significantly longer than for the coat protein in micelles. However, α_2 increases at the expense of α_3 . This indicates that in the solubilized coat protein conformation (64% β -structure as determined by CD, Figure 1) the quenching of the tryptophan fluorescence is more efficient, presumably due to changes in orientation of neighbouring amide and carbonyl groups with respect to the indole ring.

The long wavelength absorption band of the indole ring consists of two electronic transitions, 1L_a and 1L_b . The dipole moments of these transitions are almost perpendicular to each other. By excitation at 295 nm both energy levels become populated (Weber, 1960; Valeur & Weber, 1977). Between these levels energy transfer can occur easily on a subnanosecond time scale (Cross et al., 1983). Nevertheless, it cannot be excluded that energy transfer between these two states provides an additional mechanism for the multi-exponential decay of the fluorescence.

The fluorescence anisotropy is doubly exponential. The longer correlation time is assigned to the overall rotation of the coat protein-micelle complex for the following reasons. First, this correlation time is temperature dependent (Figure 3). The constancy of $kT\phi_2/\eta$ (= V, see Table II) indicates that the motion, which is characterized by ϕ_2 satisfies the Stokes-Einstein relation for isotropic rotational diffusion in solution. Second, below the CMC, i.e. under conditions in which coat protein is solubilized by detergent molecules and no micel-

les are formed, ϕ_2 increases as a result of the formation of larger coat protein-detergent aggregates. The average overall rotation of these complexes is therefore described by ϕ_2 .

Above the CMC the volume of the protein-micelle complex, V , can be used to obtain a rough estimate of the number of SDS molecules in these micelles, n . Using $V = 2M_p(v_p+h) + nM_{SDS}(v_{SDS}+h)$ in which v is the partial specific volume ($v_p = 0.74 \text{ cm}^3/\text{g}$, Cantor & Schimmel, 1980; $v_{SDS} = 0.87 \text{ cm}^3/\text{g}$, Tanford et al., 1974) and h the degree of hydration of the protein-micelle complex ($\sim 0.2 \text{ cm}^3/\text{g}$), it is calculated that n amounts to ca. 57. In this calculation two coat protein molecules per SDS micelle are assumed (Tanford & Reynolds, 1976). This value agrees very well with a previously determined ratio of 60 SDS molecules per coat protein dimer from independent measurements (Makino et al., 1975).

The shorter correlation time (0.5 ns) is independent of temperature and SDS concentration. This means that ϕ_1 characterizes a rapid, temperature-independent depolarization process within the coat protein. The mechanism, which is also present in the fluorescence anisotropy decay of coat protein in vesicles, will be discussed below.

Vesicles

In the samples of SUVs prepared by cholate dialysis the protein is dominantly in β -structure conformation (Figure 1) independent of the L/P ratio. The β -structure has been observed before by CD of M13 coat protein in model membranes (Nozaki et al., 1976;1978; Chamberlain et al., 1978). However, in the phage the structure is known to be entirely α -helix (Nozaki et al., 1976; Opella et al., 1987). This has been explained as a reflection of a major conformational change in the coat protein structure during the membrane-bound assembly of the phage (Nozaki et al., 1976).

For the triple exponential fluorescence decay of tryptophan in M13 coat protein in vesicles comparable lifetimes are found as in micelles, although the amplitude of the second lifetime, α_2 , has increased significantly at the expense of α_3 . This was also observed for solubilized coat protein in detergent solution below the CMC. The conformational change towards dominantly β -structure (94%, Figure 1) of M13 coat protein probably gives rise to a more efficient quenching process, determined by τ_2 . The constancy of the fluorescence decay as a function of L/P ratio indicates that the coat protein conformation in vesicles that favours more efficient quenching is formed independently of L/P ratio. The fact that the fluorescence decays of coat protein in SUVs and detergent solution below the CMC are both dominated by τ_2 , strongly suggests that the micro-environment of tryptophan is identical in both aggregation states of the coat protein.

The initial anisotropy, $r(0)$, of the coat protein in vesicles depends on the wavelength of excitation, 0.16 (295 nm) and 0.23 (300 nm), in agreement with previous measurements on other proteins (Lakowicz et al., 1983). From the initial and residual anisotropy the order parameter of the tryptophan in the M13 coat protein is calculated to be 0.7 ± 0.1 (at 295 and 300 nm excitation) at all L/P ratios and temperatures measured. The fluorescence anisotropy does not decay to zero since the vesicle rotation is too slow on the nanosecond time scale to contribute to the decay, in contrast to the micellar rotation (ϕ_2 in Table II). The gel to liquid-crystalline phase transition of the lipid mixture DMPC/DMPA (80/20 w/w) was determined to be completed at 26°C (unpublished results), which is 2 degrees above the phase transition of pure DMPC. Thus, it appears from the fluorescence results that the M13 coat protein is not sensitive to the phase transition and the rapid motions of lipids in the liquid-crystalline phase. This suggests that the majority of the indole rings do not experience the lipid motion because of aggregation of the coat protein. The constancy of the order parameter is in agreement with deuterium NMR measurements of

the amide sites along the M13 coat protein backbone in similar mixed bilayers, which show that the lipid motions do not affect the order of the amide deuterons along the coat protein backbone (chapter 3.2). For other single transmembrane proteins that do not aggregate, it has been found that the deuterium NMR order parameter reflects the gel to liquid-crystalline phase transition of the lipids (Pauls et al., 1985; Datema et al., 1986). For M13 coat protein it is therefore concluded that the protein in the bilayer is in an aggregated state. The concept of such protein aggregates is not in contradiction with the rigid protein structure proposed by Wolber and Hudson (1982).

Steady-state fluorescence studies of M13 coat protein in DMPC vesicles with parinaric acid have shown that the fluorescence of the tryptophan of the coat protein is quenched by radiationless energy transfer to the probe lipid (Kimelman et al., 1979). Extensive protein-protein aggregation was excluded in that paper. This is not consistent with our findings. However, it should be noted that, in a protein aggregate, quenching is still possible by inter-tryptophan energy transfer and subsequent energy trapping by the lipid acceptor.

The correlation times ϕ_1 and ϕ_2 indicate an internal tryptophan flexibility within the coat protein aggregate. The larger correlation time, ϕ_2 , is most likely related to segmental mobility of the coat protein within the aggregate. The shorter, temperature independent correlation time (0.5 ns), could arise from internal motion of the tryptophan indole ring, but also from energy transfer from one indole ring to another in the aggregate, as demonstrated for aromatic dimers in solid solution (Visser et al., 1983).

In aggregated coat protein the tryptophan rings are positioned close to each other, i.e. halfway along the peptide in the hydrophobic region. If ϕ_1 is caused by energy transfer between two nearby indole rings, then the contribution of β_1 would decrease if the excitation wavelength is shifted to the red-edge of the light absorption spectrum (Weber, 1960; Weber & Shinitzky, 1970). On the other hand, in the case

of rapid indole ring motion no such dependence is expected for β_1 . Therefore the anisotropy was measured also for 300 nm excitation. Since the relative contribution of β_1 increases if the excitation wavelength is changed from 295 to 300 nm, this observation suggests that ϕ_1 arises from rapid motion of the tryptophan ring in the coat protein.

ACKNOWLEDGEMENTS

We thank dr. B.J.M. Harmsen for providing facilities to grow E. coli and K. Vos for an introduction to the software for fluorescence data analysis.

REFERENCES

- Ameloot, M., & Hendrickx, H. (1982) J. Chem. Phys. **76**, 4419-4432.
Bartlett, G.R. (1959) J. Biol. Chem. **234**, 466-468.
Bevington, P.R. (1969) Data Reduction and Error Analysis for the Physical Sciences, McGraw-Hill, New York, NY.
Bechem, J.M., & Brand, L. (1985) Ann. Rev. Biochem. **54**, 43-71.
Cantor, C.R., & Schimmel, P.R. (1980) Biophysical Chemistry, Freeman, W.H., San Francisco
Chamberlain, B.K., Nozaki, Y., Tanford, C., & Webster, R.E. (1978) Biochim. Biophys. Acta **510**, 18-37.
Chang, M.C., Petrich, J.W., McDonald, D.B., & Fleming, G.R. (1983) J. Am. Chem. Soc. **105**, 3819-3824.
Cross, A.J., Waldeck, D.H., & Fleming, G.R. (1983) J. Chem. Phys. **78**, 6455-6467
Cross, A.J. & Fleming, G.R. (1984) Biophys. J. **46**, 45-56.
Cundall, R.B., & Dale, R.E., Eds. (1983) Time-Resolved Fluorescence Spectroscopy in Biochemistry and Biology, Plenum Press, New York, NY.
Dale, R.E., Chen, L.A., & Brand, L. (1977) J. Biol. Chem. **252**, 7500-75.
Datema, K.P., Pauls, K.P., & Bloom, M. (1986) Biochemistry **25**, 3796-3803.
Devaux, P.F., & Seigneuret, M. (1985) Biochim. Biophys. Acta **822**,

63-125.

- Garssen, G.J., Hilbers, C.W., Schoenmaker, J.G.G., & Van Boom, J.H. (1977) Eur. J. Biochem. **81**, 453-463.
- Geller, B.L., & Wickner, W. (1985) J. Biol. Chem. **260**, 13281-13285.
- Gilbert, C.W. (1983) in Time-Resolved Fluorescence Spectroscopy in Biochemistry and Biology (Cundall, R.B., & Dale, R.E., Eds.), pp605-606, Plenum Press, New York.
- Greenfield, N. & Fasman, G.D. (1969) Biochemistry **8**, 4108-4116.
- Grinvald, A., & Steinberg, I.Z. (1976) Biochim. Biophys. Acta **427**, 663-678.
- Hagen, D.S., Weiner, J.H., & Sykes, B.D. (1978) Biochemistry **17**, 5860-5866.
- Helenius, A., McCaslin, D.R., Fries, E., & Tanford, C. (1979) Meth. Enzymology **63**, 734-749.
- Hemminga, M.A. (1987) J. Chem. Soc. Faraday Trans. 1, **83**, 203-209.
- Hemminga, M.A., Datema, K.P., Ten Kortenaar, P.W.B., Kruse, J., Vriend, G., Verduin, B.J.M., & Koole, P. (1985) in Magnetic Resonance in Biology and Medicine (Govil, G., Khatrapal, C.L., & Saran, A., Eds.) pp 53-76, Tata McGraw-Hill Publishing Company Ltd., New Delhi, India.
- Heyn, M. (1979) FEBS Lett. **108**, 359-364.
- Jaehnig, F. (1979) Proc. Natl. Acad. Sci. USA **76**, 6361-6365
- Kimelman, D., Tecoma, E.S., Wolber, P.K., Hudson, B.S., Wickner, W., & Simoni, R.D. (1979) Biochemistry **18**, 5874-5880.
- Kinosita, K., Jr., Kawato, S., & Ikegami, A. (1977) Biophys. J. **20**, 289-305.
- Kinosita, K., Jr., Ikegami, A., & Kawato, S. (1982) Biophys. J. **37**, 461-464.
- Knippers, R., & Hoffmann-Berling, H. (1966) J. Mol. Biol. **21**, 281-292.
- Lakowicz, J.R., Maliwal, B.P., Cherek, H., & Balter, A. (1983) Biochemistry **22**, 1741-1752.
- Makino, S., Woolford, J.L., Jr., Tanford, C., & Webster, R. (1975) J. Biol. Chem. **250**, 4327.
- Marvin, D.A., & Wachtel, E.J. (1975) Nature **253**, 19-23.
- Munro, I., Pecht, I., & Stryer, L. (1979) Proc. Natl. Acad. Sci. USA **76**, 56-60.
- Nakashima, Y., & Konigsberg, W. (1974) J. Mol. Biol. **88**, 598-600. Biophys., in press.
- Pauls, K.P., MacKay, A.L., Soederman, O., Bloom, M., Tanjea, A.K., & Hodges, R.S. (1985) Eur. Biophys. J. **12**, 1-11.
- Peterson, G.L. (1977) Anal. Biochem. **83**, 346-356.
- Petrich, J.W., Chang, M.C., McDonald, D.B., & Fleming, G.R. (1983) J. Am. Chem. Soc. **105**, 3824-3832.
- Szabo, A.G., & Rayner, D.M. (1980) J. Am. Chem. Soc. **102**, 554-563.
- Szabo, A. (1984) J. Chem. Phys. **81**, 150-167.
- Tanford, C., Nozaki, Y., Reynolds, J.A., & Makino, S. (1974) Biochemistry **13**, 2369-2376.

- Tanford, C., & Reynolds, J.A. (1976) Biochim. Biophys. Acta **457**, 133-170.
- Valeur, B., & Weber, G. (1977) Photochem. Photobiol. **25**, 441-444.
- Van Asbeck, F., Beyreuther, K., Koehler, H., Von Wettstein, G., & Braunitzer, G. (1969) Hoppe-Seyler's Z. Physiol. Chem. **350**, 1047-1066.
- Van der Meer, W., Pottel, H., Herreman, W., Ameloot, M., Hendrickx, H., & Schroeder, H. (1984) Biophys. J. **46**, 515-523.
- Van Hoek, A., Vervoort, J., & Visser, A.J.W.G. (1983) J. Biochem. Biophys. Methods **7**, 243-254.
- Van Hoek, A., & Visser, A.J.W.G. (1985) Anal. Instrum. (N.Y.) **14**, 359-378.
- Visser, A.J.W.G., Santema, J.S., & Van Hoek, A. (1983) Photobiochem. Photobiophys. **6**, 47-55.
- Visser, A.J.W.G., Ykema, T., Van Hoek, A., O'Kane, D.J., & Lee, J. (1985) Biochemistry **24**, 1489-1496.
- Vos, K., Van Hoek, A., & Visser, A.J.W.G. (1987) Eur. J. Biochem., in press.
- Watts, A., & Depont, J.J.H.M., Eds. (1985) Progress in Protein-Lipid Interactions, Elsevier Science Publishers, New York, NY.
- Weber, G. (1960) Biochem. J. **75**, 335-345.
- Weber, G. & Shinitzky, M. (1970) Proc. Natl. Acad. Sci. USA **65**, 823-830.
- Wickner, W. (1976) Proc. Natl. Acad. Sci. USA **73**, 1159-1163.
- Wolber, P.K., & Hudson, B.S. (1982) Biophys. J. **37**, 253-262.
- Zannoni, C., Arcioni, A., & Cavatorta, P. (1983) Chem. Phys. Lipids **32**, 179-250.

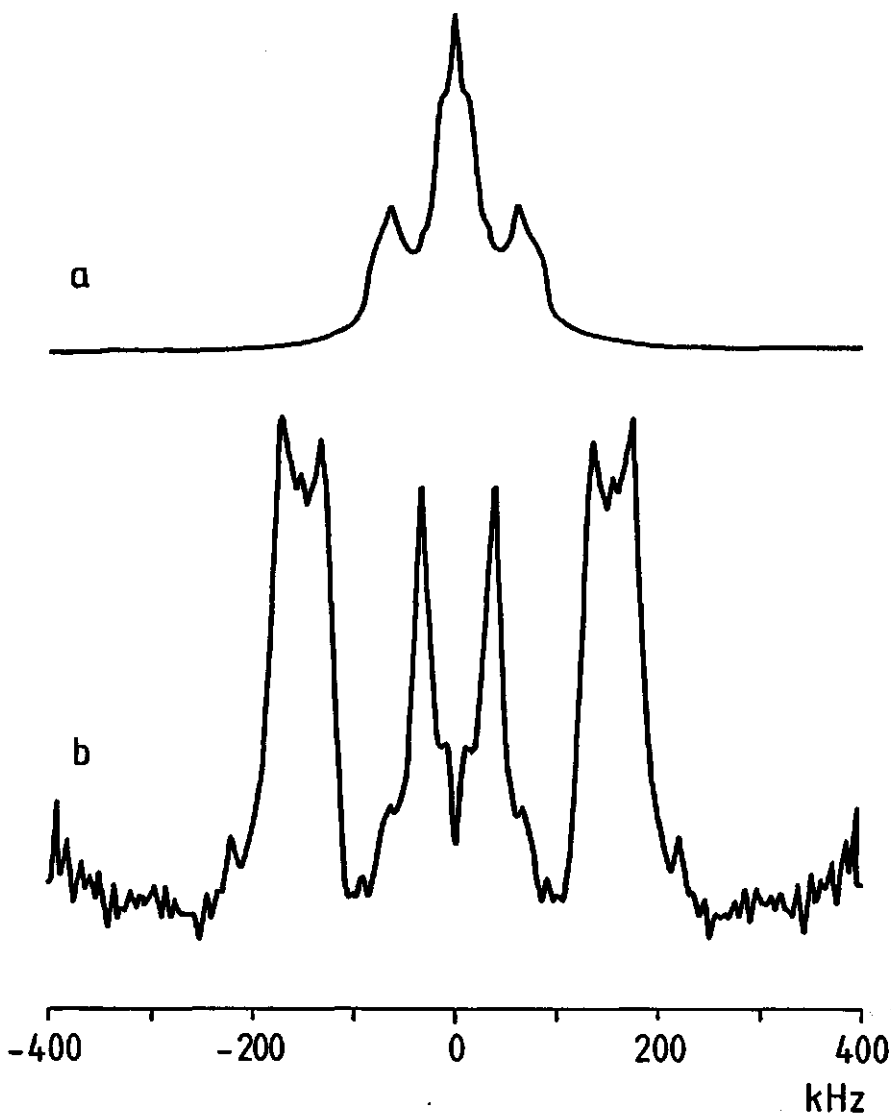
3.2 DYNAMIC PROPERTIES OF M13 COAT PROTEIN IN MIXED BILAYERS. A DEUTERIUM NMR STUDY OF EXCHANGEABLE PROTON SITES.

Klaas P. Datema, B. Jos H. van Boxtel and Marcus A. Hemminga

Bacteriophage M13 is a long rodlike nucleoprotein particle, consisting of a single strand of DNA protected by numerous copies of the major (gene 8 product) coat protein. The coat protein of M13 is small ($M=5240$) and contains 50 amino acid residues in its mature form: a basic C-terminus, a hydrophobic central core and an acidic N-terminus (1,2). The virus enters an *Escherichia coli* cell by leaving the coat proteins in the cytoplasmic membrane (3). After DNA duplication and synthesis of new coat proteins both progeny as well as parental coat proteins are stored as integral membrane protein (4). During membrane-bound assembly of new virus particles the viral DNA is complexed with these coat proteins without lysis of the host cell.

This note presents a deuterium nuclear magnetic resonance (^2H NMR) study of the exchangeable proton sites at the coat protein of M13 as a solid powder and incorporated into liposomes. It has been demonstrated that this type of experiments characterizes the dynamical properties of integral membrane proteins (5-7). The objective of this study is to obtain information about the motions of the coat protein in phospholipid bilayers, which is possibly of interest for the way in which virus infection takes place.

Fig. 1 presents the ^2H NMR powder spectrum of M13 coat protein deuterated by hydrogen exchange and the corresponding DePaked spectrum (12,13). The spectrum consists of a superposition of an asymmetric powder pattern with a quadrupolar splitting $\Delta\nu_q = 150$ kHz and an asymmetry parameter $\eta = 0.16$, a symmetric powder pattern with $\Delta\nu_q = 35$ kHz and $\eta = 0$ and a small isotropic central peak (2% of the total spectral



intensity). The spin-lattice relaxation (T_1) decay for solid M13 coat protein is complex. Two exponentials with time constants 50 and 830 ms are measured by the inversion recovery technique (7), belonging to the 35 kHz and the 150 kHz pattern, respectively, as determined from ana-

Figure 1. (a) 46.06 MHz ^2H NMR spectrum of hydrogen-exchange deuterated M13 coat protein as a solid powder at room temperature. The number of scans, $N_s = 25,343$, the relaxation delay, $T_r = 2$ s and the time between the 90° pulses of $3.4 \mu\text{s}$ in the quadrupolar echo, $\tau_2 = 35 \mu\text{s}$. Spectra were recorded on a Bruker CXP300 spectrometer. The center of the spectrum was set on resonance and a quadrupolar echo sequence is used (7,8). M13 bacteriophage was purified as described (9) and the major (gene 8 product) coat protein of M13 was isolated by the method of Knippers and Hoffmann-Berling (10). The exchangeable sites on M13 coat protein were deuterated by dissolving the protein in 10 mM sodium phosphate buffer, pH 12 in excess $^2\text{H}_2\text{O}$ at 45°C for one hour. Afterwards, the solvent was removed by overnight evaporation at reduced pressure. Circular dichroism spectra of aliquots of the protein in deoxycholate micelles were recorded before and after labelling as described (11) to ensure that the conformational change of the coat protein during deuteration at pH 12 was reversible. (b) DePaked spectrum derived from the solid M13 coat protein powder pattern of (a). Spectra were DePaked by a numerical procedure (12,13). DePakeing was continued until no difference was observed between two successive iterations. Therefore the DePaked spectrum is shown with the 12th iteration at the left side and 11th iteration at the right side in the oriented spectrum.

lysis of the relaxation in the frequency domain. The quadrupolar echo decay, however, is found to a single exponential with a spin-spin relaxation time (T_{2e}) of 200 μs .

The broad component with $\Delta\nu_q = 150$ kHz and $\eta = 0.16$ is assigned to the backbone amide groups. These values are typical for rigid amide deuterons, which are hydrogen bonded to oxygen atoms in crystalline solids (14). A similar 150 kHz powder pattern has been observed for other solid proteins, a synthetic polypeptide, $K_2\text{GL}_{24}K_2\text{A}$ -amide, (5) and gramicidin A' and S (6). Of these proteins the backbone deuterons are all hydrogen bonded in a rigid structure.

The narrow axially symmetric powder pattern with $\Delta\nu_q = 35$ kHz and $\eta = 0$ in Fig.1 is assigned to freely rotating N^2H_3 groups in the coat protein, i.e. the lysine side chains and the terminal N^2H_3 group. The same splitting has been observed for a lysine containing synthetic polypeptide (5,6). The intensity ratio of the 150 and 35 kHz component in the

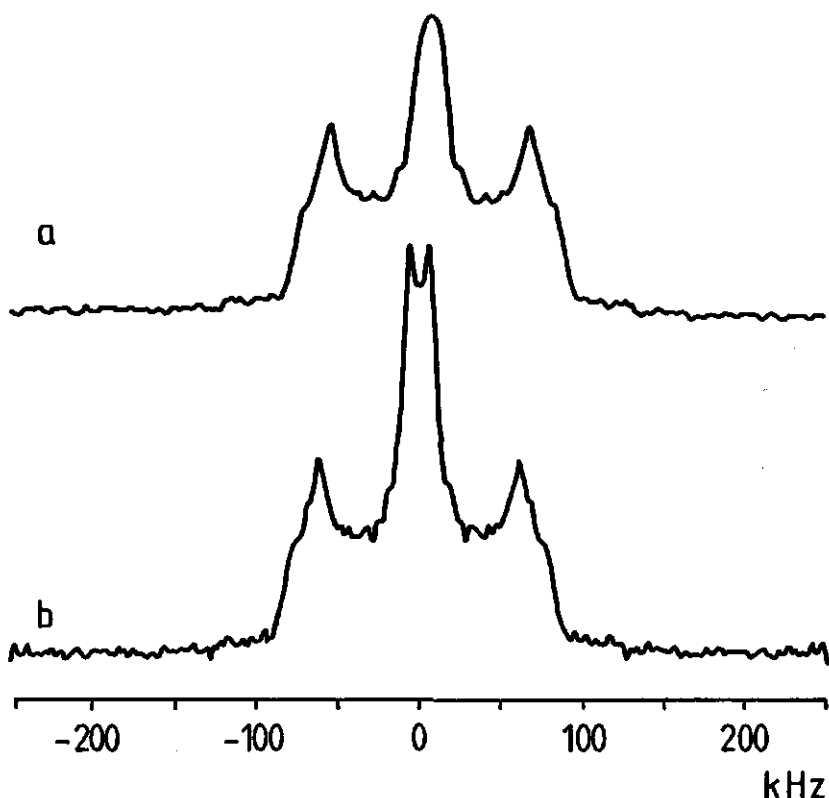


Figure 2. 46.06 MHz ^2H NMR spectra obtained from hydrogen-exchange deuterated M13 coat protein incorporated into liposomes of DMPC/DMPG (80/20 w/w, L/P = 50:1 molar ratio) in the gel phase (a) and in the liquid-crystalline phase (b) prepared in $^2\text{H}_2\text{O}$. (a) 5°C, $N_s = 120,000$, $T_r = 500$ ms, and the time between the 90° pulses of 5.0 μs in the quadrupolar echo, $\tau_2 = 35$ μs ; (b) 45°C, $N_s = 100,000$, $T_r = 333$ ms, $\tau_2 = 35$ μs . Samples of 150 mg of M13 coat protein incorporated into multilamellar lipid dispersions of DMPC/DMPG (80/20 w/w) at L/P ratio 50 were prepared by cholate dialysis (16) in $^2\text{H}_2\text{O}$ buffer or at L/P ratio 15 by sonication (data not shown). In both cases the solvent was removed from the resulting unilamellar vesicles by freeze-drying and $^2\text{H}_2\text{O}$ was added at a ratio of 1:1 (w/w). Homogeneous samples were obtained by mechanically mixing of the samples and heating them to approximately 50°C. The final lipid to protein ratio of the sample was determined as described (17,18).

the DePaked spectrum (Fig.1b) is 7:3. This is within experimental error identical to the theoretically expected ratio of 49:18. The coat protein has 50 amino acid residues, of which five residues are lysines, and a terminal amino group. Therefore, 49 exchangeable sites at the backbone are expected to contribute to the broad powder pattern, and 18 sites at the freely rotating N^2H_3 groups to the narrow powder pattern. In the determination of this ratio the intensity of the isotropic peak (2%) is neglected.

2H NMR spectra obtained with a previously described solvent subtraction technique (15) from multilamellar dispersions of dimyristoyl phosphatidylcholine/ dimyristoyl phosphatidylglycerol (DMPC/DMPG, 80/20 (w/w)) and M13 coat protein incorporated by cholera dialysis at lipid to protein molar ratio 50 are shown in Fig. 2. Incorporation by sonication at a lipid/protein (L/P) molar ratio 15 gave identical spectra. The spectra have a powder pattern with $\Delta\nu_Q = 145$ kHz and $\eta = 0.12$. The splitting of the broad component does not change over the temperature range from 5 to 55°C, although the lipids go through the phase transition (completed at 23°C, (19)). In contrast, the narrow axial symmetric pattern is temperature dependent and its $\Delta\nu_Q$ decreases from 27 kHz at 5°C to 18 kHz at 55°C (Fig. 3).

The 145 kHz splitting in the spectrum of M13 coat protein after incorporation into DMPC/DMPG (80/20 (w/w)) is only slightly smaller than the quadrupolar splitting obtained from coat protein as a powder. The 145 kHz pattern indicates little or no motion of the coat protein backbone on the 2H NMR timescale (10^{-5} s) in liquid-crystalline lipid at 45°C, in contrast to other single transmembrane polypeptides investigated so far (5-7) that show the onset of rapid axial rotation of the polypeptide at the phase transition resulting in a sharp, sharp, axially symmetric powder pattern and a strong decrease in the T_{2e} values. In case of M13 coat protein, however, T_{2e} is constant through the whole temperature range, i.e. 90 ± 10 μ s from 5 to 55°C (Fig.3). These results are best explained by aggregation of the coat

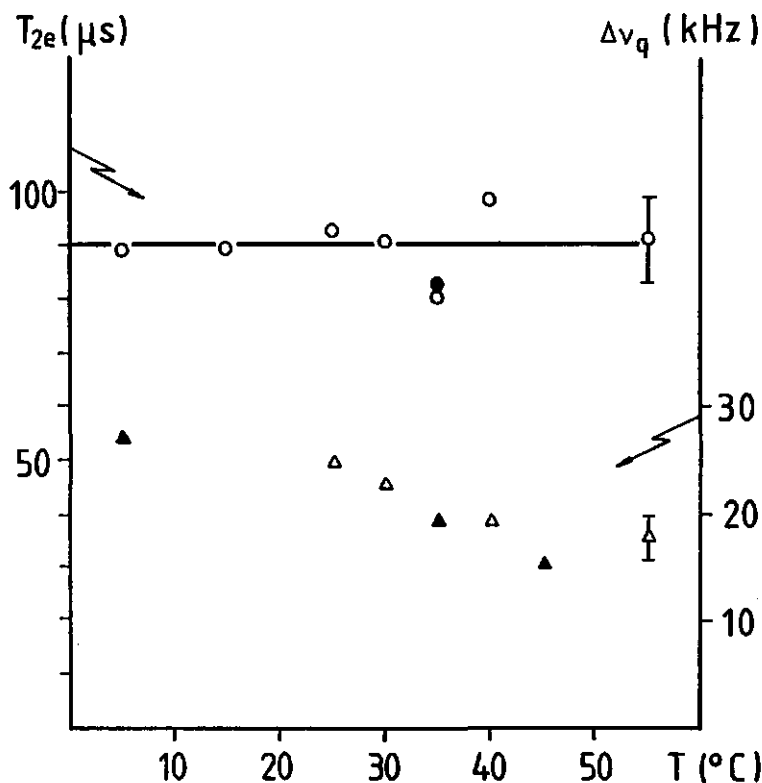


Figure 3. Temperature dependence of the quadrupolar splitting, $\Delta\nu_q$, of the narrow axial symmetric powder pattern in the 46.06 MHz ^2H NMR spectra in Figure 2 determined from the DePaked spectra (triangles, the open and closed triangles represent two different samples) and the spin-spin relaxation time, T_{2e} , of the ^2H NMR quadrupolar echo arising from the deuterons exchanged onto M13 coat protein in DMPC/DMPG (80/20 w/w) liposomes in $^2\text{H}_2\text{O}$ (solid line, open and closed circles). The phase transition of the bilayers is completed at 23°C (19). T_{2e} values were determined by varying the delay time, τ_2 , between the 90° pulses of the quadrupolar echo. Typically a range of 40–500 μs was covered by twenty measurements. Each measurement was the result of 1,000–4,000 free induction decays. The size of the quadrupolar echo signal was measured on top of the slowly decaying $^2\text{H}_2\text{O}$ signal at each τ_2 value and plotted as a function of $2\tau_2$. All decays were mono-exponential, characterized by one T_{2e} .

protein in the bilayer. M13 coat protein aggregation has also been found with time-resolved tryptophan anisotropy measurements of M13 coat protein in similar bilayers in the liquid-crystalline state (11). Measurements on the ^2H labelled alanine side chains of bacteriophage fd coat protein (which differs from the M13 coat protein by only one amino acid residue) in membranes have shown that the first 10 residues at the amino terminus and three residues at the end of the carboxyl terminus reorient rapidly at the ^2H NMR timescale (20). Since no motion is observed for the coat protein backbone using a deuterium label directly at the exchangeable sites on the coat protein backbone, the alanine side chains at the amino and carboxy terminus probably reorient to some extent independently from the coat protein backbone. This would mean that amide backbone sites are better probes for the coat protein backbone motion than the alanine sites.

The temperature dependence of the narrower axially symmetric lysine powder pattern ($\Delta\nu_Q = 35$ kHz, $\eta = 0$ for coat protein as a solid powder) indicates that the lysine side chains (one in the acidic domain at position 8 and four in the basic domain at the carboxyl terminus at the positions 40, 43, 44 and 48) are rotating more freely than the hydrogen bonded deuterons of the rigid backbone structure of the coat protein. These amino groups at the end of the lysine side chain are sensitive to motions of the surrounding lipids of the bilayer, which is seen as a decrease in the axially symmetric quadrupolar splitting in the spectra at high temperature (Fig. 3), and reflect the lysine side chain motion rather than the coat protein backbone motion.

ACKNOWLEDGEMENTS

This research was supported by the Netherlands Foundation of Biophysics, with financial aid from the Netherlands Organization for the Advancement of Pure Research (ZWO). We thank dr. T.J. Schaafsma for

reading the manuscript, Ruud B. Spruijt and Cor J.A.M Wolfs for sample preparation and characterization, dr. B.J.M. Harmsen for providing facilities to grow E. coli and Edward Sternin for providing a copy of his DePakeing program.

REFERENCES

- 1 F. Van Asbeck, K. Beyreuther, H. Koehler, G. Von Wettstein and G. Braunitzer. Hoppe-Seyler's Z. Physiol. Chem. **350**, 1047 (1969).
- 2 Y. Nakashima and W. Konigsberg. J. Mol. Biol. **88**, 598 (1974).
- 3 D.A. Marvin and E.J. Wachtel. Nature **253**, 19 (1975).
- 4 W. Wickner. Proc. Natl. Acad. Sci. USA **73**, 1159 (1976).
- 5 K.P. Pauls, A.L. MacKay, O. Soderman, M. Bloom, A.K. Tanjea and R.S. Hodges. Eur. Biophys. J. **12**, 1 (1985).
- 6 M. Bloom and I.C.P. Smith. Progress in Protein-Lipid Interactions (Watts, A. and Depont, J.J.H.H.M., eds.), Chapt. 2, pp.61-88, Elsevier Science Publishers, New York, NY (1985).
- 7 K.P. Datema, K.P. Pauls and M. Bloom. Biochemistry **25**, 3796 (1986).
- 8 J.H. Davis, K.R. Jeffrey, M. Bloom, M.I. Valic and T.P. Higgs. Chem. Phys. Lett. **42**, 390 (1976).
- 9 G.J. Garssen, C.W. Hilbers, J.G.G. Schoenmaker and J.H. Van Boom. Eur. J. Biochem. **81**, 45 (1977).
- 10 R. Knippers and H. Hoffmann-Berling. J. Mol. Biol. **21**, 281 (1966).
- 11 K.P. Datema, A.J.W.G. Visser, A. Van Hoek, C.J.A.M. Wolfs, R.B. Spruijt and M.A. Hemminga. Biochemistry, in press (1987).
- 12 M. Bloom, J.H. Davis and A.L. MacKay. Chem. Phys. Lett. **80**, 198 (1981).
- 13 E. Sternin, A.L. MacKay and M. Bloom. J. Magn. Reson. **55**, 274 (1983).
- 14 M.J. Hunt and A.L. MacKay. J. Magn. Reson. **22**, 295 (1976).
- 15 P.T. Callaghan, A.L. MacKay, K.P. Pauls, O. Soderman and M. Bloom. J. Magn. Reson. **56**, 101 (1984).
- 16 D.S. Hagen, J.H. Weiner and B.D. Sykes. Biochemistry **17**, 5860 (1978).
- 17 Peterson. Anal. Biochem. **83**, 346 (1977).
- 18 Bartlett, G.R. (J. Biol. Chem. **234**, 466 (1959).
- 19 K.P. Datema, C.J.A.M. Wolfs, D. Marsh, A. Watts and M.A. Hemminga. Biochemistry, in press (1987).
- 20 K.G. Valentine, D.M. Schneider, G.L. Leo, L.A. Colnago and S.J. Opella. Biophys. J. **49**, 36 (1986).

CHAPTER 4

EFFECT OF BACTERIOPHAGE M13 COAT PROTEIN ON THE MEMBRANE

4.1 SPIN LABEL ELECTRON SPIN RESONANCE STUDY OF BACTERIOPHAGE M13 COAT PROTEIN INCORPORATION INTO MIXED LIPID BILAYERS

Klaas P. Datema, Cor J.A.M. Wolfs, Derek Marsh, Anthony Watts
and Marcus A. Hemminga

ABSTRACT: The major coat protein of bacteriophage M13 was incorporated in mixed dimyristoyl phosphatidylcholine/dimyristoyl phosphatidyl glycerol (80/20 w/w) vesicles probed with different spin labelled phospholipids, labelled on the 14-C atom of the *sn*-2 chain. The specificity for a series of phospholipids was determined from a motionally restricted component seen in the ESR spectra of vesicles with the coat protein incorporated. At 30°C and pH 8 the fraction of motionally restricted phosphatidic acid spin label is 0.36, 0.52 and 0.72 for lipid/protein ratios of 18, 14 and 9 mole/mole, respectively. The ESR spectra, analysed by digital subtraction, resulted in a phospholipid preference following the pattern cardiolipin = phosphatidic acid > stearic acid = phosphatidyl serine = phosphatidyl glycerol > phosphatidyl choline = phosphatidyl ethanolamine. The specificities found are related to the composition of the target *E. coli* cytoplasmic membrane.

In vivo bacteriophage M13 enters the *Escherichia coli* cell leaving its coat protein in the cytoplasmic membrane (Marvin & Wachtel, 1975). After DNA duplication and coat protein synthesis both progeny as well as parental coat protein are stored as integral membrane proteins (Wickner, 1976). During the membrane bound assembly of new virions the viral DNA is complexed with many copies of the major coat protein, without lysis of the host cell.

The major (gene 8 product) M13 coat protein (MW=5240) consists of a basic carboxyl terminus, a central core of 19 hydrophobic amino acids and an acidic amino terminus (Nakashima & Koningsberg, 1974; Hagen et al., 1978). It has been shown that this hydrophobic, integral membrane protein can only be incorporated at high levels in model

membranes containing at least 20 w% negatively charged phospholipids, which results in the formation of stable vesicles (Hagen et al., 1978; Datema et al., 1987a). Also in vivo molecular association of the M13 coat protein with negatively charged cardiolipin in the E. coli membrane was suggested from altered host lipid metabolism after insertion of the M13 coat protein (Chamberlain & Webster, 1976).

Previously, the assembly and disassembly of plant viruses, the coat protein-nucleic acid interaction within the virus (for review see: Hemminga et al., 1985) and the interaction of coat protein with model membranes (Datema et al., 1987b) have been studied by magnetic resonance. An important and related problem concerns the mechanism of phage infection of the host cell. Since, as noted above, M13 coat protein can be incorporated at high levels into phospholipid bilayers only if they contain negatively-charged phospholipids (Hagen et al., 1978; Datema et al., 1987a), the interaction of the coat protein with negatively-charged phospholipids may be of importance for the mechanism of the phage entry into the cell. Electron spin resonance (ESR) measurements with spin-labelled phospholipids have been found to provide a particularly direct means of investigating the specificity of lipid interactions with integral proteins (Jost et al., 1973; Watts et al., 1979; Knowles et al., 1981; Marsh, 1981; Marsh & Watts, 1982; Griffith et al., 1982; Brophy et al., 1984; Marsh, 1985; Esmann et al., 1985; Pates et al., 1985; Devaux & Seigneuret, 1985). However, the method has not yet been applied to study the mechanism of virus infection, apart from our preliminary results with M13 coat protein reported recently (Hemminga, 1987).

In the present work the bacteriophage M13 coat protein has been incorporated in mixed phospholipid membranes composed of 80 w% dimyristoyl phosphatidyl choline (DMPC) and 20 w% dimyristoyl phosphatidyl glycerol (DMPG), probed with a variety of different spin labelled phospholipids. The presence of the M13 coat protein was found to induce a second ESR spectral component, characteristic of a motionally

restricted lipid population such as has been observed previously with other integral proteins. The two-component spectra were used to investigate the preference of the different spin labelled phospholipids for the coat protein. A high specificity was found for cardiolipin, a negatively-charged lipid of the target E. coli membrane.

MATERIALS AND METHODS

Chemicals. DMPC and DMPG were purchased from Sigma Chemical Co. and used without further purification. A series of spin labelled phospholipids labelled on the 14-C atom of the sn-2 chain was used: 14-PASL, 14-PGSL, 14-PCSL, 14-CLSL, 14-PSSL, 14-PESL and 14-SASL. All phospholipid spin labels have been synthesized from lysophosphatidyl-choline prepared from phosphatidylcholine from egg yolks, which was then acylated on the sn-2 position with the stearic acid spin label, 14-SASL. The phospholipid labels thus contain predominantly palmitic acid chains in the sn-1 position. A description of the synthesis of the spin labels can be found in Marsh & Watts (1982).

Sample preparation and characterization. Bacteriophage M13 was grown and isolated as described (Garssen et al., 1977). The major (gene 8 product) M13 coat protein was isolated according to Knippers & Hoffmann-Berling (1966). M13 coat protein was incorporated in mixed (80/20 w/w) DMPC/DMPG vesicles by cholate dialysis as described (Hagen et al., 1978) with some modifications. Typically 32 mg DMPC, 8 mg DMPG and 0.72 mg spin labelled phospholipid were suspended in 5 ml of 5 mM Tris-HCl buffer, pH 8.0 containing 8.0 M urea, 20 mM ammonium sulphate, 0.2 mM EDTA and 2 w% sodium cholate. Thus the spin label amount was 1.8 mol% of the total lipid. Dependent on the required lipid/protein ratio, M13 coat protein was added and dissolved by vortexing and incubation at 55°C until a clear solution was obtained. After incubation, the suspension was dialyzed for 48h at 4°C against 3 mM phosphate

buffer, pH 8.0, 0.02 mM EDTA, containing 10% (v/v) methanol, with buffer changes at 12, 24 and 36h. In the last dialysis no methanol was added to the buffer. Samples were concentrated by freeze-drying and resuspended in 0.15 ml H₂O. To obtain homogeneous samples of multilamellar vesicles the samples were vortexed and heated through the phase transition several times. At this point, aliquots of the samples were taken to determine the protein and the phospholipid concentration (Bartlett, 1959; Peterson, 1977), from which the lipid/protein ratio was calculated. Error in these ratios was less than 10%. The sample homogeneity was checked by sucrose density gradient centrifugation. The material was loaded onto a continuous (5-40%) sucrose gradient and centrifuged (4h, 182,000 g, 4°C). In all cases one single, sharp band was observed, indicating that each sample had a uniform L/P ratio. ³¹P NMR experiments on similar samples have indicated that all lipids are arranged in a bilayer and that the samples do not contain small vesicles, which would give rise to isotropic averaging of the chemical shift anisotropy (Datema et al., 1987a). For ESR measurements samples were transferred into 0.05 ml glass capillaries.

Electron spin resonance spectroscopy. ESR spectra were recorded on a Varian E-12 Century Line spectrometer with nitrogen gas flow temperature regulation. Spectra were digitized using a Digital Equipment Corp. LPS system and a dedicated PDP 11/10 computer with a VT 11 display. ESR spectrometer settings were: 5 mW microwave power, 0.1 mT modulation amplitude, 128 ms time constant, 240 s scan time, 10 mT scan width and 324 mT center field. Up to 13 spectra were accumulated to improve the signal/noise ratio.

RESULTS

The ESR spectra of the 14-PASL spin label in M13 coat protein-DMPC/DMPG multilayers are shown in Figure 1a-d. The spectra were taken

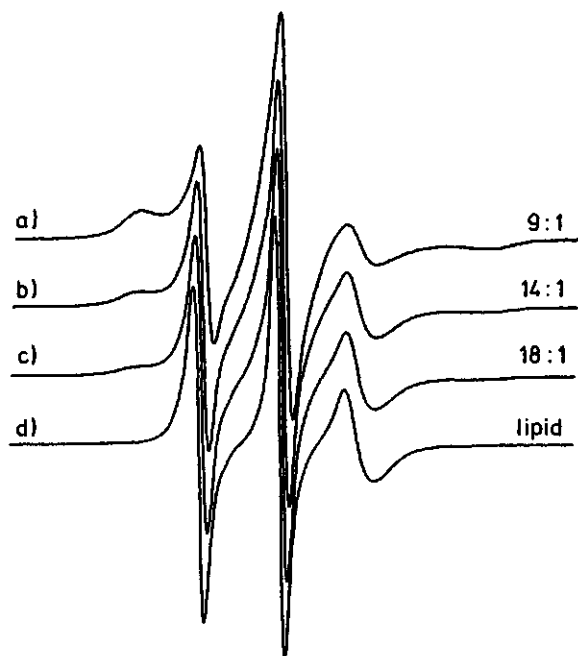


Figure 1. ESR spectra at 30°C of the 14-PASL phosphatidic acid spin label in M13 coat protein-DMPC/DMPG (80/20 w/w) complexes of different lipid/protein ratios. a) lipid/protein = 9:1 mole/mole, b) lipid/protein = 14:1 mole/mole, c) lipid/protein = 18:1 mole/mole, d) lipid alone. Total scan width = 10 mT.

at 30°C, which is well above the gel to liquid-crystalline phase transition region from 19 to 23°C of the mixed DMPC/DMPG alone, as verified by the temperature dependence of the ESR spectra (data not shown). Apart from the motionally averaged sharp three-line spectrum, typical for liquid-crystalline phase lipid, the M13 coat protein-containing samples display a second, broader component with strongly restricted motion on the ESR timescale.

The two-component spectra were analysed by spectral subtraction/addition as illustrated in Figure 2 (cf. Esmann et al., 1985). Digital subtraction of the lipid spectrum (Figure 2b, full line) from the

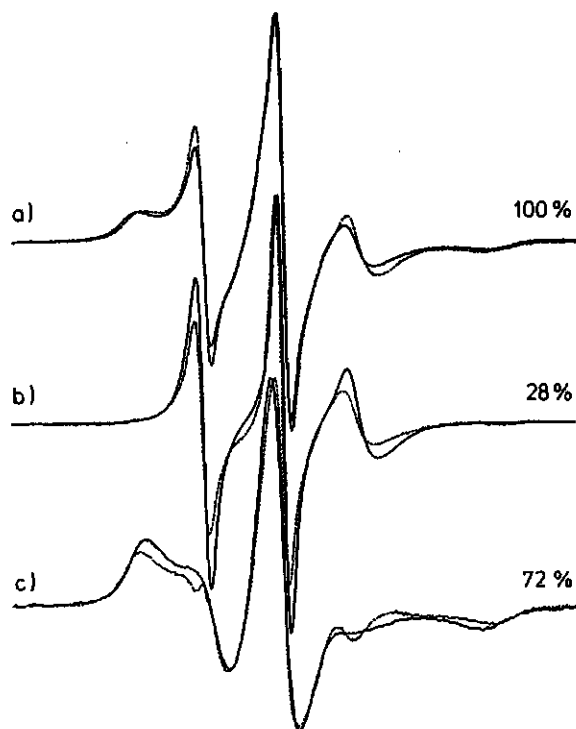


Figure 2. Spectral subtraction and addition with the 14-PASL spin label. Full lines are original spectra. a) M13 coat protein in DMPC/DMPG (80/20 w/w) at a lipid/protein ratio of 9:1 mole/mole, recorded at 30°C, b) DMPC/DMPG (80/20 w/w) alone recorded at 26°C, c) motionally restricted component comparison spectrum (14-PCSL in sonicated DMPC vesicles at 4°C). Dashed lines are summed and difference spectra. a) 28% lipid alone spectrum plus 72% motionally restricted spectrum, b) protein-lipid spectrum minus 72% motionally restricted spectrum, c) protein-lipid spectrum minus 28% lipid alone spectrum. Total scan width = 10 mT.

spectrum of M13 coat protein-DMPC/DMPG multilayers (Figure 2a, full line) yields the spectrum of the motionally restricted component (Figure 2c, dashed line). Double integration gives the percentage of this component to be 72% of the total intensity. Complementary

Table I. Fraction of Motionally Restricted 14-PASL Spin Label, f , in M13 Coat Protein-DMPC/DMPG (80/20 w/w) Complexes for Various Lipid/Protein Ratios (L/P) ^a.

Lipid/Protein mole/mole	f	(L/P)* f mole/mole
18	0.36	6.5
14	0.52	7.3
9	0.72	6.6

^afractions were determined from the ESR difference spectra of the 14-PASL at 30°C. Typical error in L/P mole/mole ratio is 10%. Typical error in f is 5%.

subtraction, ie. of a broader gel phase lipid spectrum (Figure 2c, full line) yielded the spectrum of the fluid bilayer component (Figure 2b, dashed line), which resembles the lipid spectrum in absence of M13 coat protein. By double integration of this spectrum the relative intensity of the fluid component was determined to be 28% of the total spin label intensity. These complementary quantitations agree to within an experimental error of 5%. The agreement of the addition spectrum (Figure 2a, dashed line) with the original experimental spectrum provides a further check on the consistency of the method. The fraction of motionally restricted lipid, f , obtained from the mean value of the subtractions, is given for the different lipid/protein ratios in Table I. These values were found to vary relatively little with temperature over the range for which satisfactory subtractions could be obtained

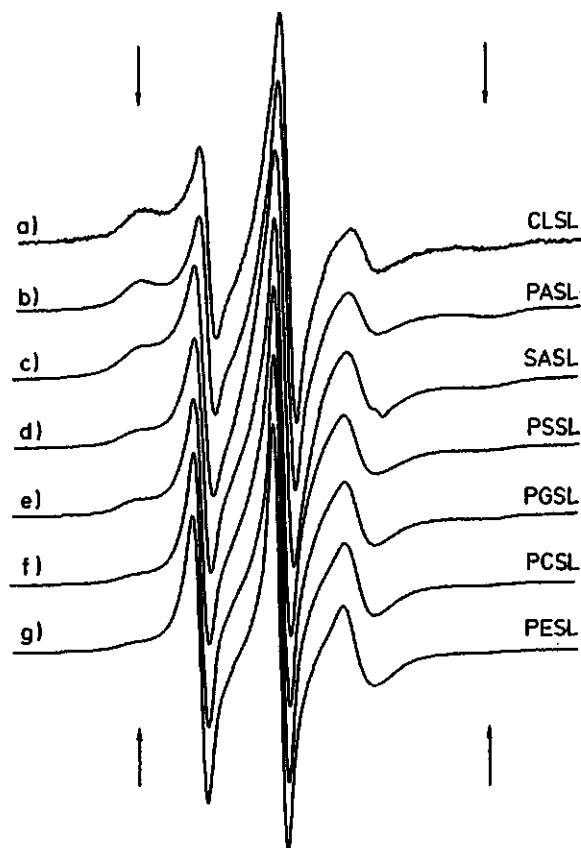


Figure 3. ESR spectra at 30°C of DMPC/DMPG (80/20 w/w) dispersions with incorporated M13 coat protein at lipid/protein ratio = 9:1 mole/mole and containing different C-14 position spin labelled lipids. a) Cardiolipin spin label, 14-CLSL; b) phosphatidic acid spin label, 14-PASL; c) stearic acid spin label, 14-SASL; d) phosphatidylserine spin label, 14-PSSL; e) phosphatidylglycerol spin label, 14-PGSL; f) phosphatidylcholine spin label, 14-PCSL; g) phosphatidylethanolamine spin label, 14-PESL. The arrows in the outer wings of the spectra indicate the motionally restricted spin label component, which is not present in the spectra of the lipids alone. Total scan width = 10 mT.

Table II. Fraction of Motionally Restricted Spin Label, f , in M13 Coat Protein-DMPC/DMPG (80/20 w/w) Complexes for Various Spin Labels ^a.

Spin Label	f	$[f/(1-f)]/[f/(1-f)]_{\text{PCSL}}$
14-CLSL	0.72	4.2
14-PASL	0.72	4.2
14-SASL	0.59	2.3
14-PSSL	0.56	2.1
14-PGSL	0.49	1.6
14-PCSL	0.38	1.0
14-PESL	0.36	0.9

^a fractions were determined from the ESR difference spectra of the spin label at 30°C for lipid/protein ratio 9:1 mole/mole. Typical error in f is 5%. $f/(1-f)$ is the ratio of motionally restricted to fluid lipid spin label component. Values are normalized to those for the 14-PCSL spin label.

(data not shown). The values bear a direct relation to the lipid/protein ratio, L/P, as seen by the approximate constancy of the product $(L/P)*f$ in Table I.

The specificity of lipid interaction with the coat protein was investigated using different lipid species, all with the spin label on the 14-C atom of the sn-2 chain. Figure 3 shows the ESR spectra at 30°C of the various spin labelled lipids in M13 coat protein-DMPC/DMPG multilayers of lipid/protein molar ratio 9:1. In all spectra a well resolved motionally restricted component is superimposed on the fluid

component. The motionally restricted components are very similar in maximum outer hyperfine splitting value, $2A_{\text{max}} = 6.2$ mT, but have different relative intensities. The fraction of motionally restricted component, obtained by spectral subtraction, for each of the spin labelled lipids is given in Table II. For comparison of the relative selectivities the normalized ratio of motionally restricted to fluid components is also given in Table II. For a single lipid host, these values would give the ratios of the relative association constants for the different spin labelled lipids (see eg. Marsh, 1985). Because of the presence of the obligatory negatively-charged lipid in the mixtures, the values in Table II, therefore represent lower limits for the selectivity relative to the pure phosphatidyl choline.

DISCUSSION

Incorporation of the M13 coat protein at high levels in stable bilayers requires the presence of negatively-charged lipids (Hagen et al., 1978; Datema et al., 1978a). This is especially interesting in view of the lipid composition of the target *E. coli* membrane which is: phosphatidyl ethanolamine, 74%; phosphatidyl glycerol, 19%; and cardiolipin, 3% (Burnell et al., 1980). The spin label ESR results presented here show that the coat protein exhibits different interactions with the different negatively-charged spin labelled lipids. A clear second component is seen in the ESR spectra of vesicles containing M13 coat protein. The fraction of motionally restricted component depends directly on the amount of protein present in the bilayer (see Figure 1). The product of the fraction of motionally restricted lipid and the lipid/protein ratio remains approximately constant (Table I), although for a mixed lipid system this can only indirectly be related to the total number of lipids interacting with the protein. Furthermore, the

apparent temperature dependence of the fraction of motionally restricted lipid is small (data not shown). Also the ratio of the fraction of restricted 14-PCSL and 14-PGSL is constant over the temperature range of 30 to 50°C. The influence of M13 coat protein on the phase transition at 19 to 23°C, is small. The temperature range is only slightly broader, 18 to 25°C in the presence of the protein (data not shown). These results clearly indicate that the motionally restricted component represents lipid molecules directly influenced by the coat protein (cf. Marsh, 1985).

The total percentage of motionally restricted lipid at L/P = 9 mole/mole, as determined from the fractions of motionally restricted 14-PCSL ($f=0.38$) and 14-PGSL ($f=0.49$) in the mixed DMPC/DMPG (80/20 w/w) is approximately 40%. This means that at L/P = 9 mole/mole approximately 4 moles of lipid molecules are directly associated with the protein per mole of M13 coat protein, while approximately 5 moles of lipid are in a fluid lipid environment. The ratio of motionally restricted to fluid lipids of 0.40 is lower than one would expect on the basis of a model in which a single M13 coat protein molecule spans the membrane as a monomer. Therefore, the spin-label ESR results indicate protein aggregation, in agreement with time-resolved fluorescence anisotropy (Chapter 3.1) and ^2H NMR measurements (Chapter 3.2).

The protein-associated spectrum in Figure 2c, has a hyperfine splitting of 6.2 mT, indicating a considerably reduced motion relative to that of the bilayer lipids. Since the fluid and the restricted components are well resolved (see Figure 2) the rate of exchange between the lipid molecules interacting with the protein and the free bilayer lipids is slow on the ESR time scale (Marsh, 1981; Devaux & Seigneuret, 1985). Comparing our spectra with simulations based on two-site exchange (Horvath, L.I., Brophy, P.J., & Marsh, D., personal communication) suggests that the exchange rate of the lipid molecules between the two components is of the order of 10^7 s^{-1} .

The specificity of the M13 coat protein for several phospholipids,

determined from the fractions of restricted component for the different phospholipids can be divided into three groups as seen in Table II. 14-PCSL and 14-PESL, both zwitterionic phospholipids, show little specificity ($f=0.37$) and consequently little preferential interaction with the coat protein. Phosphatidyl ethanolamine which accounts for 74% of the lipids in the *E. coli* target membrane (Burnell et al., 1980), has the smallest interaction with the coat protein and, therefore, provides a good reference for comparison with the other phospholipids. The negatively charged phospholipids, all bearing one negative charge per two fatty acid chains at pH 8, consist of two groups, one comprising 14-PSSL, 14-PGSL and the fatty acid 14-SASL, displaying an intermediate specificity ($f=0.55$), and the other comprising 14-PASL and 14-CLSL, that show a larger specificity for the protein ($f=0.72$). Consequently, the specificity cannot simply be explained by electrostatic interaction, and, as the hydrocarbon chains are all the same for the phospholipid labels used, the configuration of the phospholipid headgroup must play a role in the interaction with the protein. A preference for negatively-charged phospholipids, as found here, is seen also for most integral membrane proteins so far investigated, with the exception of rhodopsin (Watts et al., 1979), although the detailed specificity pattern differs between the different proteins (Marsh, 1985). The specificity of M13 coat protein for 14-CLSL is in good agreement with molecular association of cardiolipin with the coat protein as suggested from altered host lipid metabolism after infection of *E. coli* with M13 bacteriophage, indicating increased cardiolipin synthesis (Chamberlain & Webster, 1976). The limited selectivity for phosphatidyl glycerol may also be significant, since there is a relatively high proportion of phosphatidyl glycerol (19% of the total lipids) in the *E. coli* cytoplasmic membrane (Burnell et al., 1980), which does not increase after infection (Chamberlain & Webster, 1976).

The lipid specificity pattern for the M13 coat protein may there-

fore be essential for understanding the molecular mechanisms underlying (1) infection of the host cell by the bacteriophage, (2) storage of the coat protein in the host cytoplasmic membrane during reproduction of the viral DNA and (3) membrane bound assembly of the bacteriophage.

ACKNOWLEDGEMENTS

We thank Dr. B.J.M. Harmsen for providing facilities to grow E. coli and R.B. Spruijt for help with the preparation of bacteriophage M13 coat protein.

REFERENCES

- Bartlett, G.R. (1959) J. Biol. Chem. **234**, 466-68.
- Brophy, P.J., Horvath, L.I., & Marsh, D. (1984) Biochemistry **23**, 860-865.
- Burnell, E., Van Alphen L., Verkleij, A., & De Kruijff, B. (1980) Biochim. Biophys. Acta **597**, 492-501.
- Chamberlain, B.K., & Webster, R.E. (1976) J. Biol. Chem. **251**, 7739-45.
- Datema, K.P., Spruijt, R.B., Wolfs, C.J.A.M., & Hemminga, M.A. (1987a) submitted for publication.
- Datema, K.P., Spruijt, R.B., Verduin, B.J.M., & Hemminga, M.A. (1987b) Biochemistry, in press.
- Datema, K.P., Visser, A.J.W.G., Van Hoek, A., Wolfs, C.J.A.M., Spruijt, R.B., & Hemminga, M.A. (1987c) Biochemistry, in press.
- Datema, K.P., Van Bortel, B.J.H., & Hemminga, M.A. (1987d) submitted for publication.
- Devaux, P.F., & Seigneuret, M. (1985) Biochim. Biophys. Acta **822**, 63-125.
- Esmann, M., Watts, A., & Marsh, D. (1985) Biochemistry **24**, 1386-93.
- Garssen, G.J., Hilbers, C.W., Schoenmaker, J.G.G., & Van Boom, J.H. (1977) Eur. J. Biochem. **81**, 453-63.
- Griffith, O.H., Brothorus, J., & Jost, P.C. (1982) in Lipid-Protein Interactions (Jost, P.C., & Griffith, O.H., Eds) Vol. II, pp 225-237, Wiley-Interscience, New York.
- Hagen, D.S., Weiner, J.H., & Sykes, B.D. (1978) Biochemistry **17**.

- 5860-6.
- Hemminga, M.A., Datema, K.P., Ten Kortenaar, P.W.B., Krüse, J., Vriend, G., Verduin, B.J.M., & Koole, P. (1985) in Magnetic Resonance in Biology and Medicine (Govil, G., Khetrpal, C.L., & Saran, A., Eds.) pp. 53-76, Tata McGraw-Hill Publishing Company Ltd, New Dehli, India.
- Hemminga, M.A. (1987) J. Chem. Soc., Faraday Trans. 1 **83**, 203-209.
- Jost, P.C., Griffith, O.H., Capaldi, R.A., & Vanderkooi, G.A. (1973) Proc. Natl. Acad. Sci. USA **70**, 4756-4763.
- Knippers, R., & Hoffmann-Berling, H. (1966) J. Mol. Biol. **21**, 281-292.
- Knowles, P.F., Watts, A., & Marsh, D. (1981) Biochemistry **20**, 5888-94.
- Marsh, D. (1981) in Membrane Spectroscopy (Grell, E., Ed.) pp 51-142, Springer-Verlag, Berlin-Heidelberg-New York.
- Marsh, D., & Watts, A. (1982) in Lipid-Protein Interactions (Jost, P.C., & Griffith, O.H., Eds.) Vol. II, pp 53-126, Wiley-Interscience, New York.
- Marsh, D. (1985) in Progress in Protein-Lipid Interactions (Watts, A., & De Pont, J.J.H.M., Eds.) Chapt. 4, pp 143-172, Elsevier Science Publications, New York.
- Marvin, D.A., & Wachtel, E.J. (1975) Nature **253**, 19-23.
- Nakashima, Y., & Koningsberg, W. (1974) J. Mol. Biol. **88**, 598-600.
- Pates, R.D., Watts, A., Uhl, R., & Marsh, D. (1985) Biochim. Biophys. Acta **814**, 389-97.
- Peterson, G.L. (1977) Anal. Biochem. **83**, 346-56.
- Watts, A., Volotovskii, I., & Marsh, D. (1979) Biochemistry **18**, 5006-12.
- Wickner, W. (1976) Proc. Natl. Ac. Sci. USA **73**, 1159-63.

4.2 DEUTERIUM NUCLEAR MAGNETIC RESONANCE INVESTIGATION OF BACTERIOPHAGE M13 COAT PROTEIN IN DIMYRISTOYL PHOSPHATIDYLCHOLINE LIPOSOMES USING PALMITIC ACID AS A PROBE

Klaas P. Datema, Ruud B. Spruijt, Cor J.A.M. Wolfs
and Marcus A. Hemminga

ABSTRACT: Deuterium NMR has been used in combination with deuterated palmitic acid as bilayer probe in DMPC liposomes. The effect of incorporation of M13 bacteriophage coat protein on the bilayer order and acyl chain motion was investigated using deuterium and phosphorus NMR and additional spin label ESR. The secondary structure of the M13 coat protein in these bilayer systems was determined from circular dichroism spectra. The phase transition of DMPC liposomes at 24°C is shifted upward and broadened, to the range of 29 to 38°C in the presence of 27% (w/w) palmitic acid. Phosphorus NMR spectra of the mixed liposomes are characteristic for DMPC organized in bilayers, also after incorporation of various levels of M13 coat protein. Circular dichroism spectra of the coat protein indicate that the protein conformation is predominantly β -structure (92% at lipid/protein molar (L/P) ratio 56). At L/P molar ratio 39 all deuterium labelled positions along the acyl chain are found to have equal order as in the reference bilayers. In contrast, the spin-spin relaxation times decrease in the presence of the coat protein, especially at the terminal carbon-16 position, but also at the carbon-9 and carbon-2 position. The spin label ESR spectra of the same system using 14-doxyl stearic acid as a label, show a second, motionally-restricted component, that is not observed by deuterium NMR. Its intensity (typically 10% at L/P molar ratio 39) depends on the lipid to protein ratio (10% at L/P molar ratio 39). The NMR and ESR results are consistent with a model, in which the fatty acid molecules are in a fast two-site exchange (at a rate of approximately 10^7 Hz) between the sites in the bulk of the lipid bilayer and the motionally-restricted sites.

The investigation of membranes by magnetic resonance has been very succesful in the last decade. Especially phosphorus and deuterium nuclear magnetic resonance (NMR) have developed to powerful techniques,

that provide structural and dynamical information of the lipid molecules in membranes [1,2]. These developments have been prompted by the notion that the structure of membranes depends on lipid composition (for a review see: [3]) and that its functioning is influenced by the physical properties of the lipids [4].

In model membranes of well-defined mixed lipids, proteins have been reconstituted to relate lipid-protein interactions to protein functioning, thus obtaining a better insight in the properties of integral membrane proteins. In these studies the fatty acyl chain order and motions have been characterized extensively in presence of a variety of proteins. The results have been summarized and evaluated in a number of recent reviews [5-8].

The objective of our work is to study the infection mechanism of non-enveloped viruses, like bacteriophage M13 and plant viruses, at a molecular level. A number of stages of the virus life cycle can be studied well by physical techniques such as NMR and spin label ESR. The assembly and disassembly of virus particles and coat protein-nucleic acid interaction within the virus itself have already been studied for some plant viruses in our laboratory (for a review see: [9]). A suitable system to study the interaction of viral coat proteins with membranes is the M13-Escherichia coli system.

The major (gene-8 product) M13 coat protein is present in the long rodlike virus particle in numerous copies and functions as protection for its single stranded DNA. The virus enters the E. coli host cell by leaving the coat proteins in the cytoplasmic membrane [10]. The coat protein of M13 (M=5240) consists of 50 amino acid residues: a basic C-terminus, a hydrophobic central core of 19 amino acid residues and an acidic N-terminus [11,12]. After DNA duplication and synthesis of new coat proteins both progeny as well as parental coat proteins are stored as integral membrane protein [13]. During the membrane bound assembly of new virus particles the viral DNA is complexed with these coat proteins without lysis of the host cell.

As an initial step towards a model for virus penetration into the host cell we have reconstituted the coat protein of M13 in model membranes [see also: 14,15]. In this study a mixed lipid system consisting of neutral dimyristoyl phosphatidylcholine and negatively charged palmitic acid was chosen for the following reasons. Stable bilayers containing M13 coat protein have been prepared using a mixed lipid system with negatively charged lipids [16]. Using a free fatty acid instead of negatively charged lipids this incorporation procedure enabled us to use deuterium NMR in combination with specifically deuterated palmitic acid as probe. Recently the effect of palmitic acid on membrane structure has been investigated by deuterium NMR, showing that palmitic acid is an accurate reporter molecule in membranes [17].

In the present study perdeuterated ($[U-^2H_{31}]$) and specifically deuterated ($[2,2-^2H_2]$, $[9,9-^2H_2]$ and $[16,16,16-^2H_3]$) palmitic acid in DMPC liposomes have been used with various incorporation levels of M13 coat protein. The effect of the coat protein on membrane structure and motion is investigated with deuterium NMR of these labels and additional spin label ESR of stearic acid labelled at the carbon-14 position of the acyl chain and phosphorus NMR. CD spectra were taken of the M13 coat protein in these bilayer systems to determine the secondary structure.

MATERIAL AND METHODS

DMPC (1,2-dimyristoyl-sn-glycero(3)phosphocholine, 99% purity), palmitic acid (99% purity) were obtained from Sigma Chemical Co. and used without further purification. $[U-^2H_{31}]$ (99.1 atom% 2H), $[2,2-^2H_2]$ (98.8 atom% 2H), $[9,9-^2H_2]$ (99.3 atom% 2H), and $[16,16,16-^2H_3]$ palmitic acid (99 atom% 2H) were obtained from MSD Isotopes, Montreal. 14-SASL (14-doxyl stearic acid) was prepared as described [18].

M13 bacteriophage was purified as described [19]. The major (gene-8 product) coat protein of M13 was isolated by the method of Knippers and Hoffmann-Berling [20].

(a) Samples for determination of the amount of coat protein in stable vesicles and CD measurements. Samples were prepared by cholate dialysis, as described [16], with a few modifications. For each DMPC/palmitic acid ratio 1 mg M13 coat protein and a total amount of 10 mg DMPC and palmitic acid were suspended in 1.0 ml of 8.0 M urea/ 5.0 mM Tris-HCl/ 2% (w/w) sodium cholate/ 0.1 mM EDTA/ 20 mM ammonium sulphate buffer (pH 8.0). A clear, homogeneous suspension was obtained by vortexing and heating the sample to 55°C. Subsequently, the suspension was dialysed at 4°C against 4x1 L of 10 mM Tris-HCl/0.2 mM EDTA/ 10% (v/v) methanol buffer (pH 8.0) for a total of 48 h with changes at 12, 24 and 36 h. In the last step no methanol was added to the buffer. This results in dispersions of unilamellar vesicles, that are opalescent in absence of protein. For CD measurements samples were sonicated under nitrogen with a Branson cell disruptor B30 (duty cycle: 90%, power setting 4 (max. 350 W at setting 10)) to avoid spectral distortion by light scattering of the vesicles. The resulting dispersion of SUVs was checked by measuring its UV absorption spectrum (300 - 190 nm) and no significant light scattering was observed.

(b) Samples for ESR were prepared as under (a), with small modifications. Typically, 32 mg DMPC, 8 mg palmitic acid and 0.36 mg 14-SASL was suspended in urea/cholate buffer (pH 8.0). Thus the spin label amounted to 1.8 mol% of the total lipid. Coat protein was added and dissolved by vortexing and incubation at 55°C until a clear solution was obtained. Incorporation was checked visually and no precipitate of unincorporated, water insoluble coat protein was observed. Samples were concentrated by freeze-drying and redissolved in 0.15 ml H₂O. To obtain homogeneous samples of multilamellar bilayers, the samples were

vortexed and heated through the phase transition several times. Before the ESR measurements aliquots of the samples were taken to determine the protein [21] and phosphatidylcholine content [22] yielding the L/P ratio of the samples. The samples were homogeneous as determined by sucrose gradient centrifugation. Before measurement the samples were transferred into 0.05 ml glass capillars.

(c) Samples for ^2H and ^{31}P NMR were prepared as described under (a), with the following modifications. Typically, 177.2 mg DMPC, 50 mg deuterated palmitic acid and 0, 22.7, 49.9 or 127.8 mg M13 coat protein were suspended in 10, 10, 20 or 40 ml urea/cholate buffer (pH 8.0), respectively. After dialysis and removal of the solvent by freeze-drying, 10 mM of Tris-HCl buffer (pH 8.0) prepared from deuteriumoxide depleted water was added to the solid mixture at a ratio of 2:1 (w/w). Before measurement, the L/P ratio of the samples was determined as described under (b) and the homogeneity of the samples was checked by sucrose gradient centrifugation.

Determination of the amount of coat protein in stable vesicles. Vesicle suspensions were centrifuged (8,800g, 10 min) to precipitate water insoluble aggregates of M13 coat protein and lipid. The amount of M13 coat protein present in stable vesicles in the supernatant was determined as described [21].

Determination of DMPC to palmitic acid ratio. The DMPC to palmitic acid ratio was determined by gas chromatography. After ^2H NMR measurement the samples were freeze-dried. Typically, 15 mg of the powder was dissolved in 0.5 ml of 2 M sodiummethanolate/methanol to re-esterify the myristic acid chains of DMPC. Next, 1 ml of 2 M sulfuric acid/methanol was added to the solution to also esterify the palmitic acid. The esters were extracted into hexane for gas chromatography. After separation of hexane from the aqueous fraction, sodium sulphate (anhydrous) was added to remove residual water in the hexane solvent.

CD spectra were recorded at room temperature on a Jobin-Ivon Auto-Dichrograph Mark V in the wavelength range 250-190 nm. A sample cell of 1-mm path length was used. Spectra are the average of four scans taken from the same sample. To determine the secondary structure the CD spectra were fitted to reference spectra of Greenfield and Fasman [23] by a least-square fit procedure using spectral points in the 250 to 190 nm range with 5-nm steps.

^{31}P NMR spectra of DMPC/palmitic acid systems were obtained with a Bruker CXP300 Fourier Transform spectrometer at a frequency of 121.48 MHz. For the spectra a multiplication equivalent to 50 Hz in the frequency domain was applied. All spectra were recorded in the presence of broadband proton decoupling (20W/12dB) using a 16 μs 45° pulse with a repetition rate of 1 s and a spectral width of 50,000 Hz. The CSA was determined from the powder spectrum.

ESR spectra were recorded as described [15].

^2H NMR spectra were recorded at 46.06 MHz with a Bruker CXP300 Fourier Transform spectrometer. All spectra were recorded with the center of the spectrum on resonance using the quadrupolar echo sequence [24,25]. For measurements of the $[\text{16,16,16-}^2\text{H}_3]\text{palmitic acid}$ samples 180° pulses were inserted at $t = \tau_2/2$ to also refocus possible dephasing from dipolar interactions [26, K.P. Datema, P.A. de Jager and M.A. Hemminga, unpublished results]. Quadrature detection was used and both signals from the in-phase and out-of-phase channel were taken for Fourier transformation. The temperature of the sample was regulated by a Bruker variable temperature unit B-VT 1000. For temperatures below room temperature nitrogen gas, evaporated from a Dewar containing liquid-nitrogen, was used for temperature regulation. Measurements were started at low temperature and after each temperature increase the samples were allowed to equilibrate for at least half a hour.

Spin-spin relaxation times, T_{2e} , were determined by varying the delay time, τ_2 , between the 90° pulses of the quadrupolar echo. Typically a range of 40-1,000 μs was covered by twenty measurements, with exception of the $[16,16,16\text{-}^2\text{H}_3]\text{palmitic acid}$ samples for which a range of 40-5,000 μs was taken. Each measurement was the result of 2,500-8,000 FIDs. The top of the quadrupolar echo signal was measured at each τ_2 value and plotted as a function of $2\tau_2$.

RESULTS

M13 coat protein incorporation in stable vesicles

The formation of stable DMPC/palmitic acid vesicles that contain M13 coat protein at 4°C was determined as a function of the amount of palmitic acid. By comparison of the amount of protein found in the vesicles formed after cholate dialysis to the initial amount of protein added to the micellar solution (1 mg) the percentage of incorporated protein in the vesicles was calculated. It was found that at 20% (w/w) palmitic acid or more, the protein was maximally incorporated in vesicle structures (Figure 1a). It is also evident that no stable pure DMPC vesicles with coat protein are formed by cholate dialysis at 4°C (Figure 1a). At the ratio of 73/27 (w/w) DMPC/palmitic acid, M13 coat protein incorporation was determined as a function of the amount of protein initially added (Figure 1b). Up to 30% (w/w) protein incorporation is complete. At higher amounts of protein, aggregates of coat protein with lipid in non-vesicle structure were formed, which decreased the amount of M13 coat protein in stable vesicles.

These incorporation experiments demonstrate that the initially added amounts of coat protein and phosphatidylcholine do not provide an accurate number for the L/P ratio in the vesicles after cholate

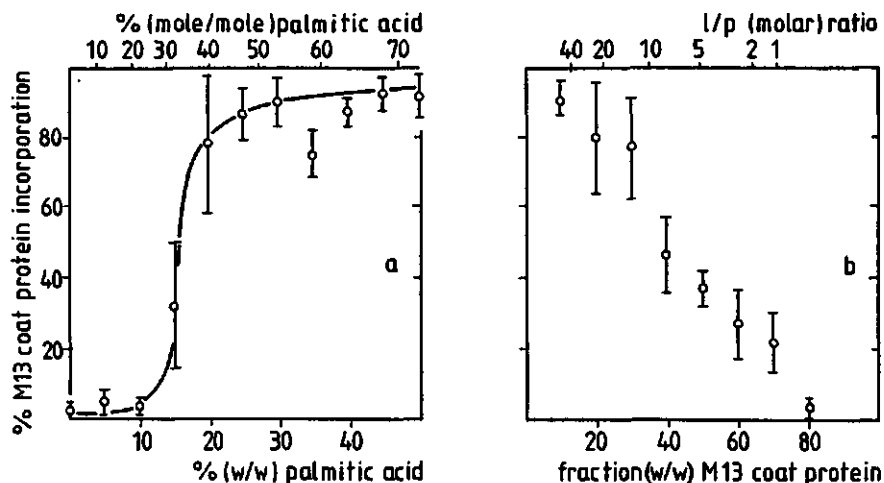


Figure 1. M13 coat protein in stable DMPC/palmitic vesicles prepared by cholate dialysis as a function of the amount of palmitic acid in the DMPC bilayers at a constant coat protein content (10 % (w/w) of the bilayer material, (a)) and as a function of the amount of coat protein initially added to DMPC/palmitic acid mixtures that form bilayers with a (final) ratio of 73/27 (w/w) (b). The symbols represent average values of 3 different samples.

dialysis. Therefore, aliquots of the ^{31}P NMR, ^2H NMR and spin label ESR samples were taken to determine the final L/P ratio. The phosphatidylcholine and coat protein, that was initially added to the micellar solution, had a L/P ratio of 60, 30 and 15. Dialysis decreases the ratios to 39, 20 and 9, respectively. These values are reproducible within 10%.

By gas chromatography the myristic to palmitic acid molar ratio in the ^2H NMR samples was found to be: 2.1 ± 0.2 for all samples in the range from 0 to 36% (w/w) coat protein. This implies that the initial weight percentage (20% (w/w)) of palmitic acid has increased to 27% (w/w).

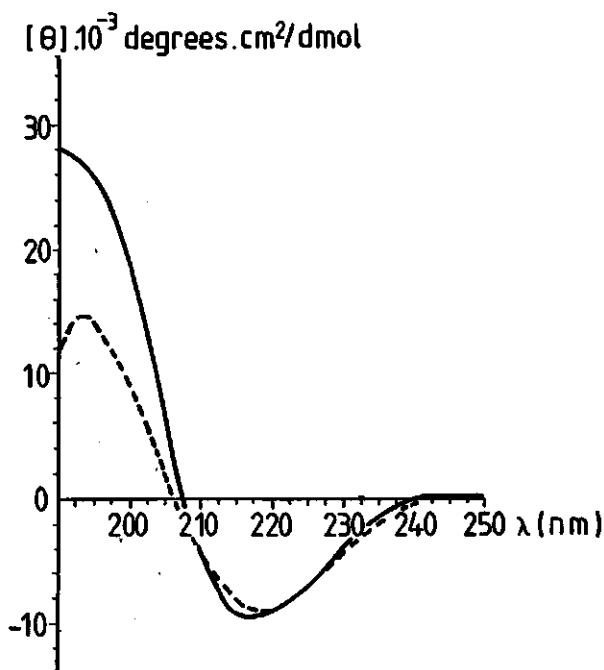


Figure 2. Circular dichroism spectra at room temperature of M13 coat protein in DMPC/palmitic acid (73/27 (w/w)) SUVs at L/P ratio 56 (solid line) and 1.5 (dashed line). Spectra are the average of four scans from the same sample. Mean residue ellipticities are shown.

CD spectra

In Figure 2 CD spectra are shown of M13 coat protein incorporated in DMPC/palmitic acid (73/27 (w/w)) SUVs at L/P ratios of 56 (solid line) and 1.5 (dashed line). Analysis of these spectra yields the following secondary structure: no α -helix, 92% β -structure, 8% other structure at L/P ratio 56 and no α -helix, 75% β -structure, 25% other structure at L/P ratio 1.5. In between these L/P ratios intermediate amounts of secondary structure were found (data not shown).

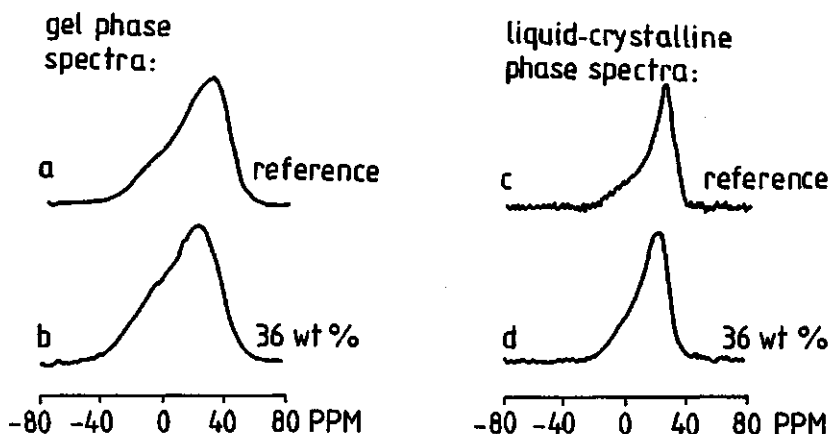


Figure 3. 121.48 MHz ^{31}P NMR spectra at 0°C (a,b) and 45°C (c,d) of DMPC/palmitic acid (73/27 (w/w)) systems without (a,c) and with (L/P ratio 9) M13 coat protein (b,d). The number of scans was 74,676 (a), 1,500 (b), 1,539 (c) and 851 (d). In all cases the spectra were recorded under proton decoupling with 20W/12dB, a relaxation delay of 1 s, a 45° pulse of 16 μs and a spectral width of 50,000 Hz.

^{31}P NMR spectra

Figure 3 shows ^{31}P NMR spectra in the gel and in the liquid-crystalline phase of the phosphatidylcholine molecules in the DMPC/palmitic acid (73/27 (w/w)) system with (L/P ratio 9) and without coat protein. All spectra are powder spectra with a low field shoulder and a high field peak characteristic for DMPC organized in bilayers. At 0°C the spectra are broad with a CSA parameter of 66 ppm (Figure 3a,b). At 45°C the CSA parameter was 43 ppm (Figure 3c,d). No difference in CSA of the sample with and without coat protein is observed. Also in none of the spectra intensity is seen (1) at the isotropic peak position (0 ppm), that could arise from the presence of rapidly tumbling phosphatidylcholine molecules [27], or (2) from H_{II} phase lipids [28]. The

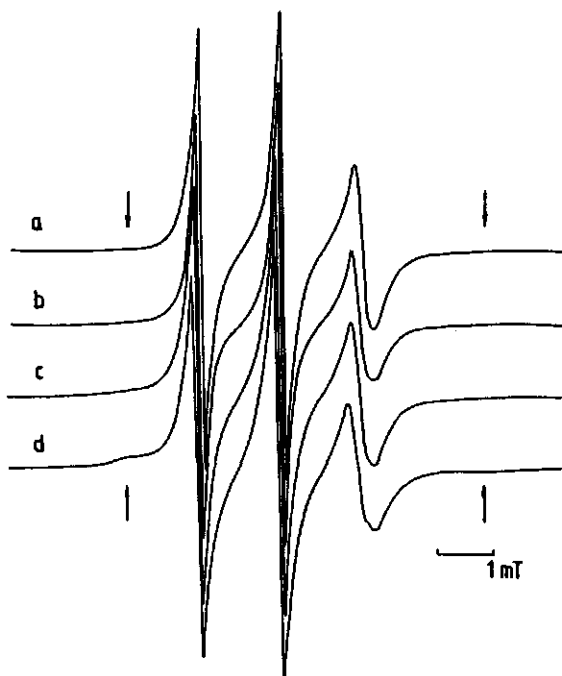


Figure 4. ESR spectra at 45°C of the 14-SASL stearic acid spin label in DMPC/palmitic acid (73/27 (w/w)) systems without (a) and with coat protein at L/P ratio 39 (b), 20 (c) and 9 (d). Arrows indicate the motionally restricted component.

phase transition, which is visible in a temperature dependent series as a decrease in the CSA parameter [1], ranges from 29 to 38°C in both samples (data not shown).

ESR spectra

In Figure 4 the ESR spectra of 14-SASL spin label in DMPC/palmitic acid (73/27 (w/w)) systems with M13 coat protein are shown at various L/P ratios. The spectra were taken at 45°C, which is well (7°C) above

the phase transition as observed by ^{31}P NMR (data not shown) and ^2H NMR (Figure 7, to be discussed below). Apart from the motionally averaged sharp three-line spectrum, typical for liquid-crystalline phase lipid, the samples with M13 coat protein have a second, broader component with strongly restricted motion on the ESR time scale. The intensities of these components, determined by a previously described analysis [8,15], were found to be 0, 10, 19 and 36% of the total spin label intensity at L/P ratios of ∞ , 39, 20 and 9, respectively.

^2H NMR spectra

^2H NMR spectra of $[9,9-^2\text{H}_2]$ -palmitic acid/DMPC (27/73 (w/w)) with M13 coat protein at various L/P ratios are shown in Figure 5. In the gel phase (0°C) the spectra are broadened by slow motions ($\tau_c > 10^{-5}$ s) of the labelled acyl chain [29,30]. The spectra are typical for gel phase lipid, covering a range of approximately 125 kHz (Figure 5a-d). In the liquid-crystalline phase at 45°C typical powder pattern line-shapes [5,31], are observed with quadrupolar splittings, $\Delta\nu_q$, of 28, 28, 28 and 26 kHz for L/P ratios of ∞ , 39, 20 and 9, respectively (Figure 5e-h). For samples with a low coat protein content (L/P ratio ≥ 20) $\Delta\nu_q$ is the same as for the reference sample. However, due to the coat protein the spectra are broadened. The phase transition is visible in a temperature dependent series as double component spectra from 29 to 38°C for the reference sample, which is not changed by the presence of coat protein in the range of L/P ratios tested (data not shown). The ^2H NMR spectra of all reference samples have an isotropic peak of small intensity, which is best seen in the liquid-crystalline phase at 45°C (Figure 5e and also 6i-l, that increases at increasing coat protein content (3, 5 and 20% intensity in Figure 5f,g,h, respectively).

^2H NMR spectra of $[\text{U}-^2\text{H}_{31}]$, $[2,2-^2\text{H}_2]$, $[9,9-^2\text{H}_2]$ and $[16,16,16-^2\text{H}_3]$ palmitic acid in DMPC/palmitic acid (73/27 (w/w)) systems with (L/P

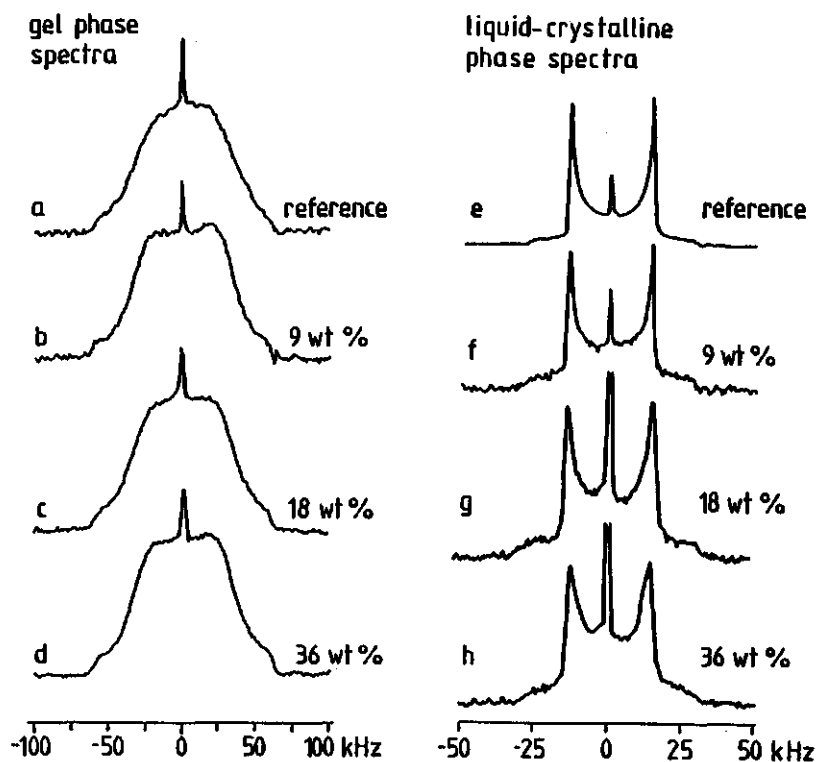


Figure 5. 46.06 MHz ^2H NMR spectra of a DMPC/[9,9- $^2\text{H}_2$]palmitic acid system (73/27 (w/w)) at 0°C (a-d) and 45°C (e-h) without (a,e) and with coat protein at L/P ratio 39 (b,f), 20 (c,g) and 9 (d,h). The number of scans was 40,000 (a-e), 16,000 (f-h) with a relaxation delay of 333 ms, τ_2 of 40 μs , a 90° pulse length of 5.8 μs , and a line broadening of 100 Hz.

ratio 39) and without coat protein in the gel and liquid-crystalline phase are shown in Figure 6. In the gel phase spectra of the reference sample and the sample with M13 coat protein a sharp powder pattern with $\Delta\nu_Q$ of 12 kHz of the mobile, terminal C^2H_3 group is visible on top of several superimposed broadened lineshapes (Figure 6a,e), that arise from immobile C^2H_2 -sites along the acyl chain [17]. At 41°C the spectrum (Figure 6i) consists of several overlapping powder patterns

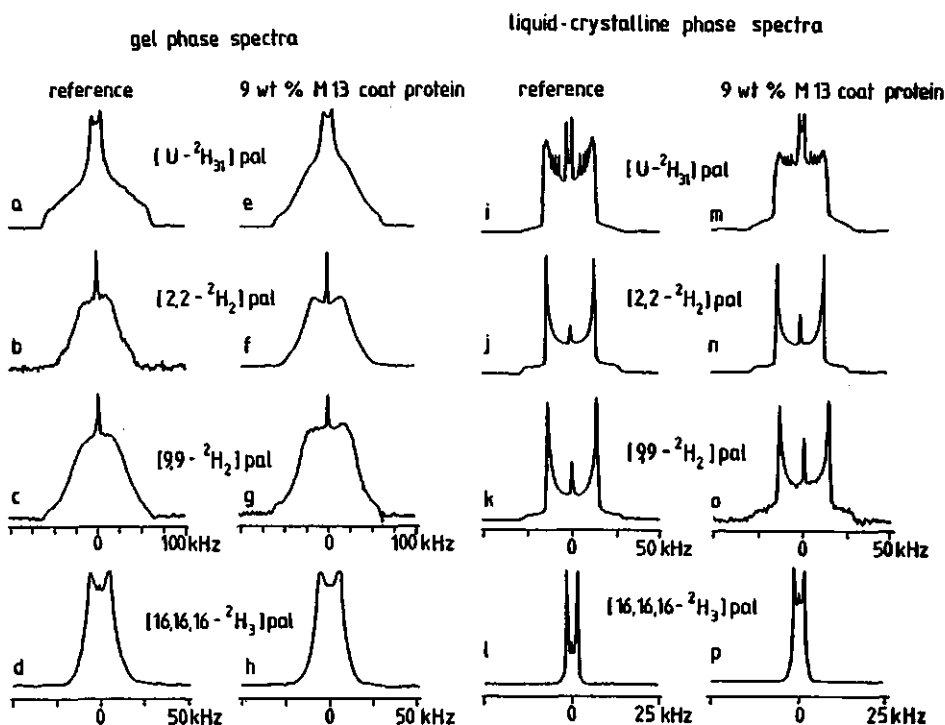


Figure 6. 46.06 MHz ^2H NMR spectra of a $[\text{U}-^2\text{H}_{31}]$ (a,e,i,m), $[\text{2,2}-^2\text{H}_2]$ (b,f,j,n), $[\text{9,9}-^2\text{H}_2]$ (c,g,k,o) and $[\text{16,16,16}-^2\text{H}_3]$ (d,h,l,p) palmitic acid /DMPC (27/73 (w/w)) system without (a-d and i-l) and with (e-h and m-p) M13 coat protein (L/P ratio 39) in the gel phase (a-h) and in the liquid-crystalline phase (i-p). The number of scans and the temperature were 5,000 and 0°C (a), 2,000 and 10°C (b), 40,000 and 0°C (c), 20,000 and 0°C (d), 2,000 and 0°C (e), 20,000 and 12°C (f), 40,000 and 0°C (g), 20,000 and 0°C (h), 2,500 and 41°C (i), 25,000 and 45°C (j), 40,000 and 45°C (k), 20,000 and 41°C (l), 2,000 and 41°C (m), 25,000 and 45°C (n), 16,000 and 45°C (o) and 20,000 and 41°C (p). In all cases a relaxation delay of 333 ms, a τ_2 of 40 μs , a 90° pulse length of 5.8 μs and a line broadening of 100 Hz was applied.

of nine resolved quadrupolar splittings of 29, 27, 25, 24, 22, 19, 15 and 11 kHz of deuterated sites along the acyl chain and 2.7 kHz of the terminal C^2H_3 site. The sample with M13 coat protein gives iden-

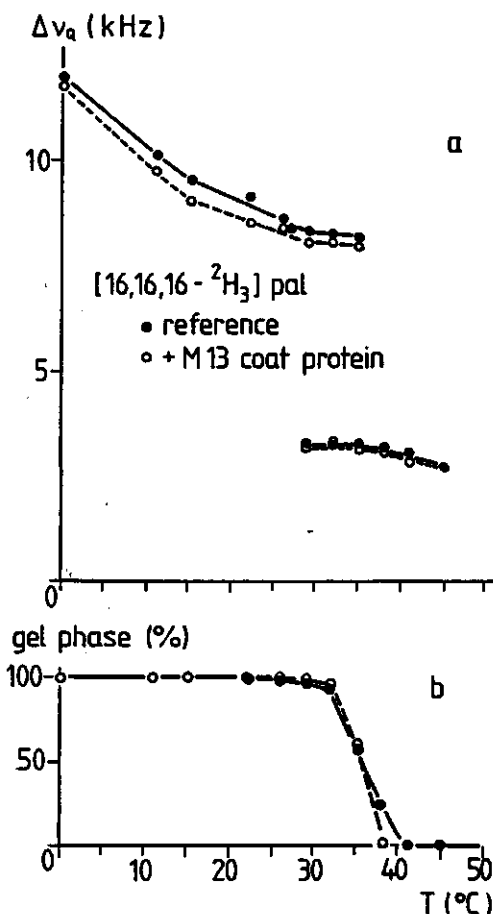


Figure 7. Quadrupolar splittings, $\Delta\nu_q$, as a function of temperature from ^2H NMR spectra of a DMPC/[16,16,16- $^2\text{H}_3$]palmitic acid (73/27 (w/w)) system without (a, solid line) and with (a, dashed line) M13 coat protein (L/P ratio 39). The gel phase percentage, as determined from the intensity distribution in the double component ^2H NMR spectra, is also plotted (b).

tical values (Figure 6m). However, all peaks in this spectrum are broadened due to the presence of M13 coat protein (Figure 6i,m).

In the gel phase the ^2H NMR spectra of samples with palmitic acid selectively labelled at the C-2 or C-9 position resulted in broad

lineshapes covering a range of approximately 100 kHz both in the reference sample (Figure 6b,c) as well as in the sample containing M13 coat protein (Figure 6f,g). In the liquid-crystalline phase, at 45°C both labels give sharp single powder pattern spectra with $\Delta\nu_Q$ of 28 kHz (Figure 6j,k). Again, a distinct line broadening is observed in samples with coat protein (Figure 6n,o).

^2H NMR spectra of samples with palmitic acid labelled at the C-16 display a powder spectrum with a $\Delta\nu_Q$ of 12 kHz at 0°C (Figure 6d) and of 2.7 kHz at 41°C (Figure 6l), in agreement with the values found for the terminal group in the perdeuterated sample (Figure 6a,i). In Figure 7a the quadrupolar splitting from this sample is plotted as a function of temperature. Due to its high mobility the terminal C^2H_3 site also gives sharp powder spectra in the gel phase. This property is used to determine the amount of gel phase lipid as a function of temperature (Figure 7b). The phase transition region is seen from 29 to 38°C as double component spectra. From 29 to 35°C $\Delta\nu_Q$ of the fluid component remains constant at 3.2 kHz and decreases above 35°C with increasing temperature for both samples, with and without coat protein (Figure 7b). In the gel phase, the spectral width of the sample with coat protein is slightly smaller than in the reference sample.

Quadrupolar echo decay measurements

Quadrupolar echoes of samples with $[2,2\text{-}^2\text{H}_2]$, $[9,9\text{-}^2\text{H}_2]$ and $[16,16,16\text{-}^2\text{H}_3]$ palmitic acid/DMPC (27/73 (w/w)) systems with (L/P ratio 39) and without M13 coat protein were measured at 45°C as a function of twice the spacing between the 90 degree pulses of the quadrupolar echo sequence, $2\tau_2$, at 45°C. The decays are mono-exponential, characterized by one spin-spin relaxation time, T_{2e} . The T_{2e} values obtained in this way are listed in Table I.

Table I. Spin-spin relaxation times along the acyl chain in mixed bilayers with M13 coat protein at 45°C.

label position at the acyl chain	T _{2e} (M13) (μs)	T _{2f} (Ref) (μs)	T _{2b} [*] (calc) (μs)
C- 2	540	620	320
C- 9	430	480	220
C-16	3500	5400	880

* For the calculation of T_{2b} from equation (1) the specifically deuterated palmitic acid (27% (w/w) in DMPC bilayers) is assumed to undergo a fast two-site exchange between the sites in the bulk of the lipid bilayer and the motionally-restricted sites (10% as seen by ESR in Figure 4). The coat protein was incorporated at L/P ratio 39. Typical error in T_{2e} and T_{2f} is 5%.

DISCUSSION

M13 coat protein incorporation in stable vesicles

Formation of stable vesicles of mixed DMPC/palmitic acid and coat protein was maximal at 20% (w/w) palmitic acid or more. Therefore, incorporation of the coat protein at high levels in stable bilayers

requires the presence of negatively charged palmitic acid. From previous spin label ESR work it is known that the coat protein has a high preference for the negatively charged lipids, like cardiolipin and also for stearic acid and phosphatidylglycerol [15]. This agrees with incorporation results obtained for a lipid system containing 80% (w/w) phosphatidylcholine, 10% (w/w) phosphatidic acid and 10% (w/w) cardiolipin [16]. Maximal incorporation in vesicles is only possible at relatively low coat protein content (L/P ratio \geq 20, Figure 1b). At high protein content not all the coat protein is incorporated in the SUVs (50% at L/P ratio 9, Figure 1b). Simultaneously palmitic acid with almost isotropic motion is seen by ^2H NMR as a broad isotropic peak (contributing 20% of the intensity, Figure 5h). It is therefore concluded that the coat protein associates partly with part of the palmitic acid molecules in a non-bilayer organization at these high protein levels. It should be noted that the narrow isotropic peak in the reference spectra (Figure 5e and 6i-1) belongs to free palmitic in solution.

M13 coat protein secondary structure

From the CD spectra in Figure 2 it is clear that the dominant conformation of the M13 coat protein in the lipid system is β -structure (75 - 92%) for L/P ratios from 1.5 to 56. A β -structure for an integral membrane protein is remarkable, since many proteins are known to span the membrane by an α -helix [7,8]. However, a β -structure conformation of fd coat protein (which differs from M13 coat protein in only one amino acid residue) has been observed before in model membrane [32-35], even though the M13 and fd coat protein are known to be entirely in an α -helix conformation in the virus [36,37]. This has been explained in terms of a major conformational change during the membrane-bound assembly of the bacteriophage [32]. From time-resolved

tryptophan anisotropy measurements [35] and deuterium NMR measurements of the exchangeable sites at the coat protein backbone [38] in similar mixed bilayers, protein aggregation was concluded. In analogy, in mixed DMPC/palmitic acid bilayers the coat protein is probably also aggregated. Within the aggregate the positively charged C-terminus and negatively charged N-terminus [11,12] can very well cross-link to form antiparallel β -sheet structures. Also a U-shaped conformation of the protein monomer, which has been considered before [34], can be present in the protein aggregates. It is not clear whether the β -structure is the protein conformation *in vivo* in the *E. coli* membrane, although a model for M13 coat protein assembly has been proposed [39], which includes a U-shaped procoat, in which the nature coat protein domain could well form an antiparallel β -structure conformation with its N-terminal leader sequence.

Lipid structure after coat protein incorporation

DMPC/palmitic acid (73/27 (w/w)) systems with M13 coat protein at L/P ratio ∞ , 39, 20 and 9 have been analyzed by ^{31}P and ^2H NMR.

(1) Reference lipid system. The spectra obtained at 45°C by ^{31}P NMR from the phospholipids (Figure 3c) and by ^2H NMR from the palmitic acid labelled at the C-9 position (Figure 5e), show powder patterns, that are characteristic for lipid and palmitic acid organized in a bilayer in the liquid-crystalline phase.

(2) DMPC/palmitic acid mixtures with a high amount of coat protein. The ^{31}P NMR powder patterns (Figure 3b,d) indicate that also in presence of a high amount of coat protein (L/P ratio 9) all phospholipids are in a bilayer structure. The ^2H NMR spectrum of Figure 5h, however, displays a broad isotropic peak contributing 20% to the total spectral intensity. This shows that the major part (80%), but not all palmitic acid, is organized in a bilayer-type organization. Clearly at this

protein content and higher, part of the palmitic acid (20%) does no longer reflect the acyl chain behaviour of the phosphatidylcholine molecules in the bilayer.

A similar ^2H NMR spectrum has been reported for a system consisting of a very high amount (67% (w/w)) of f1 coat protein in DMPC labelled at the terminal C-14 atom position of the *sn*-2 chain [40]. Since f1 coat proteins has an almost identical amino acid sequence as M13 coat protein it may be concluded from these results that at extremely high protein contents the coat protein is no longer incorporated in phospholipids in a bilayer type of aggregation.

(3) DMPC/palmitic acid systems with lower levels of coat protein. At L/P ratio 39 the ^{31}P (data not shown) and ^2H (Figure 5f) NMR spectra show that all phosphatidylcholine molecules and more than 95% of the palmitic acid are in a bilayer structure. In the liquid-crystalline phase the order parameter of the deuterons at the C-9 atom is not changed by incorporation of the coat protein (Figure 5f).

Free fatty acid acyl chain order and dynamics

(a) Previous spin label ESR experiments have shown that incorporation of M13 coat protein into phosphatidylcholine bilayers with negatively charged phospholipids results in a second, motionally-restricted component [14,15]. In the ^2H NMR spectrum of Figure 5f no other component is seen apart from the narrow isotropic peak, which is assigned to freely rotating palmitic acid in solution. Additional spin label ESR spectra were obtained from DMPC/palmitic acid (73/27 (w/w)) systems probed with the 14-SASL spin label to enable direct comparison with the ^2H NMR spectra. The results in Figure 4 show that the coat protein interacts preferentially with 14-SASL in the DMPC/palmitic acid bilayers. The intensity of the motionally-restricted component is proportional to the protein content. This is in agreement with the

previous results [15]. The 14-SASL spin label results can be compared directly with the ^2H NMR spectra of Figure 6i-p. Since in the ESR spectra two distinct sites, i.e. of a motionally-restricted and of a fluid component, are seen these sites are in slow exchange on the ESR timescale (slower than 10^{-9} s). The motionally-restricted component is well-resolved from the fluid component, similar as previously reported for 14-doxyl dimyristoyl phosphatidylglycerol spin label (14-PGSL) in mixed DMPC/dimyristoyl phosphatidylglycerol (80/20 (w/w)) bilayers [15]. Therefore the fatty acid spin label in the mixed DMPC/palmitic acid is likely to exchange at approximately the same rate, i.e. 10^{-7} s^{-1} [15]. As a consequence no second component is seen in the ^2H NMR spectra of deuterated palmitic acid, i.e. The two sites, seen in the spin label ESR spectra, are in fast exchange with respect to the ^2H NMR timescale (10^{-5} s). The two fatty acid sites, seen as distinct components in the ESR spectrum, are time-averaged to reference-like ^2H NMR spectra as seen in Figure 6m-p.

(b) ^2H NMR. M13 coat protein was incorporated at low protein content (L/P ratio 39) in samples with palmitic acid labelled at three different positions along the acyl chain. The coat protein did not affect the order at the C-2, C-9 and C-16 position in the liquid-crystalline phase, as reflected by the quadrupolar splitting (Figure 6j and n, k and o, l and p). However, the presence of coat protein increases the linewidth of the spectra (Figure 6i-p). In the liquid-crystalline phase the bilayer order decreases gradually along the acyl chain [5], which is seen in the ^2H NMR spectra as a series of decreasing quadrupolar splittings. The smallest originates from the terminal C^2H_3 site. At all measured temperatures above the phase transition, i.e. at 35, 38, 41 (data not shown) and 45°C the order along the acyl chain, seen as individual splittings in the spectra from the perdeuterated sample was the same as in presence of M13 coat protein (Figure 6i and m). These results agree with those of the samples with

C-2, C-9 and C-16 labelled acyl chains (Figure 6j-p).

The phase transition region, observed by ^{31}P NMR (data not shown) and ^2H NMR (Figure 7b), for the mixed reference bilayers is broadened to a range of 9°C and shifted upward as compared to the phase transition of pure DMPC (24°C). Both are caused by palmitic acid (27% (w/w)) as reported before for phospholipid bilayers containing free fatty acids [41]. Free fatty acids are assumed to fill the voids that exist between the phospholipids. The voids arise from crowding of the headgroups, that have a larger excluded area in the bilayer plane than the lipid acyl chains [42,43]. As a consequence of this, the phase transition is shifted upward. In the phase transition region of our samples preferential partitioning of the fatty acid in the gel phase is observed by the constancy of the order parameter of the terminal C^2H_3 group from 29 to 35°C (Figure 7), consistent with previous results [17]. At the onset of the phase transition the liquid-crystalline phase is gradually enriched with palmitic acid as the temperature increases at the onset of the phase transition. The enrichment of the liquid-crystalline phase with palmitic acid increases the order parameter. This is compensated by the decrease of the bilayer order at higher temperatures, that is typical for the liquid-crystalline phase. Therefore, the order parameter is constant from 29 to 35°C .

From Table I it is seen that in the liquid-crystalline phase the coat protein decreases T_{2e} at all three sites along the fatty acid acyl chain. To analyse these data we use a model in which the free fatty acid molecules are in fast two-site exchange (at a rate of 10^7 s^{-1} , as concluded above) between the sites in the bulk of the lipid bilayer and the motionally-restricted sites. Then T_{2e} is the weighted average of the spin-spin relaxation times of free palmitic acid in the bulk of the lipid bilayer (T_{2f}) and at the motionally-restricted sites (T_{2b}).

$$1/T_{2e} = f/T_{2b} + (1-f)/T_{2f} \quad (1)$$

where f is the fraction of motionally-restricted fatty acid, as seen by ESR (which is 0.10 at L/P ratio 39, Figure 4). The calculated values for T_{2b} are given in Table I. For the C-2 and C-9 position the T_{2b} values are a factor of 2 smaller than T_{2f} of the reference sample. At the C-16 position the difference is a factor of 6 (Table I). Assuming that the limit of fast motion applies for the relaxation behaviour of these systems [5,44] the observed decrease of T_{2e} values corresponds to a decrease in mobility. In this concept the motions of the palmitic acid are restricted most by the coat protein at the terminal position.

ACKNOWLEDGEMENTS

This research was supported by the Netherlands Foundation of Biophysics, with financial aid from the Netherlands Organization for the Advancement of Pure Research (ZWO). We thank dr. T.J. Schaafsma for reading the manuscript and valuable comments, dr. D. Marsh for the gift of 14-SASL spin label and access to his ESR spectrometer, dr. B.J.M. Harmsen for providing facilities to grow *E. coli*, and R.B.M. Koehorst and W.Ch. Melger for gas chromatography determinations.

REFERENCES

- 1 Seelig, J. and Seelig, A. (1980) Quart. Rev. Biophys. 13, 19-61.
- 2 Jacobs, R.E. and Oldfield, E. (1981) Prog. Nucl. Magn. Reson. Spectrosc. 14, 113-136.
- 3 De Kruijff, B., Cullis, P.R., Verkleij, A.J., Hope, M.J., Van Van Echteld, C.J.A., Taraschi, T.F., Van Hoogevest, P., Killian, J.A., Rietveld, A., and Van Der Steen, A.T.M. (1985) in Progress in Protein-Lipid Interactions (Watts, A. and De Pont, J.J.H.H.M., eds.), Ch. 3, pp. 89-143, Elsevier Science Publications, NY.
- 4 McElhaney, R.N. (1982) Curr. Top. Membr. Transp. 17, 317-380.
- 5 Davis, J.H. (1983) Biochim. Biophys. Acta 737, 177.

- 6 Devaux, P.F., (1983) in *Biological Magnetic Resonance* (Berliner, L.J. L.J., and Reuben, J., eds.), Vol. 5, pp. 183-299, Plenum Press, NY.
- 7 Bloom, M. and Smith, I.C.P. (1985) in *Progress in Protein-Lipid Interactions* (Watts, A. and De Pont, J.J.H.H.M., eds.), Ch. 2, pp. 61-88, Elsevier Science Publishers, NY.
- 8 Marsh, D. (1985) in *Progress in Protein-Lipid Interactions* (Watts, A. and De Pont, J.J.H.H.M., eds.), Ch. 4, pp. 143-172, Elsevier Science Publications, NY.
- 9 Hemminga, M.A., Datema, K.P., Ten Kortenaar, P.W.B., Kruse, J., Vriend, G., Verduin, B.J.M. and Koole, P. (1985) in *Magnetic Resonance in Biology and Medicine* (Govil, G., Khetrapal, C.L. and Saran, A., eds.), pp. 53-76, Tata McGraw-Hill Publishing Company Ltd., New Delhi, India.
- 10 Marvin, D.A. and Wachtel, E.J. (1975) *Nature* 253, 19-23.
- 11 Van Asbeck, F., Beyreuther, K., Koehler, H., Von Wettstein, G. and Braunitzer, G. (1969) *Hoppe-Seyler's Z. Physiol. Chem.* 350, 1047-1066.
- 12 Nakashima, Y. and Konigsberg, W. (1974) *J. Mol. Biol.* 88, 598-600.
- 13 Wickner, W. (1976) *Proc. Natl. Acad. Sci. USA* 73, 1159-1163.
- 14 Hemminga, M.A. (1987) *J. Chem. Soc. Faraday Trans. 1* 83, 203-210
- 15 Datema, K.P., Wolfs, C.J.A.M., Marsh, D., Watts, A. and Hemminga, M.A. (1987), *Biochemistry*, in press.
- 16 Hagen, D.S., Weiner, J.H. and Sykes, B.D. (1978) *Biochemistry* 17, 5860-5866.
- 17 Pauls, K.P., MacKay, A.L. and Bloom, M. (1983) *Biochemistry* 22, 6101-6109.
- 18 Marsh, D. and Watts, A. (1982) in *Lipid-Protein Interactions* (Jost, P.C. and Griffith, O.H., Eds.), Vol. 2, pp 53-126, Wiley-Interscience, New York, NY.
- 19 Garssen, G.J., Hilbers, C.W., Schoenmaker, J.G.G. and Van Boom, J.H. (1977) *Eur. J. Biochem.* 81, 453-463.
- 20 Knippers, R. and Hoffmann-Berling, H. (1966) *J. Mol. Biol.* 21, 281-292.
- 21 Peterson, G.L. (1977) *Anal. Biochem.* 83, 346-56.
- 22 Bartlett, G.R. (1959) *J. Biol. Chem.* 234, 466-468.
- 23 Greenfield, N. and Fasman, G.D. (1969) *Biochemistry* 8, 4108-4116.
- 24 Davis, J.H., Jeffrey, K.R., Bloom, M., Valic, M.I. and Higgs, T.P. (1976) *Chem. Phys. Lett.* 42, 390-394.
- 25 Datema, K.P., Pauls, K.P. and Bloom, M. (1986) *Biochemistry* 25, 3796-3803.
- 26 Siminovich, D.J., Rance, M. and Jeffrey, K.R. (1984) *J. Magn. Reson.* 58, 62-75.
- 27 Burnell, E.E., Cullis, P.R. and De Kruijff, B. (1980) *Biochim. Biophys. Acta* 603, 63-69.
- 28 Van Echteld, C.J.A., De Kruijff, B., Verkleij, A.J., Leunissen-Bijvelt, J. and De Gier, J. (1982) *Biochim. Biophys. Acta* 692, 126-138.

- 29 Westerman, P.W., Vas, M.J., Strenk, L.M. and Doane, J.W. (1982) *Proc. Natl. Acad. Sci. USA* 79, 2890-2894.
- 30 Wittebort, R.J., Blume, A., Huang, T.-H., Das Gupta, S.K., and Griffin, R.G. (1982) *Biochemistry* 21, 3487-3502.
- 31 Seelig, J. and Seelig, A. (1974) *Biochemistry* 13, 4839-4845.
- 32 Nozaki, Y., Chamberlain, B.K., Webster, R.E. and Tanford, C. (1976) *Nature* 259, 335-337.
- 33 Nozaki, Y., Reynolds, J.A. and Tanford, C. (1978) *Biochemistry* 17, 1239-1246.
- 34 Chamberlain, B.K., Nozaki, Y., Tanford, C. and Webster, R.E. (1978) *Biochim. Biophys. Acta* 510, 18-37.
- 35 Datema, K.P., Visser, A.J.W.G., Van Hoek, A., Wolfs, C.J.A.M., Spruijt, R.B. and Hemminga, M.A. (1987) *Biochemistry*, in press.
- 36 Valentine, K.G., Schneider, D.M., Leo, G.L., Colnago, L.A. and Opella, S.J. (1986) *Biophys. J.* 49, 36-38.
- 37 Opella, S.J., Stewart, P.L. and Valentine, K.G. (1987) *Quart. Rev. Biophys.*, in press.
- 38 Datema, K.P., Van Boxtel, B.J.H. and Hemminga, M.A. (1987) submitted for publication.
- 39 Kuhn, A., Wickner, W. and Kreil, G. (1986) *Nature* 322, 335-339.
- 40 Oldfield, E., Gilmore, R., Glaser, M., Gutowski, H.S., Hshung, J.C., Kang, S.Y., King, T.E., Meadows, M. and Rice, D. (1978) *Proc. Natl. Acad. Sci. USA* 75, 4657-4660.
- 41 Kantor, H.L. and Prestegard, J.H. (1978) *Biochemistry* 17, 3592-3597.
- 42 Mabrey, S. and Sturtevant, J.M. (1977) *Biochim. Biophys. Acta* 486, 444-450.
- 43 McIntosh, T.J. (1980) *Biophys. J.* 29, 237-246.
- 44 Brown, M.F. and Williams, G.D. (1985) *J. Biochem. Biophys. Methods* 11, 71-81.

CHAPTER 5

SUMMARIZING DISCUSSION

5 SUMMARIZING DISCUSSION

In this thesis some new aspects of the infection process of non-enveloped viruses are reported. The interaction of a rod-shaped (TMV) and three spherical (CCMV, BMV, SBMV) plant viruses, of the filamentous bacteriophage M13, and of their coat proteins with membranes have been investigated. A comparison is made between the infection mechanisms of these non-enveloped viruses.

1 EFFECT OF PLANT VIRUSES ON MEMBRANES

All plant viruses studied interact with membranes. This is demonstrated by turbidity measurements of small unilamellar vesicles with different surface charges (chapter 2). The interaction is either electrostatic or hydrophobic.

Neutral vesicles always interact with viral capsids by indirect hydrophobic interaction. On the other hand, charged vesicles always interact with opposite charges at the capsids by electrostatic interaction. The location of the coat protein after interaction has been determined to test Durham's model for plant virus infection, in which the coat protein becomes an integral membrane protein, similarly as for M13 infection. The results indicate that as a result of the interactions, multilamellar vesicles are formed, containing all the protein in case of electrostatic interaction. The coat protein is associated at the bilayer surface. However, after hydrophobic interaction no protein is found in the multilamellar vesicles. For the latter type of interaction a mechanism is proposed, in which the coat protein behaves as a catalyst, only enhancing the rate of fusion and multilamellar vesicle formation. Since in either case no lipid-protein complex is formed, that is stabilized by direct hydrophobic lipid-protein inter-

actions, Durham's model for plant virus infection is very likely to be incorrect.

The recently proposed co-translational disassembly model for plant virus infection, in which the viral particle dissociates during translation of its RNA by the host ribosomes, does not include a specific role for membranes during disassembly. However, before the co-translational disassembly takes place, the particles need to be destabilized. At this moment no specific mechanism for this process has been proposed. Also the fate of the coat protein after particle disassembly remains unspecified in any model, with exception of Durham's model. The observed electrostatic interaction at the bilayer surface (e.g. with the N-terminal arm of the coat proteins, released upon assembly may play a significant role in the infection mechanism.

From the experiments described in this thesis no results contradictory to co-translational disassembly have been found. Therefore, to our present opinion, the best model for plant virus infection is the co-translational disassembly model. In this view it is assumed implicitly that the virus particles arrive intact in the cytoplasm, for example by passage through the cell wall and the plasma membrane by local, transient wounding.

2 EFFECT OF THE MEMBRANE ON BACTERIOPHAGE M13 COAT PROTEIN

M13 coat protein has been incorporated as an intrinsic protein in micelles and model membranes (chapter 3-4). The secondary structure of coat protein in SDS micelles is predominantly α -helix (60%), while in membranes (DMPC/DMPA 80/20 w/w) the structure is entirely β -structure.

In micelles at high detergent protein ratio the protein is dimeric with the central core in β -structure. The termini of the coat protein (30 residues or 60%) are in α -helix structure. The dynamics of the micellar system, investigated by time-resolved fluorescence anisotropy

measurements, is characterized by rotation of the complex on the nanosecond timescale (10 ns at 20°C) and additional mobility of the Trp-26 sidechain on the subnanosecond timescale (0.5 ns). The complex has a temperature dependent overall rotation, that satisfies the Stokes-Einstein relation for spherical rotation. From this dependence it has been determined that the complex consists of two coat protein molecules and approximately 57 SDS molecules.

In membranes, regardless of the lipid to protein ratio, the coat protein is aggregated. This is concluded from three independent measurements. Fluorescence anisotropy decay measurements indicate that the single tryptophan-26 in the hydrophobic core is highly ordered on the nanosecond timescale in liquid-crystalline bilayers, whereas the surrounding lipids are not. ^2H NMR measurements indicate that all the exchangeable sites at the backbone are ordered on the microsecond timescale. Both results are consistent with protein aggregation. Finally, the fraction of motionally restricted lipid, determined from spin label ESR is too low for a monomeric state of the coat protein in the membrane, also in agreement with protein aggregation.

The state of the M13 coat protein in model membranes used in the experiments of this thesis is therefore best described as a β -polymeric state. Within the polymer the orientation of the coat protein is unknown. For comparison, in vivo, the coat protein in the E. coli cytoplasmic membrane is known to be oriented. Its secondary structure and state of aggregation, however, are up to now unknown.

3 EFFECT OF BACTERIOPHAGE M13 COAT PROTEIN ON THE MEMBRANE

In model membranes also the effect of M13 coat protein incorporation on the lipids has been investigated (chapter 4). Upon introduction of coat protein in the membrane as an intrinsic protein a fraction of the lipid molecules becomes motionally restricted.

The spin labelled phospholipids show a difference in their selectivity for the coat protein: cardiolipin = phosphatidic acid >> stearic acid = phosphatidylserine = phosphatidylglycerol >> phosphatidylcholine = phosphatidylethanolamine. The selectivities found are related to the composition of the target *E. coli* cytoplasmic membrane. Typically, neutral phosphatidylethanolamine accounts for 74% of the lipid in the membrane, constituting the bulk of the lipid, while phosphatidylglycerol is present for 19% and cardiolipin for 3%. The high selectivity of cardiolipin for the coat protein forms direct, biophysical evidence for a previously suggested molecular association of cardiolipin with the coat protein. This was concluded from an increase in the cardiolipin synthesis after infection of *E. coli* by M13. No increase in phosphatidylglycerol synthesis, the major negatively charged lipid, is observed after infection.

Using selectively deuterated palmitic acid as probe lipid, spectral broadening has been observed in presence of M13 coat protein. This result, as well as the ESR results, agrees with a two-site exchange model for the probe lipid between sites in the bulk of the membrane and motionally-restricted sites at the protein. The exchange rate is fast on the nanosecond timescale of the ESR technique, but slow on the microsecond timescale of the ^2H NMR technique. The exchange rate of 10^7 Hz, deduced from simulation of the spin label ESR spectra, is in excellent agreement with these upper and lower limits.

SAMENVATTING

Virussen zijn onderverdeeld in membraan- en niet-membraanvirussen. Van de meeste membraanvirussen is in het algemeen het penetratiemechanisme bekend: ze passeren het membraan door fusie van het eigen en gastheermembraan. Van de niet-membraanvirussen, waartoe de meeste plantevirussen en sommige bacterievirussen behoren, is het penetratiemechanisme niet bekend. Zelfs voor M13, een veel bestudeerde colifaag, is dit het geval.

In dit proefschrift is de interactie van enkele niet-membraanvirussen, een staafvormig (TMV) en enkele bolvormige (CCMV, BMV, SBMV) plantevirussen en de bacteriofaag M13, met membranen onderzocht met geavanceerde spectroscopische technieken. Bovendien is een vergelijking gemaakt tussen de infectiemechanismen van deze virussen.

1 HET EFFECT VAN PLANTEVIRUSSEN OP MEMBRANEN

Alle bestudeerde plantevirussen hebben een interactie met membranen. Dit is aangetoond met turbiditeitsmetingen van kleine unilamellaire vesikels met verschillende oppervlaktelading. De kleine unilamellaire vesikels vormen modelmembranen voor het natuurlijke plasmamembraan van de gastheercel.

Vesikels met een neutrale oppervlaktelading hebben een interactie met virale eiwitten door middel van een indirecte hydrofobe interactie. Vesikels met een geladen oppervlak hebben altijd een elektrostatistische interactie met tegengestelde ladingen op de eiwitmoleculen. Als test voor Durham's model voor penetratie van plantevirussen, waarin het manteleiwit wordt opgeslagen als intrinsiek eiwit in het membraan op een zelfde manier als het manteleiwit bij infectie door M13, is het

lot van het manteleiwit van de plantevirussen na de interactie nagegaan. De resultaten tonen aan dat multilamellaire vesikels worden gevormd. Deze bevatten al het virale eiwit bij elektrostatische interactie: het manteleiwit is dan geassocieerd aan het oppervlak. Echter, na hydrofobe interactie wordt geen eiwit teruggevonden in de gevormde multilamellaire vesikels. Voor deze interactie wordt in dit proefschrift een mechanisme voorgesteld waarbij het manteleiwit zich gedraagt als een katalysator, die alleen de membraanfusie en multilamellaire vesikelvorming versnelt, maar waarbij het eiwit niet geïncorporeerd wordt in het membraan. Aangezien in beide gevallen geen lipide-eiwitcomplex gevormd is, dat gestabiliseerd wordt door directe hydrofobe interacties, is Durham's model voor plantevirusinfectie hoogst waarschijnlijk onjuist.

Een ander, onlangs voorgesteld "co-translational disassembly" model voor plantevirusinfectie, veronderstelt dat tijdens de translatie van het virale RNA door de gastheerribosomen het virusdeeltje dissocieert. Dit model bevat geen specifieke membraanfunctie bij de disassemblage van het virusdeeltje, maar het virusdeeltje moet wel vooraf gedestabiliseerd worden. Op het moment is dit mechanisme niet bekend. De bestemming van het manteleiwit na disassemblage van het deeltje wordt in het midden gelaten in het "co-translational disassembly" model, terwijl Durham's model onjuist is gebleken op dit punt. De waargenomen elektrostatische interactie aan het membraan-oppervlak kan een rol van betekenis spelen tijdens het infectieproces.

De experimentele resultaten zijn niet tegenstrijdig met het "co-translational disassembly" mechanisme. Daarom wordt dit model hier als het beste beschouwd voor plantevirusinfectie. In dit concept is tevens impliciet verondersteld dat de virale deeltjes intact arriveren in het cytoplasma van de gastheercel, bijvoorbeeld door passage door de celwand en het plasmamembraan tijdens lokale, tijdelijke verwonding.

2 HET EFFECT VAN HET MEMBRAAN OP HET BACTERIOFAAG M13 MANTELEIWIT

M13 manteleiwit is geïncorporeerd als intrinsiek eiwit in micellen en modelmembranen (hoofdstuk 3-4). De secundaire structuur van het manteleiwit in SDS micellen heeft voornamelijk α -helix karakter (69%), terwijl de secundaire structuur in membranen vrijwel geheel β -structuur is (90%).

In micellen bij hoge detergens/eiwit-verhouding is het eiwit aanwezig als dimeer met het centrale deel in β -structuur en beide uiteinden (30 residuen ofwel 60% van het totaal) in α -helix structuur. De dynamica van het micellaire systeem, onderzocht met tijd-opgeloste fluorescentie-anisotropiemetingen, wordt gekarakteriseerd door rotatie afkomstig van het eiwit-micelcomplex op de nanoseconde tijdschaal (10 ns bij 20°C) en een extra sub-nanoseconde beweeglijkheid (0.5 ns) van de tryptofaan-26 zijketen. Het complex heeft een temperatuur-afhankelijke rotatiebeweging, die voldoet aan de Stokes-Einstein relatie voor een bol. Met behulp van deze afhankelijkheid is bepaald dat het complex bestaat uit twee eiwit sub-eenheden en 57 detergens moleculen.

In membranen is het manteleiwit geaggregeerd. Dit is waargenomen met drie onafhankelijke technieken. Tijd-opgeloste fluorescentieanisotropiemetingen laten zien dat het tryptofaan-26 in het hydrofobe gedeelte van het manteleiwit in hoge mate geordend is op de nanoseconde tijdschaal, ook als dit niet zo is voor de omringende lipiden. Deuterium-NMR metingen, gevoelig voor beweeglijkheid op de microseconde tijdschaal, laten zien dat alle uitwisselbare plaatsen van de $[-CO-NH-CR-]$ -keten van het eiwit eveneens geordend zijn. Beide resultaten zijn in overeenstemming met eiwitaggregatie. Tenslotte blijkt de fractie van de lipiden, die in hun beweeglijkheid worden beperkt door de aanwezigheid van het manteleiwit, gekwantificeerd met spinlabel-ESR metingen, te laag te zijn voor een monomere toestand van het eiwit in het membraan. Ook dit is in overeenstemming met eiwitaggregatie.

De toestand van het M13-manteleiwit in de gebruikte modelmembraan

systemen, wordt het best beschreven als een β -polymere toestand. In een dergelijk polymeer is de oriëntatie van het eiwit echter onbekend. Ter vergelijking, in vivo is van het M13-manteleiwit bekend dat het georiënteerd voorkomt in het cytoplasmamembraan van E. coli. In tegenstelling tot de oriëntatie zijn de secundaire structuur en aggregatietoestand van het manteleiwit tot nu toe onbekend.

3 HET EFFECT VAN HET BACTERIOFAAG M13 MANTELEIWIT OP HET MEMBRAAN

Het effect van M13-manteleiwit op de lipiden in modelmembranen is onderzocht in hoofdstuk 4. Zodra M13-manteleiwit geïncorporeerd is als intrinsiek eiwit in het membraan wordt een fractie van de lipiden beperkt in hun beweeglijkheid. Fosfolipiden, voorzien van een spinlabel, laten een verschil zien in hun selectiviteit voor het M13-manteleiwit: cardiolipine = fosfatidezuur >> stearinezuur = fosfatidylserine = fosfatidylglycerol >> fosfatidylcholine = fosfatidylethanolamine. Het waargenomen selectiviteitspatroon is duidelijk gerelateerd aan de samenstelling van het E. coli cytoplasma membraan. Dit bestaat voor 74% uit fosfatidylethanolamine, 19% fosfatidylglycerol en 3% cardiolipine. De zeer hoge specificiteit voor cardiolipine vormt een direkt, biofysisch bewijs voor een al eerder veronderstelde moleculaire associatie van cardiolipine met M13 manteleiwit. Dit werd destijds door andere onderzoekers geconcludeerd uit een toename van de synthese van cardiolipine na infectie van E. coli met M13.

Met gebruikmaking van selectief deuterium-gelabeld palmitinezuur als probe is een verbreding van het deuterium-NMR spectrum waargenomen in aanwezigheid van M13-manteleiwit. Dit resultaat, evenals de spinlabel-ESR resultaten, stemmen overeen met een uitwisselingsmodel voor de gelabelde lipiden in de bulk van het membraan en naast het eiwit, waar de beweeglijkheid van de lipiden beperkt is. De uitwisselingsnelheid is snel op de nanoseconde tijdschaal (ESR), maar langzaam op

de microseconde tijdschaal (deuterium NMR). De uitwisselingsnelheid van 10^{+7} Hz, bepaald door simulatie van de spin-label ESR spectra zijn zeer goed in overeenstemming met deze onder- en bovengrens.

ABBREVIATIONS

A _{550nm}	turbidity at 550 nm
BMV	brome mosaic virus
¹³ C	carbon-13
CCMV	cowpea chlorotic mottle virus
CD	circular dichroism
14-CLSL	1-(3- <u>sn</u> -phosphatidyl)-3-[1-acyl-2-[14-(4,4-dimethyl-oxazolidine- <u>N</u> -oxyl)stearoyl]glycero-3-phospho]- <u>sn</u> -glycerol
CMC	critical micelle concentration
CSA	chemical shift anisotropy
CTAB	cetyl trimethyl ammonium bromide
DLPA	1,2-dilauroyl- <u>sn</u> -glycero-3-phosphatidic acid
DLPC	1,2-dilauroyl- <u>sn</u> -glycero-3-phosphocholine
DMPA	1,2-dimyristoyl- <u>sn</u> -glycero-3-phosphatidic acid
DMPC	1,2-dimyristoyl- <u>sn</u> -glycero-3-phosphocholine
DMPG	1,2-dimyristoyl- <u>sn</u> -glycero-3-phosphoglycerol
DNA	desoxyribonucleic acid
$\Delta\sigma$	residual CSA
$\Delta\nu_q$	quadrupolar splitting
D ₂ O	deuterium oxide
EDTA	ethylene diamine tetraacetic acid
EM	electron microscopy
ESR	electron spin resonance
η	asymmetry parameter
f	fraction
FID	free induction decay
ϕ	correlation time
H	spin hamiltonian
H _{II}	hexagonal phase of type II
¹ H	proton
² H	deuterium
² H ₂ O	deuterium oxide
L/P ratio	phospholipid to coat protein molar ratio
L _{pc} /P ratio	phosphatidylcholine to coat protein molar ratio
M	molecular weight
M13	bacteriophage M13
NMR	nuclear magnetic resonance
N _s	number of scans
OD _{280nm}	optical density at 280 nm
PALCHOL	palmitoyl choline
³¹ P	phosphorus-31
14-PASL	1-acyl-2-[14-(4,4-dimethyloxazolidine- <u>N</u> -oxyl)stearoyl]- <u>sn</u> -glycero-3-phosphoric acid
14-PCSL	1-acyl-2-[14-(4,4-dimethyloxazolidine- <u>N</u> -oxyl)stearoyl]- <u>sn</u> -glycero-3-phosphocholine

14-PESL	1-acyl-2-[14-(4,4-dimethyloxazolidine- <u>N</u> -oxyl)stearoyl]- <u>sn</u> -glycero-3-phosphoethanolamine
14-PGSL	1-acyl-2-[14-(4,4-dimethyloxazolidine- <u>N</u> -oxyl)stearoyl]- <u>sn</u> -glycero-3-phosphoglycerol
pI	iso-electric point
ppm	parts per million
14-PSSL	1-acyl-2-[14-(4,4-dimethyloxazolidine- <u>N</u> -oxyl)stearoyl]- <u>sn</u> -glycero-3-phosphoserine
RNA	ribonucleic acid
r	radius
r(0)	initial anisotropy
r(∞)	residual anisotropy
S	order parameter
SDS	sodium dodecyl sulphate
SDS-PAGE	sodium dodecyl sulphate poly acryl amide gel electrophoresis
14-SASL	14-(4,4-dimethyloxazolidine- <u>N</u> -oxyl)stearic acid
SBMV	southern bean mosaic virus
SUVs	small unilamellar vesicles
$\sigma_{11,22,33}$	principal axis chemical shift anisotropy tensor values
T	triangulation number or Tesla
TMV	tobacco mosaic virus
Tris	tris(hydroxymethyl)aminomethane
T ₁	spin-lattice relaxation time
T _{2b}	spin-spin relaxation time of bound palmitic acid, motionally restricted by coat protein
T _{2e}	spin-spin relaxation time determined from the decay of the quadrupolar echo
T _{2f}	spin-spin relaxation time of free palmitic acid in the bulk of the lipid bilayer
θ	mean residue ellipticities
τ_c	rotational-correlation time
τ_f	fluorescence lifetime
τ_1	relaxation delay
τ_2	delay between 90° pulses of quadrupolar echo sequence
V _{xx,yy,zz}	principal axis quadrupolar tensor values

CURRICULUM VITAE

Klaas Pieter Datema werd geboren op 8 februari 1959 in Kesteren. In 1977 legde hij het eindexamen gymnasium- β af, waarna hij begon met de studie biologie aan de Landbouwwuniversiteit in Wageningen.

In 1981 behaalde hij het kandidaatsexamen biologie (oriëntatie cel) en moleculaire wetenschappen (fysisch-chemische oriëntatie). De dok-toraalvakken voor moleculaire wetenschappen waren: moleculaire fysica (hoofdvak), biochemische genetika (hoofdvak) en wiskunde (bijvak). De praktijktijd bracht hij door in het NMR Laboratory, Department of Physics, University of British Columbia in Vancouver, Canada. In 1983 legde hij het ingenieursexamen af.

Van september 1983 tot september 1987 verrichtte hij, in dienst van de Stichting van Biofysica met financiële hulp van de Nederlandse Organisatie voor Zuiver Wetenschappelijk Onderzoek (ZWO), het onderzoek dat leidde tot dit proefschrift. Vanaf september 1987 werkt hij als onderzoeker in de NMR groep van het Koninklijke/Shell-laboratorium in Amsterdam.